REPUBLIQUE ALGERIENNE DEMOCRATIQUE ET POPULAIRE
MINISTERE DE L'ENSEIGNEMENT SUPERIEUR ET DE LA RECHERCHE SCIENTIFIQUE

UNIVERSITE ABOU-BEKR BELKAID – TLEMCEN

THÈSE LMD

Présentée à :

FACULTE DES SCIENCES – DEPARTEMENT DE MATHÉMATIQUES

Pour l'obtention du diplôme de :

DOCTORAT

Spécialité : **Analyse**

Par :

Mlle Zineb KAID

Sur le thème

Modélisation de la croissance tumorale et interaction avec le système immunitaire

---

Soutenue publiquement le 25/10/2023 à Tlemcen devant le jury composé de :

Mr. M.YEBDRI	Professeur	Université de Tlemcen	Président
Mr. A.LAKMECHE	Professeur	Université de Sidi Bel Abbès	Directeur de thèse
Mr. J. CLAIRAMBAULT	Directeur de recherche	Sorbonne Université/INRIA	Examinateur
Mr. C. POUCHOL	Maître de Conférences	Université de Paris	Examinateur
Mr. A. CHEKROUN	Maître de Conférences A	Université de Tlemcen	Examinateur
Mr. M. BOUIZEM	Maître de Conférences A	Université de Tlemcen	Examinateur
Mr. M. HELAL	Professeur	Université de Sidi Bel Abbès	Invité

Laboratoire des Systèmes Dynamiques et Applications
BP 119, 13000 Tlemcen - Algérie

This thesis has been prepared at

Dynamical Systems and Applications Laboratory **(SDA)**
Department of Mathematics, Faculty of Sciences
Abou Bekr Belkaid University
BP 119, 13000 Tlemcen, Algeria
Phone/Fax: (+213)43216375

Biomathematics Laboratory **(LBIOMATH)**
Department of Mathematics, Faculty of Exact Sciences
Djillali Liabes University
BP 89, 22000 Sidi Bel-Abbes, Algeria
Phone/Fax: (+213)48799006

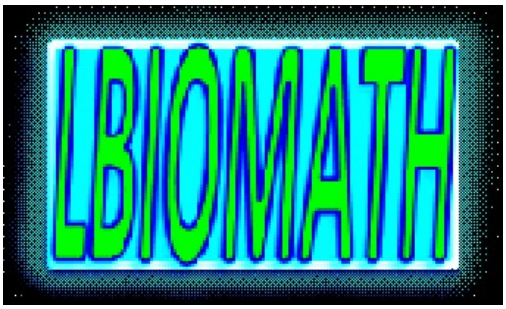

À ma mère, je dis qu'aucun langage ne saurait rendre hommage à ton dévouement à notre éducation et aux longues années de ta vie consacrées à notre réussite. Je dédie ce travail à la mémoire de mes deux tantes, Mama et Malika, décédées récemment, elles ne verront malheureusement pas l'aboutissement de ma thèse et à ma tante Rabia, en reconnaissance de leur bonté exceptionnelle. À vous trois, j'adresse ma profonde gratitude.

Acknowledgements

Achever une thèse est un travail de longue haleine, un effort personnel en continu auquel plusieurs personnes, du plus proche au plus éloigné, ont contribué. Il me sera difficile de remercier l'ensemble des personnes, nombreuses qui, grâce à leur aide, j'ai pu mener cette thèse à son terme.

Je voudrais tout d'abord remercier grandement mon directeur de thèse, le professeur Abdelkader Lakmèche, qui a bien voulu accepter de diriger ma thèse et m'orienter dans mon travail avec délicatesse. Je suis ravie d'avoir travaillé en sa compagnie car, outre son appui scientifique, il a toujours été là pour me soutenir et me conseiller au cours de l'élaboration des nombreuses étapes de ce travail.

Ma gratitude et ma reconnaissance vont au professeur Jean Clairambault et à Camille Pouchol, maître de conférences qui n'ont ménagé aucun effort pour faire advenir cette thèse. Leur disponibilité et leur patience m'ont redonné confiance dans les moments de doute. Leur co-encadrement scientifique d'une grande efficacité m'a permis d'apprendre et d'avancer dans le raisonnement et la modélisation d'un sujet difficile mais passionnant. Cette thèse est le fruit d'une collaboration de plusieurs années avec eux. C'est à leur côté que j'ai compris ce que rigueur et précision signifient.

Je tiens à remercier le professeur Mustapha Yebdri d'avoir accepté de présider le jury de cette thèse. Les professeurs Mohamed Bouizem et Abdennasser Chekroun m'ont fait l'honneur d'être examinateurs de la thèse. Ils ont pris le temps de lire, d'évaluer mon manuscrit. Pour tout cela, je les remercie.

J'adresse mes remerciements aussi au professeur Mohamed Helal pour sa participation scientifique active tout au long de nos nombreuses séances de travail au laboratoire des biomathématiques. Il m'est impossible d'oublier toute l'équipe du Laboratoire Jacques Louis-Lions (JLL) pour son apport précieux notamment, lors des débats sur les modèles d'application et les séminaires riches pendant mes séjours d'accueil scientifique. Mes remerciements vont singulièrement aux professeurs Emmanuel Trélat, Benoît Perthame, Louis Almeida, Nicolas Vauchelet et aux doctorants de JLL

qui m'ont aidée par leurs suggestions et critiques pertinentes : Emma, Georgia, Nicolas, Noemie et Jesús. C'est grâce à cette équipe que j'ai pu concilier avec bonheur recherche théorique et appliquée au bénéfice de cette thèse.

Les professeurs Ali Moussaoui, Karim Yadi qui m'ont initiée à la recherche et prodigué de nombreux conseils pour démarrer cette thèse, le professeur Bedr Eddine Aïnseba a su trouver des passerelles pour une réorientation de ma recherche et mon encadrement, qu'ils en soient chaleureusement remerciés. Je tiens à exprimer, en particulier, mon respect affectueux à ma tante Rabia Bekkar, chercheure, pour les nombreuses discussions, son suivi et ses conseils d'organisation de mon travail qui m'ont enrichie tout au long de mon cursus universitaire, notamment lors de l'élaboration de cette thèse.

Je remercie les deux équipes des laboratoires auxquels je suis rattachée pour leur accueil : laboratoire des systèmes dynamiques et applications de l'Université Abou Bekr Belkaïd de Tlemcen et le laboratoire des biomathématiques de l'Université Djillali Liabes de Sidi -Bel-Abbès.

Le soutien de mon ami Alexandre a été inestimable les trois dernières années. J'ai partagé avec lui mon intérêt pour la question de la croissance tumorale. Il a bien voulu suivre mon travail et m'a fait profiter de ses remarques avec bienveillance et attention. Je n'oublierai jamais qu'il m'a fait répéter l'exposé que je devais présenter au séminaire "Café Mamba". Un énorme merci à Nastassia pour son aide, ses conseils et pour tous les moments de mots croisés. Je souhaite bien évidemment exprimer une reconnaissance toute particulière à mon ami Anes pour son soutien inconditionnel pendant toutes ces années d'études universitaires. Sa présence attentive, sa disponibilité m'ont été précieuses. Enfin, je ne remercierai jamais Tonton Philippe. Merci infiniment pour les encouragements dans cette dernière ligne droite et aussi pour tous les conseils sur les formalités administratives.

Zineb KAID

Glossary of biological terms

In what follows, we give the terminology for some biological concepts encountered in this thesis. We refer the reader to ([83], [85], [84]).

Antigen: Any substance that can stimulate an immune response against it. Two main categories of antigens are recognized: foreign antigens also called heteroantigens, and autoantigens (or self-antigens). Heteroantigens include bacteria, viruses, fungi, chemicals, toxins, and any substance that originated outside the body. Autoantigens, on the other hand, originate within the body. Antigens are present on the surface of pathogens, normal cells, and even tumour cells.

Angiogenesis inhibitors: A chemical that interferes with the signals to form new blood vessels is called an angiogenesis inhibitor. Antiangiogenic therapy is a treatment that prevents the growth of cancer by blocking new blood vessels from forming.

Antigen presenting cells (APCs): A heterogeneous group of immune cells that mediates the cellular immune response by processing and presenting antigens for recognition by specific lymphocytes such as T cells. APCs include macrophages (which are the primary ones), dendritic cells, and B cells.

AXL Tyrosine kinase receptor: A member of the TAM (TYRO3-AXL-MER) family of receptor tyrosine kinases (RTKs). Recent studies have revealed a crucial role for AXL

signalling in tumour proliferation, stem cell phenotype, and resistance to cancer therapy.

Cell dedifferentiation: The process by which cells grow reversely from a partially or terminally differentiated stage to a less differentiated stage within their own lineage.

Cytotoxic T-lymphocyte antigen 4 (CTLA4): A protein receptor that downregulates immune responses. It functions as an immune checkpoint for T cells and helps prevent them from killing other cells, particularly cancer cells when it is bound to another protein called B7.

Humoral response: A type of immune response, in which Target cells are eliminated indirectly via the production of antibodies by B cells.

Immune checkpoint: A particular type of protein produced by some types of immune cells, including cytotoxic T lymphocytes and some tumour cells. Their role is to prevent immune responses from being so strong.

Immune checkpoint inhibitors (ICIs): A class of drugs that block different checkpoint proteins and boost the immune system to fight cancer. Examples of checkpoint inhibitors include the anti-PD-L1 or anti-PD-1 drugs (which block the binding of PD-L1 to PD-1) and the anti-CTLA-4 drugs (which block the binding of CTLA-4 to B7-1/B7-2).

Major histocompatibility complex (MHC): A set of genes that code for proteins found on the surfaces of cells that help the immune system recognize foreign substances. The MHC molecules play an important role in the development of both humoral and cellular immunity, it enables T lymphocytes to identify antigen-presenting cells.

Melanoma: A skin cancer that starts in melanocytes (cells that make melanin) and can spread to other organs in the body. Unlike other skin cancers, melanoma is the most malignant.

MIT transcription factors: Are master regulators of cellular adaptation to a wide variety of stressful conditions.

Natural killer cell (NK cell): A lymphocyte cell type. NK cells are classified as part of a heterogenous group called innate lymphoid cells, which respond quickly to a wide variety of pathogens and tumours.

Programmed cell death 1(PD-1): An immune checkpoint, expressed on the surface of T and B cells. When PD-1 is bound to another protein called PD-L1, it helps keep T cells from killing other cells, including cancer cells.

Phenotype: The set of observable characteristics of an individual, resulting from the interaction of its genotype with the environment; observable characteristics are not necessarily visibly observed but may be internal traits, e.g., related to some epigenetic, reversible, modification by a graft of a chemical radical (methyl, acetyl...) on some base of the DNA before transcription or on some amino acid in a histone protein, such traits being possibly evidenced after some dynamic stimulation only.

T Lymphocyte cell (CTL): A type of leukocyte (white blood cell) that determines the specificity of the immune response to antigens. It derives from hematopoietic stem cells in the bone marrow and matures in the thymus. T cells are one of the most important components of the immune system in the fight against cancer.

Tumour microenvironment: A set of cellular and molecular components that surround, feed and interact with tumour cells. The tumour microenvironment includes normal cells, immune cells, molecules, blood vessels, fibroblasts and the extracellular matrix.

Targeted therapy: A type of drug that targets specific genes and proteins which help cancer cells survive and grow.

Yamanaka genes: A set of four genes that can reprogram the cells in our body and are essentially used to regenerate old cells or grow new organs.

Contents

Acknowledgements iii

Glossary of biological terms iv

1 General introduction 3
- 1.1 Motivations . . . 3
- 1.2 Biological context . . . 6
  - 1.2.1 Tumour development . . . 6
  - 1.2.2 Cancer immunology . . . 7
  - 1.2.3 Tumour immune escape mechanisms . . . 10
  - 1.2.4 Immunotherapy . . . 10

2 Mathematical modelling of tumour-immune response dynamics 14
- 2.1 Review of modelling strategies . . . 14
  - 2.1.1 Mathematical modelling of tumour-immune dynamics . . . 14
- 2.2 Contributions of the thesis . . . 20

3 Dynamics of tumour growth and of the immune response 22
- 3.1 Biological motivations . . . 22
- 3.2 Model formulation . . . 23
- 3.3 Qualitative analysis of the model . . . 25
  - 3.3.1 Steady state analysis . . . 26
  - 3.3.2 Local stability analysis . . . 26
  - 3.3.3 Global stability of interior equilibrium $E^\star$ . . . 32
- 3.4 Hopf bifurcation analysis . . . 33
- 3.5 Numerical simulations . . . 35
- 3.6 Discussion and conclusions . . . 37

4 A phenotype structured model for the tumour-immune response 39
- 4.1 Biological background . . . 39
- 4.2 The model . . . 41
  - 4.2.1 The cell populations . . . 41
  - 4.2.2 Biological motivations . . . 42

4.2.3 Modelling choices for the mathematical functions of phenotypes . . . 43
4.2.4 Goals of the present study . . . 47
4.3 Asymptotic analysis . . . 48
4.3.1 Asymptotics in the absence of treatment . . . 48
4.4 Numerical simulations . . . 57
4.4.1 Simulations in the absence of treatment . . . 57
4.4.2 Numerical simulations with constant drug doses . . . 70
4.5 Discussion, conclusions and research perspectives . . . 75
4.5.1 Summary of the mathematical results . . . 75
4.5.2 Biological interpretations. . . . 77
4.5.3 Possible generalisations. . . . 78

5 Conclusion and research perspectives **80**
5.1 Discussions and conclusions . . . 80
5.2 Research perspectives . . . 82

A Appendix **85**
A.1 Proof of lemma 3.3.1 . . . 85
A.2 Proof of theorems 3.3.5-3.3.7 . . . 87
A.3 Proof of theorem 3.3.8 . . . 92
A.4 Proof of theorem 3.4.1 . . . 95

Bibliography **99**

Chapter 1

General introduction

1.1 Motivations

With an incidence of 58.000 new cases per year, cancer is the second leading cause of death in Algeria (International Agency for Research in Cancer, 2020) [1]. Cancer differs from other diseases by its ability to hijack normal cell functions, initiate uncontrolled cell proliferation, and to adapt to environmental stresses such as the aggressive environment produced by a host body's immune response or by any anti-cancer treatment ([17], [72]). There are three standard types of cancer treatment which have been used for centuries to target tumour cells more broadly, depending on their type, progression level, and many other factors. (i) Surgery: the first treatment option used when the size and location of the tumour are optimal. (ii) Radiotherapy treatments, which use high doses of radiation to destroy the tumour cells. (iii) Chemotherapy uses chemotherapeutic agents, which inhibit cell division (i.e., mitosis) or induce DNA damage. However, the side effects of these treatments can be significant, including nausea, hair loss, infertility, and psychological problems and the most severe effect is the toxicity to healthy tissue. Nowadays, several novel strategies for cancer treatment, which target specific cells within the tumour microenvironment are emerging, involving hormone therapy, angiogenesis inhibitors, and immunotherapy. They are less harmful (not completely harmless, though) to human tissue than traditional treatments. Despite significant advancements in technology and research in oncology, cancer is still broadly prevalent in our country.

[1] Cancer in Algeria, https://www.iarc.who.int

A striking finding of studies conducted in recent years is that the immune system plays a primary role, providing early tumour control [67]. In fact, tumour cells are characterized by a variety of genetic and epigenetic processes leading to the appearance of specific antigens on their surface which allow them to be detected not only by the immune system cells but also to trigger a specific anti-tumoral immune response ([25], [71]). Briefly, in an adaptive anti-tumour immune response, tumour-expressed neoantigens are captured by antigen-presenting cells (APCs) such as dendritic cells (DCs), which activate naïve T cells in the lymphoid organs, resulting in the activation of effector T cells responses against the cancer-specific antigens. The activated and proliferating effector T cells then migrate to the tumour microenvironment, where they function not only as an extrinsic tumour suppressor but also as tumour immunogenicity inhibitors. This process refers to the cancer-immunity cycle [16]. In summary, the tumour-immune cell interactions result in three distinct and asymptotic states encompassed in the concept of cancer immunoediting and are called: **(i) elimination, (ii) equilibrium, and (iii) escape** ([71], [23]). However, loss of antigen presentation is a frequent and important mechanism used by tumour cells, and, more particularly, the malignant ones to escape immune recognition and destruction. Furthermore, tumour cells secrete immunosuppressive factors and express inhibitory costimulatory molecules to directly inhibit effector immune system cells and mainly T-lymphocyte cells' activation through various different mechanisms ([7], [10]). Tumours also express proteins such as PD-L1 which can bind to PD-1 receptors on activated T cells, thereby inhibiting their cytotoxic activity [37].

By boosting the immune system's intrinsic ability to kill tumour cells, 2018 Nobel Prize in Physiology laureates James P. Allison and Tasuku Honjo revolutionised cancer treatment, leading to an increased number of options and better results for patients, including many with metastatic disease [47]. This new therapeutic method consists of targeting immune checkpoint inhibitors such as PD-L1, which inhibit the immune response against tumours. Immune checkpoint inhibitor therapy has been particularly successful in the treatment of melanoma, for which anti-PD-1 (nivolumab and pembrolizumab) and anti-CTLA-4 (ipilimumab) are currently approved [68]. However, not all cancers appear to respond to these immunomodulatory treatments as well as melanoma (for which, nevertheless, the rate of cures does not exceed 20%), and the causes of this failure are still not fully understood to date. This could be due to the highly complex nature of the interactions between tumour cells and immune system cells, involving various molecules, proteins, receptors, and cells that

either inhibit or foster the immune response against cancer. In this context, understanding the key mechanisms, or hallmarks, that enable the tumour to evade immune destruction, as well as the various biological phenomena underlying tumour-immune system interactions, is a major challenge for cancer immunotherapy, particularly immune checkpoint inhibitor immunotherapy. In this framework, mathematical models could help describe these complex biological phenomena and provide a comprehensive review of the different outcomes of tumour-immune response interactions.

Gathering knowledge from different scientific fields, in this thesis, we propose two mathematical models to describe tumour-immune response interactions. We found it illuminating for our subject to report biological concepts about cell population heterogeneity and different aspects of evolution in general that are still widely ignored in the community of cancer immunology, with the ultimate aim of proposing new theoretical therapeutic strategies for immunotherapy with immune checkpoint inhibitors. Mathematical models represent a simplification of reality and, as a result, they do not allow for fully absolute conclusions on the underlying biological dynamics of the studied phenomenon. However, their analysis allows us to assess the value of the involved biological parameters as well as the accuracy of the hypothesis. This thesis has been motivated by questions from cancer immunology and the recent clinical results of immunotherapy with immune checkpoint inhibitors, particularly in the treatment of melanoma. The concept of immune dysfunction, in conjunction with the tumour progression and its various links to the selection of malignant cancers, is what motivates us in this thesis in particular. Among the mathematical questions at stake we will in particular deal with the mathematical analysis of an ordinary differential equations model from population dynamics (Chapter 3) as a particular case of an integro-differential equations model, where the heterogeneity of the cell populations is taken into account by structuring variables that are continuous internal traits, resulting in a model for which the asymptotic analysis, as well as the selection dynamics, are the object of study (Chapter 4), with the ultimate aim of proposing theoretical therapeutic strategies with immune checkpoint inhibitor immunotherapies.

We began this thesis by describing the biological framework leading to the development of the models under study.

1.2 Biological context

As already mentioned, the interaction of tumour cells with immune system cells is a highly complex system involving many different cell types and molecules. Therefore, some of the concepts described in the following sections may be simplifications of the actual mechanisms underlying immune responses to tumours. These simplifications are directly related to the assumptions that led to the development of mathematical models.

The first part briefly describes the general mechanisms involved in the tumour development process. In the second part, we present an overview of the cancer-immunity cycle. More precisely, we describe some of the key biological and immunological mechanisms involved in the recognition of tumour cells, such as the expression of tumour antigens (APCs), as well as those implicated in the activation of the anti-tumour immune response. In the third part, we present some of the characteristics of tumour cells that allow them to evade the immune response. Finally, we will conclude the section by considering several immunotherapy strategies that have been developed recently, focusing on the current understanding of how to reverse T-cell exhaustion through immune therapies such as checkpoint blockade.

1.2.1 Tumour development

Typically, normal cells grow and divide, but have many mechanisms that regulate their growth. They grow only when stimulated by growth factors. When cells are damaged, a molecular brake acts, stopping cell division until they are repaired. If their repair is not possible, they commit programmed cell death (apoptosis). Moreover, they can only divide a limited number of times (the so-called Hayflick limit) and as part of their tissue structure, they remain where they belong. All cells have processes of regulation within them that prevent cell growth and division, the formation of a cancerous tumour, its growth, and its invasion of distant tissues. These processes are orchestrated by proteins known as tumour suppressor genes. Cancer cells, however, have the ability to grow without these growth factors. In fact, cancer cell transformation is caused by the accumulation of mutations in cells, which leads to the deregulation of a relatively restricted number of key pathways, enough for tumour formation and progression [24]. In particular, a tumour suppressor gene (there are many of them) is inactivated by those mutations, the protein it encodes is not produced or becomes non-functional, and as a result, uncontrolled cell division may occur.

As hypothesized by Hanahan and Weinberg [36], all cancers share six common hallmarks that govern the transformation of normal cells into cancer cells: (i) self-sufficiency in growth signals; (ii) insensitivity to growth-inhibitory signals; (iii) evasion of programmed cell death; (iv)limitless replication potential;(v) sustained angiogenesis; and (vi) tissue invasion and metastasis. In 2011, four new hallmarks were added by Weinberg and Hanahan [35]:(i) abnormal metabolic pathways; (ii) inflammation; (iii) genome instability; and (iv) evading the immune system.

Briefly, a tumour is defined as an abnormal growth of body tissue. It occurs when cells divide and grow excessively in the body. Cause or consequence, loss of control on proliferation is always accompanied by loss of control on differentiations [8]. Tumours are classified into several different categories based on their location, origin of tumour cells, and ability to metastasize. The most prevalent classification is based on invasiveness. (i) Benign or non-cancerous tumours, which are rarely life-threatening, don't typically affect nearby tissue nor spread to other parts of the body. (ii) Malignant or cancerous tumours are more dangerous and can spread into nearby tissue, glands, and other parts of the body [12]. Furthermore, tumour cells have been shown to hijack normal cell functions, initiate uncontrolled cell proliferation, to adapt to extracellular insults or environmental stresses.

In this thesis, we have limited ourselves to describe the phenomenon of uncontrolled proliferation, taking into account the cellular plasticity of tumours linked to the dedifferentiation phenotype. Loss of differentiation is associated with increased tumour cell invasiveness and drug resistance, and a particular interest in this thesis is the connection between tumour cell loss of differentiation and immune evasion.

1.2.2 Cancer immunology

The immune system is the body's defence system that consists of cells, tissue, and organs, which all together protect the body from any foreign attack. The primary role of the immune system cells is to recognise pathogens that invade the human body and eliminate them from the organism. Despite the diversity and heterogeneity of cancers, it has been shown that the immune system can control their progression. The concept that the immune system can recognise and destroy early tumours in the absence of treatments was originally embodied

in the cancer immunosurveillance hypothesis of Burnet and Thomas ([9], [77]). However, the hypothesis could not be experimentally tested because too little was known at the time about the detailed mechanisms underlying the process. Immunosurveillance theory suggests that the immune system is able to detect and eliminate the so-called neoantigens (antigens that are different from those of the body), and the validity of this theory has been established recently with a series of experiments [69]. There are two main parts of the immune system, namely, innate (non-specific) immunity and adaptive (specific) immunity. Both of them have their own unique strategies and abilities to protect the human body and interact with one another to detect and eliminate pathogens, including tumours.

Innate immune response and cancer The innate immune response is the body's first line of defence against pathogens. It recruits specific immune cells at the infected site, initiates an inflammatory environment to remove the foreign substances, and activates the adaptive immune response [14]. Innate immune cells also interact with tumour cells and try to eliminate them from the organism. They are recruited either directly at the tumour site, as lots of them are patrolling everywhere in the organism, or from distant lymphoid organs stimulated by cytokines such as interleukins. More particularly, natural killer (NK) cells, as part of the innate immune cells of lymphoid origin, are responsible for killing cancer cells that lack the expression of major histocompatibility complex (MHC) molecules without requiring activation by other immune cells [44]. Briefly, NK cells are capable of secreting type-1 cytokines, inducing the apoptosis of tumour cells. However, experimental advances have revealed that tumour cells can alter the extracellular environment by producing immunosuppressive cytokines, such as TGFβ, which significantly reduce NK-cell functionality and infiltration. Moreover, recent findings in [64] report that PD-1 signalling might enhance the exhaustion of NK cells and downregulate the innate responses against tumours.

Adaptive (specific) immune response and cancer The adaptive immune response is the body's second line of defence, which is highly specific to each particular pathogen. The adaptive immune system requires more time to produce an effective response but offers long-term protection. In the context of tumours, T cells are the most important adaptive immune cell types. The activation of the adaptive immune response requires the expression of antigens (APCs) on the surface of tumour cells and their presentation on the surface of

APCs by MHC molecules. When APCs process antigens, they migrate to lymph nodes to present them to the naive T lymphocytes. The naive T cells are a type of T lymphocyte that has matured and been released by the thymus but has not yet encountered its corresponding antigen. These cells are endowed with specific receptors, the so-called T cell receptor (TCR) on their membrane surfaces, which allow them to recognise specific antigens and initiate an antigen-specific immune response. Martínez-Lostao and colleagues [56], state that the activation process depends on co-stimulatory such as CD28 and co-inhibitory (e.g., CTLA-4, PD-1) proteins. Depending on complementary proteins and the antigen-MHC complex, subsequently, naive T lymphocytes can differentiate into different groups. The following are the most critical T-cell subsets involved in the anti-tumour immune response include: (i) the helper CD4+ T lymphocytes, which stimulate the activation of APCs and CD8+ T cells by releasing cytokines, such as interleukin 2 (IL-2), and expressing a variety of co-stimulatory proteins on their surface; (ii) the cytotoxic CD8+ T lymphocytes are able to directly eliminate tumour cells;(iii) the regulatory T lymphocytes modulate the other immune system cells and prevent them from attacking healthy tissue [73]. Activated T cells then proliferate and migrate to the tumour site through blood vessels, where they bind to and induce tumour cell apoptosis. This process, which is referred to as the "tumour-immunity cycle", continues until either the tumour has been removed or the tumour adapts to and evades, targeted by the T cells. This cycle is subject to various obstacles, and tumour cells can adapt to evade the immune response through a process known as immunoediting (see, Figure 1.1).

In this thesis, we focus on the interaction dynamics occurring between tumour cells and the immune system cells consisting of CD8+ T lymphocytes (for the adaptive response) and NK lymphocytes (for the innate response).

Immunoediting At the beginning of the 2000s, Robert Schreiber and colleagues proposed a new theory to describe the dynamic process wherein the immune system not only controls tumour progression but also shapes tumour immunogenicity. The term was introduced instead of the traditional "cancer immunosurveillance" to describe the three different stages of the anti-tumour immune response: elimination, equilibrium and escape referred to as "the three Es of cancer immunoediting".

- *Elimination:* This stage is initiated by inflammation in the tumour site, followed by recruiting innate and adaptive immune cells, and synthesis of pro-inflammatory and immunomodulatory, which facilitate the recognition and elimination of tumour cells. If, however, some tumour cells are able to evade immune destruction, they enter the equilibrium stage.
- *Equilibrium:* The longest stage of the cancer immunoediting process in which, the surviving cells from the elimination phase enter the equilibrium stage, in which the adaptive immune cells prevent tumour cell outgrowth and edit tumour cell immunogenicity. The resisting tumour cells from the elimination stage create clones with cumulative numbers of mutations and enter the escape stage.
- *Escape:* During the escape stage, the immune cells lose control of the tumour cells. These later, continue to grow and expand in an uncontrolled manner and may eventually lead to metastases.

1.2.3 Tumour immune escape mechanisms

As previously mentioned in Section 1.2.1, one of the hallmarks of cancer is the ability to avoid immune destruction. Tumour cells use various strategies to evade immune surveillance. These include: (i) down-regulation of the antigen presentation machinery and instigating an immunosuppressive tumour microenvironment [6], tumour cells alter their antigen presentation machinery and become invisible to the adaptive immune system cells; (ii) inducing T cell exhaustion and dysfunction [81], where cytotoxic T cells are characterized by an overexpression of multiple inhibitory receptors, including PD-1, CTLA-4.

1.2.4 Immunotherapy

Belonging to the general class of so-called "targeted therapies", immunotherapy is becoming a very promising approach in cancer treatment. Immunotherapy is, as most targeted therapies, that act on specific intracellular or extracellular pathways without killing cells, a class of anti-cancer treatments aiming to be less toxic than the traditional anti-cancer therapies, chemotherapy and radiation therapy, that either enhance (or boost) the anti-tumour immune response or reverse (or block) the tumour's immunosuppressive effects. Immunotherapy aims

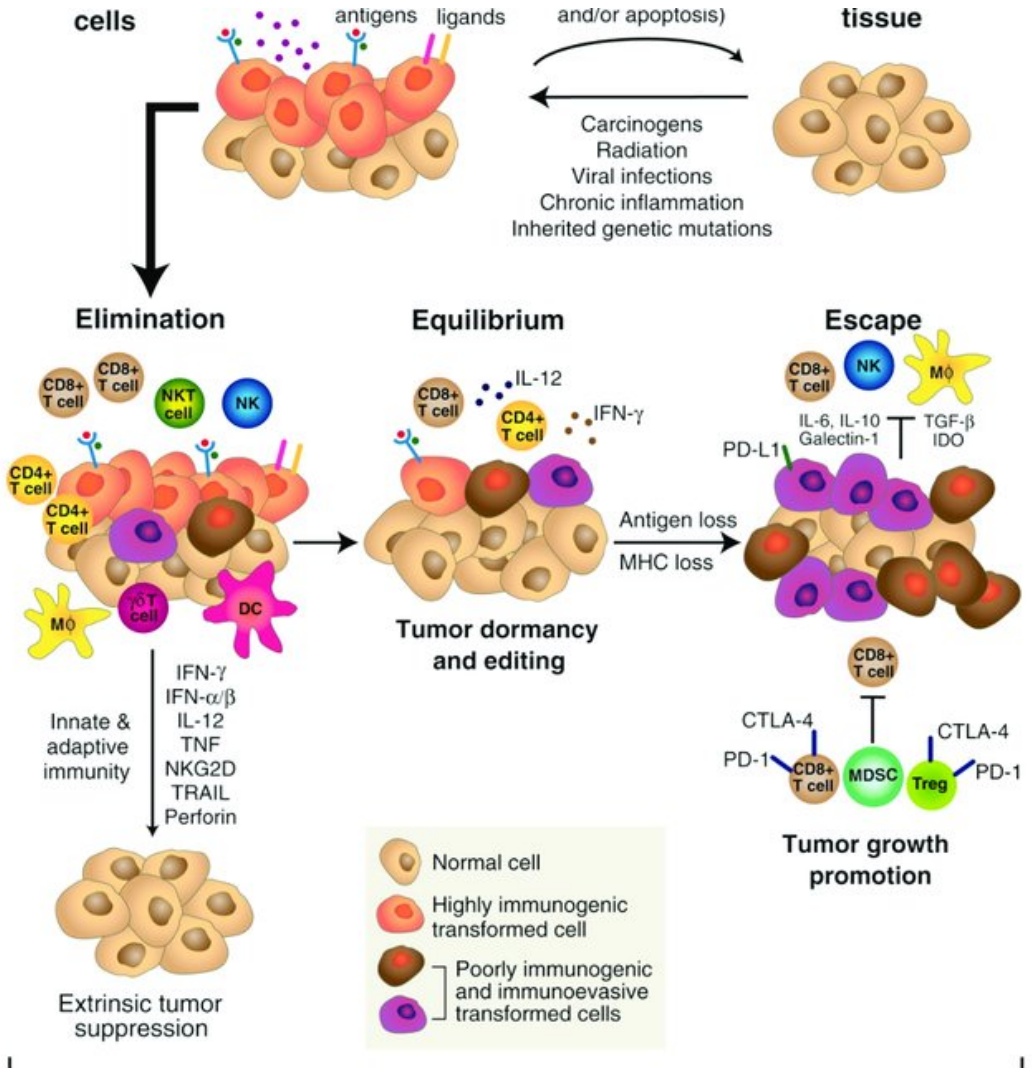

Figure 1.1: **The cancer immunoediting process after R. D. Schreiber, Science 2011 [71]. It proceeds according to three possible situations termed elimination, equilibrium and escape. In the present mathematical framework of the model studied in Chapter 4, we classify the different outcomes of the tumour-immune interactions according to the levels of the tumour population density values (as compared to the theoretical and numerical values of the tumour carrying capacity), themselves dependent on the parameters of the activation term by the APCs towards T-cells in lymphoid organs (specificity of the immune response) or by humoral messages sent by patrolling NK-cells to resident NK-cells in lymphoid organs or tissues to favour their proliferation (innate, non-specific immune response).**

at inducing loss of the dedifferentiation capacity of tumour cells [51], which may be seen as an expression of their malignancy.

- **Immunotherapy using monoclonal antibodies** The main monoclonal antibodies used in immunotherapy are immune checkpoint inhibitors. Monoclonal antibodies are antibodies created in the lab and are designed to bind to specific proteins expressed on the surface of tumour cells. The aim of therapies based on these specific antibodies is to block the immune checkpoints. As already mentioned in the motivations part, the immune checkpoint proteins, cytotoxic T lymphocyte-associated 4 (CTLA-4), and programmed cell death protein 1 (PD-1), are receptors expressed on the surface of cytotoxic T-cells that respectively bind to their ligands PD-1 and B7 receptors, leading to the suppression of the anti-tumour immune response. In particular, CTLs that are in contact with tumour cells expressing PD-L1 ligands are inhibited and become exhausted. Therefore, anti-PD1/anti-PDL1 treatments (such as nivolumab, pembrolizumab, and lambrolizumab) that block PD-1 and PD-L1 interactions are able to restore the effector activity of exhausted CTLs. Similarly, the anti-CTLA-4, ipilimumab treatment inhibits the interactions between the checkpoint proteins CTLA-4 and B7 which restore T cell activation mechanisms in secondary lymph nodes. Both anti-PD1 and anti-CTLA-4 were proven clinically beneficial in terms of long-term survival in patients with advanced melanoma ([68], [80]) and later in patients with other types of cancers including non-small cell lung cancer, and renal cell carcinoma [39].
- **Adoptive cell transfer therapy** T cells are one of the essential components of the immune system in the fight against tumours. However, in many tumours, the number of tumour antigen-specific CTLs is extremely limited. Two novel immunotherapy strategies were recently introduced to address this problem: tumour-infiltrating lymphocytes (or TIL) therapy and modified cell transfer therapy. Tumour-infiltrating lymphocytes (TIL) therapy involves isolating tumour-infiltrating CTLs that are specific to tumour antigens from fresh patient biopsy specimens and cultivating them in the presence of particular cytokines (such as IL-2) to increase their growth. The cultivated cells are then backwards administered into the patient's body after the requisite number of CTLs has been reached. There are two benefits that tumour-infiltrating CTLs therapy offers that no other modality of cancer therapy does: it is more adaptive and personalised for each patient ([22], [40]). However, most of the time, it is difficult to isolate TIL from tumour tissue. Moreover, as reported in [33], targeting common antigens carries the risk of attacking healthy cells, which might result in severe side effects. Modified cell transfer therapy requires the genetic modification of

the patient's cytotoxic T cells to result in the effective recognition of specific tumour antigens. CAR-T cell therapy is one of the most well-known treatments based on modified cell transfer therapy. Chimeric antigen receptors (CARs) are designed receptor proteins that provide CTLs with the capacity to target a specific antigen. Their clinical uses have demonstrated significant advancements in several types of cancers, including melanoma [61]. However, there are still safety concerns, which were recently highlighted, regarding the occurrence of subsequent autoimmune reactions [70].

- **Vaccination strategies** Are cell-based vaccines intended for use in cancer patients and can be generated from the patient's tumour cells, tumour-associated antigens, or dendritic cells. Examples of cancer vaccines include oncolytic virus therapy ([16], [40]).

A number of novel immunotherapies have been designed to either enhance/boost the immune response or reverse/block the immunosuppressive effects of the tumour. In the mathematical model developed in Chapter 4, we investigate how the effects of constant doses of anti-PD-1 treatment, may vary the success of the immune response against tumour cells.

Chapter 2

Mathematical modelling of tumour-immune response dynamics

2.1 Review of modelling strategies

In this chapter, we discuss the literature on mathematical models that have been developed to describe tumour-immune interactions. These models were selected from key papers in the history of mathematical modelling of tumour-immune interactions. Note that a detailed overview of the first models for this process can be found in Grace Mahlbacher and collaborators' paper *Mathematical modeling of tumor-immune cell interactions* [55]. In this article, the effect of different types of immune cells on tumour progression is discussed, with sections following offering an overview of tumour-immune interactions modelling approaches. The first part of this chapter discusses different mathematical modelling approaches used to describe tumour-immune interactions, which include ordinary differential equations models, and phenotype-structured models. The second part will be devoted to a summary of the contributions of the thesis.

2.1.1 Mathematical modelling of tumour-immune dynamics

As previously mentioned in Chapter 1, the development of tumours and the functioning of the immune system is an extremely complex process, as a consequence, the interactions

between tumour cells and immune cells are still not yet fully understood by either experimentalists or theoreticians. In recent decades, mathematical models for tumour-immune response dynamics have become increasingly popular and are used as a tool that helps researchers understand the interplay between tumour growth and the immune response, and the mechanisms of tumour escape. Incorporating the effect of various therapeutic strategies including immunotherapies into these models might also help biologists and clinicians to predict the different outcomes of cancer treatment protocols.

2.1.1.1 Mathematical modelling approaches

The anti-tumour immune response is increasingly recognised as crucial for mounting a prolonged and effective response to tumours. As the understanding of tumour-immune response interactions has advanced, experimental investigation has been complemented by mathematical modelling aimed at quantifying and predicting these interactions. Several modelling approaches have been used to describe the interactions between a tumour and the immune system cells, including deterministic continuum models in the form of ordinary differential equations (ODEs), intégro differential equations (IDEs), and partial differential equations (PDEs); stochastic discrete models; and hybrid models, i.e., the combination of both. The deterministic continuum models allow for a more efficient representation of the tissue-scale level, whereas, the discrete models are well-suited for representing individual cells (the reason why they are also known as individual-based or agent-based models, as well as cellular automata models) and their interactions at the microscopic scale and over a short timescale. Finally, the hybrid models integrate both continuum and discrete models, which allow for a multiscale description of the system under study. In this third category of models, cells may be modelled as individuals, using a cellular automata description, in a spatial domain in which other substances are described as a continuum of variables. The choice of the modelling approach depends on the biological phenomena considered, the physical representation of the system (discrete or continuous), the spatial and temporal scales, and the type of information the mathematician had on the phenomena. Note that, the first models developed to describe tumour-immune interactions were two-species nonspatial models formulated by means of ordinary differential equations (ODEs). In this thesis, we will develop deterministic continuum models to describe the tumour-immune response dynamics. Therefore, we will discuss some of the key models from the literature that motivated our modelling choices.

2.1.1.2 Deterministic nonspatial models

Ordinary differential equations models (ODEs) are commonly used to represent systems with only time as the independent variable. In the tumour-immune setting, most of the ODE's models view tumour-immune (in particular, CTLs) interactions as prey-predator systems, where immune cells are the predator population, while tumour cells are considered as the prey population. This modelling approach allows us to characterize both local and global stability of steady states and also identify model parameters which have an important issue on tumour evolution. The Kuznetsov model is the classical representation of this approach [46]:

$$\begin{cases} \dfrac{dE}{dt} = S + \dfrac{pET}{g+T} - mET - dE, \quad E \equiv E(t) : \text{CTLs} \\ \dfrac{dT}{dt} = aT\,(1 - bT) - nET, \quad T \equiv T(t) : \text{tumour cells} \end{cases} \tag{2.1}$$

where E represents the population of effector T-cells that enter the system with constant influx S, are recruited at rate $\frac{pET}{g+T}$, and are killed or inhibited at a rate proportional to the density of tumour cells, with a constant of proportionality m, and die at rate d due to natural death. While Tumour cells grow at a logistic rate $aT\,(1 - bT)$ with carrying capacity $\frac{1}{b}$, and are killed at a rate proportional to the density of CTLs, with a constant of proportionality n. This model is used to describe the growth and regression kinetics of the B lymphoma BCL1 in the mouse spleen. The model exhibits a number of phenomena that are observed in vivo, including immunostimulation of tumour development, "sneaking through" of the tumour, and formation of a tumour "dormant state", a mechanism for which a small tumour continues to exist but is maintained at a restricted size by the immune system. This model is the basis for numerous extensions and generalizations, examples include ([11], [74], [30], [29]).

To explore the role of helper T cells, in addition to cytotoxic T cells, Kirschner and Panetta [45] proposed a system of three ODEs for the cytokine IL-2 produced by the helper T cells, cytotoxic T cells and tumour cells. The interactions between the populations of cells and

the IL-2 cytokines are modelled as follows:

$$\begin{cases} \dfrac{dE}{dt} = cT - \mu_2 E + \dfrac{p_1 EI}{g_1 + I} + s_1, \quad E \equiv E(t) : \text{CTLs} \\ \dfrac{dT}{dt} = r_2(T)T - \dfrac{aET}{g_2 + T}, \quad T \equiv T(t) : \text{tumour cells}, \\ \dfrac{dI}{dt} = \dfrac{p_2 ET}{g_3 + T} - \mu_2 I + s_2, \quad I \equiv I(t) : \text{ the concentration of IL-2}. \end{cases} \tag{2.2}$$

For the population of cytotoxic T cells E, c stands for the tumour's antigenicity, s_1 represents an external source for E, while, $\frac{1}{\mu_2}$ models their natural lifespan. Tumour growth is modelled by a logistic function $r_2(T)$, and a represents the immune response strength. The results obtained shed light on the impact of tumour antigenicity on tumour progression. The authors also identified stable periodic solutions, reflecting clinical observations of tumour suppression and regrowth. A detailed review of this model can be found at [27]. On the other hand, Byrne and colleagues incorporated interactions of tumour cells with both helper and cytotoxic T cells taking into account immunosuppressive effects. Their aim was to investigate how the anti-tumour immune response varies with the level of infiltrating helper and cytotoxic T cells. The model exhibits the three E's of cancer immunoediting [26]. Other several ODEs models have been proposed, consisting of many cell types (e.g. innate and adaptive immune cells) and molecules (e.g. cytokines), see and the references [27] therein.

2.1.1.3 Phenotype-structured models

The heterogeneity of populations is one of the fundamental difficulties in population biology. In fact, individuals do not all respond to their environment with exactly the same laws. In order to take into account this fact, the phenotype is thus a natural structuring variable (always denoted by x below) to study the evolutionary dynamics in a certain population. Individuals' size and age are two classical examples of structuring parameters. These evolve during an individual's life and are not addressed in this thesis.

In what follows, we present the formulation of a prototypal mathematical model of one population (coming from adaptive dynamics) from which we can derive models that include

precise effects:

$$\begin{cases} \frac{\partial n}{\partial t}(t,x) = R\left(x,\rho(t)\right) n(t,x), \quad x \in [0,1], \quad t > 0, \\ n(0,x) = n^0(x), \\ \rho(t) = \int_0^1 n(t,x)dx. \end{cases} \tag{2.3}$$

Roughly $n(t,x)$ denotes the density of individuals at time t with phenotype x, and the function $R(\cdot,\cdot)$ so-called fitness function represents the growth (and death) rates, which depends generally on the total density of the population due to competition for nutrients and space. This is the meaning of the notation $[n(t,\cdot)]$. We have decided to state the problem in $[0,1]$ for later purposes but it would be also possible to extend the study in $\mathbb{R}^m$.

The most typical example for R is

$$R(x,\rho(t)) = r(x) - d(x)\rho(t),$$

here the individuals have different selection and death rates $r(x)$ and $d(x)$ depending on the phenotype x. This model stems from the classical logistic ODE

$$\begin{cases} \frac{dN(t)}{dt} = \left(r - dN(t)\right) N(t), \quad t > 0, \\ N(0) = N_0 \geq 0, \end{cases} \tag{2.4}$$

where r is the net growth rate, the so-called reaction rate (proliferation-death), and dN is the logistic death rate (increasing in N: intraspecific competition). Regarding the asymptotic behaviour of the simple integro-differential model (2.3), a very well-known result due to Jabin et al [38] ensuring convergence and concentration:

Theorem 2.1.1. *([21], [38])*

i) *ρ converges to $\rho^\star$, the smallest value ρ such that $r(x) - d(x)\rho \leq 0$ on $[0,1]$* $\left(i.e., \rho^\star = \max_{[0,1]} \frac{r(x)}{d(x)} \right)$.

ii) *The population $n(t,\cdot)$ viewed as a Radon measure supported on $[0,1]$ concentrates on the phenotype set $\{x \in [0,1], r(x) - d(x)\rho^\star = 0\}$.*

iii) *Furthermore, if this set is reduced to a singleton x^∞, then $n(t,\cdot) \rightharpoonup \rho^\star \delta_{x^\star}$ as $t \to +\infty$ in $\mathcal{M}^1([0,1])$.*

Here $\mathcal{M}^1([0,1])$ denotes the set of Radon measures supported in $[0,1]$.

A general discussion on this model as well as an existence proof can be found in [21]. The proof of theorem 2.1.1 can be found in [65], it consists of proving that ρ is a bounded variation (BV) function on $[0,+\infty)$. We mentioned that it is also possible to prove both convergence and concentration by using an appropriate Lyapunov functional designed by Pierre-Emmanuel Jabin and Gaël Raoul in [38]. Starting from this simple model, further models were developed to incorporate various biological and ecological effects based on the emergence of the fittest trait in a structured population (see [63] and the references therein).

Biological evidence suggests that phenotypic heterogeneity in the cancer cell population is a major challenge in oncology. In fact, for a given tumour microenvironment (e.g., nutrients, growth factors, drug exposure), several experiments have shown that the fittest cells are selected. For example, some subpopulations of cancer cells may be more resistant to certain therapies than others. Another effect of the emergence of the fittest trait in a cancer cell population is the potential for increased aggressiveness. Cancer cells that are more aggressive are able to migrate and spread to other parts of the body more effectively, making it more difficult to treat cancer. Several other effects have been studied based on the emergence of the fittest trait in a structured population. In this context, phenotype-structured models, which are usually stated in terms of non-local partial differential equations or integro-differential ones have been widely used to describe phenotype heterogeneity in tumour cell populations. In these models, the phenotypic state is represented by a continuous real variable x, modelling different biological characteristics such as viability and fecundity, see ([3], [4], [52], [65]) and the references therein. Such models, which can be derived from stochastic individual-based models [13], are known to possibly lead to the concentration of populations on one or several phenotypes. In ([3], [65]), the biological motivation to use these types of models stems from drug resistance in cancer. For instance, in [65], the authors proposed an integro-differential system for the time evolution of densities of cancer and healthy cells, structured by a continuous phenotypic variable (which is related to the expression level of a particular gene that controls the cellular level of cytotoxic-drug resistance), representing their level of resistance to chemotherapy to which they are exposed. The long-time asymptotic behaviour of the solutions to the model equation has been studied in the presence of constant drug doses. Moreover, an optimal control problem consisting of minimizing the number of cancer cells at the end of a given therapeutic window was also studied by means of optimal control

methods. This model is further developed in [60] to incorporate epimutations, namely the heritable changes in DNA expression, which are frequent in tumour development.

Under the action of immune cells (the adaptive immune cells CTLs or the innate ones NK cells) which are part of the tumour microenvironment, the more malignant tumour cells are selected. In order to take into account this fact, it is relevant to take into account the heterogeneity of the cell populations by structuring them by internal traits modelling different biological characteristics of populations. To the best of our knowledge, the first phenotype-structured model for tumour-immune interactions was proposed by Delitala and Lorenzi [20], where a tumour cell population characterised by heterogeneous antigenic expressions is exposed to the action of antigen-presenting cells and immune T-cells. More precisely, their model incorporates five populations of cells. All populations but one are assumed in [20] to be structured by a real continuous variable in $[0, 1]$ representing an internal phenotypic state of the cell. Their model reproduces well the selective recognition and learning processes in which immune cells are involved. In recent works, Louis Almeida and collaborators [2] have developed an individual-based model for the coevolutionary dynamics between cytotoxic T lymphocytes (CTLs) and tumour cells. In this model, each cell is viewed as an individual agent and is structured by a variable representing a parameterisation of the antigen expression profiles for tumour cells and a parameterisation of the target antigens of T-cell receptors (TCRs) for CTLs. The main findings support the idea that TCR tumour antigen binding affinity may be a good intervention target for immunotherapy and provide a theoretical foundation for the development of anti-cancer therapies.

2.2 Contributions of the thesis

As mentioned in the introduction, there may be a strong correlation between tumour progression and immune system dysfunction that has not yet been fully explained and may be responsible for both tumour escape and treatment failure, including immunotherapies with immune checkpoint inhibitors. In this context, mathematical models could help to understand the interactions between tumour growth and the immune response, as well as possible ways in which tumour cells may escape immune surveillance. This in turn may provide different frameworks to help immunologists and clinicians design new immunotherapy strategies that significantly improve the overall effectiveness of the anti-tumour immune response.

This thesis is organized into two main chapters. Each chapter is divided into four sections: the first summarises the relevant biological background to inform the reader on the empirical evidence motivating the model hypothesis; the second presents the mathematical framework; the third is dedicated to the presentation of the analytical and numerical results; and the final section discusses the model's results and research perspectives.

Chapter 3. Dynamics of tumour growth and of the immune response. Chapter 3 deals with the basic results of an ordinary differential equations model describing tumour-immune response interactions. This model is a simplified version of an integro-differential equations model developed in Chapter 4 further in order to explicitly include the phenotype heterogeneity of the cell populations. For the sake of simplicity, we will present the analytical results of the simplified model. We first discuss several results regarding the existence, uniqueness and positivity of the solutions. We then characterize the existence of the steady states. Moreover, we decompose parameter space into distinct regions according to the linear stability of the coexistence steady state, as well as identify regions of parameter space in which a Hopf bifurcation exist. Finally, we present numerical simulations which confirm the predicted stability of the steady-state solutions.

Chapter 4. A phenotype-structured model for the tumour-immune response. In Chapter 4, we develop a mathematical model for tumour-immune response interactions in the perspective of immunotherapy by immune checkpoint inhibitors (ICIs). The model is of the integrodifferential nonlocal Lotka-Volterra type, in which heterogeneity of the cell populations is taken into account by structuring variables that are continuous internal traits (aka phenotypes) representing a lumped "aggressiveness", i.e., for tumour cells, the ability to thrive in a viable state under attack by immune cells or drugs - which we propose to identify as a potential of de-differentiation, or malignancy -, and for immune cells, the ability to kill tumour cells, or anti-tumour efficacy. We analyse the asymptotic behaviour of the model in the absence of treatment. By means of two theorems, we characterise the limits of the integro-differential system under an a priori convergence hypothesis. We illustrate our results with numerical simulations, which show that our model exemplifies the three Es of immunoediting: elimination, equilibrium, and escape.

Chapter 3

Dynamics of tumour growth and of the immune response

3.1 Biological motivations

In this chapter, we analyze a simple mathematical model of tumour-immune response interactions between cell populations. The model differs from most others in the literature in that it is a simplified version of an integro-differential model, in which heterogeneity of the cell populations is taken into account by structuring variables that are continuous internal traits (aka *phenotypes*) representing a lumped "aggressiveness" proposed in [42]. The model analysed in [41] is written as follows

$$\begin{cases} \dfrac{\partial n}{\partial t}(t,x) = [R(x,\rho(t)) - \varphi(t)]n(t,x), \\ \dfrac{\partial \ell}{\partial t}(t,y) = p(t,y) - \nu(y)(1+\rho(t))\ell(t,y), \\ \dfrac{\partial p}{\partial t}(t,y) = \chi(t,y)p(t,y) - kp^2(t,y). \end{cases} \tag{3.1}$$

with the total densities at time t

$$\rho(t) = \int_0^1 n(t,x)dx, \quad \varphi(t,y) = \int_0^1 \psi(y)\ell(t,y)dy, \quad \chi(t,y) = \int_0^1 \omega(t,x)n(t,x)dx. \tag{3.2}$$

The fitness function R is given by:

$$R(x, \rho(t)) = r(x) - d(x)\rho(t).$$

For the tumour cell population of density $n(t, x)$, x represents the malignancy trait, meaning stemness (ability to de-differentiate) or fecundity trait (ability to proliferate), with two biological interpretations: $x = 0$ for lower malignancy, meaning lower de-differentiation capacity with higher proliferation capacity, and $x = 1$ for higher malignancy, meaning higher de-differentiation capacity with lower proliferation capacity. On the other hand, y represents the anti-cancer aggressiveness trait, such that: $y = 0$ when T-lymphocytes are weakly aggressive and less competent, while $y = 1$ when T-lymphocytes are highly aggressive and more competent. Each term of the system (3.1) modelize a different phenomenon describing what is physiologically known on the interaction between tumour cells $n(t, x)$ and T-lymphocytes, naive in lymphoid organs, $p(t, y)$ and effector, $\ell(t, y)$ in close contact with tumour cells. The study of this integro-differential model will be developed in Chapter 4. We specifically wish to explore here situations in which the interaction between cancer cells and immune T-cells leads to the concentration (Dirac-like) of populations on one or several phenotypes, or conversely if the distribution of phenotypes is uniform on $[0, 1]$. In either case of these simplifying assumptions, by integration with respect to the phenotypes, the system (3.1) can be reduced to a system of ODEs (below (3.3)), which admits stationary solutions. The stability analysis helps in understanding the role of the parameters of the model. We mention that we will give more details on the functions and their biological interpretation in the next chapter.

3.2 Model formulation

To describe tumour-immune interactions, we consider three different cell population densities: a cancer cell population $\rho(t)$ at time t, a cytotoxic T-lymphocyte population $\sigma(t)$ interacting with cancer cells ρ at the tumour site, and a population of naïve T-lymphocytes $\gamma(t)$ produced by distant lymphoid organs, source of the population of cytotoxic T-lymphocytes at the tumour site, informed at the lymphoid organ site by **APCs** (antigen-presenting cells, which are not represented here), see figure 3.1. This leads to the following time-dependent, ODE system

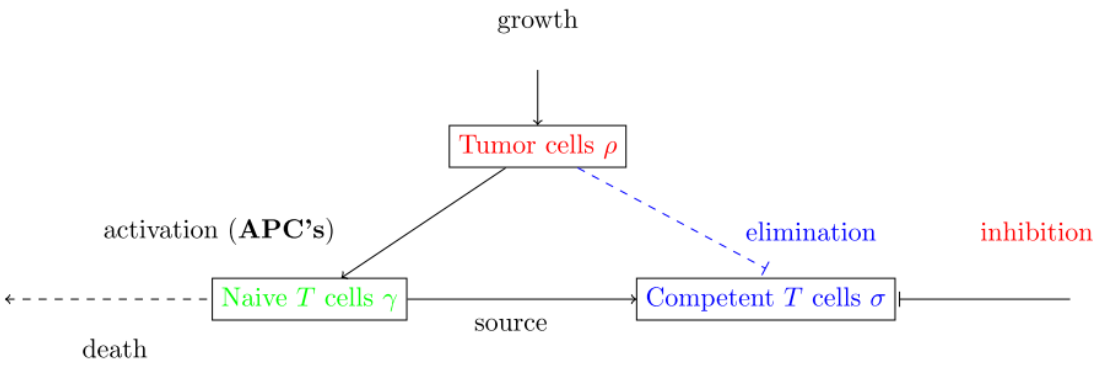

Figure 3.1: **Scheme of the tumor-immune cell interactions included in (3.3).**

$$\begin{cases} \dfrac{d\rho}{dt} = (r - d\rho)\rho - \sigma\rho, \\ \dfrac{d\sigma}{dt} = \gamma - \nu(1+\rho)\sigma, \\ \dfrac{d\gamma}{dt} = \gamma\rho - k\gamma^2, \end{cases} \tag{3.3}$$

where,

$$\sigma(t) = \int_0^1 \ell(t,y)dy, \quad \gamma(t) = \int_0^1 p(t,y)dy,$$

with positive initial conditions

$$\rho(0) = \rho_0, \quad \sigma(0) = \sigma_0, \quad \gamma(0) = \gamma_0. \tag{3.4}$$

In fact, as regards the equation for tumour cells, we expect at steady-state concentration of the density $n(t,x)$ on a single phenotype x, and distribution close to uniform for the populations $p(t,y)$ and $\ell(t,y)$; that is why we study the asymptotic of system (3.1) with ω constant in (x,y), so that without loss of generality $\chi(t,y) = \rho(t)$ at equilibrium, and we also take r and d constant in x. Similarly, we assume that functions ν and ψ of y are also constants, and we will take $\varphi = \sigma$ at the assumed steady state. We then integrate the equations respectively with respect to x and y, which leads to the above ODE model. We assume that in the absence of an immune response, the tumour undergoes a logistic growth, with a proliferation rate r and a natural death rate d. We assume further that, once an immune response has been stimulated, the tumour cells interact with cytotoxic T cells at a rate which is proportional to the product of both population densities. These

interactions lead to tumour cell death. We also assume that the evolution of both naive and cytotoxic T -cells is dominated by growth in response to the tumour cells and cell death. More specifically, naive T-cells which are produced by distant lymphoid organs are directly stimulated by tumour cells, and therefore a population of these naive T cells are represented as a source for cytotoxic T cells. We suppose that the tumour cells inhibit the cytotoxic T-cells at rate ν. We assume that the two T -cell populations die at rates ν and k. Of course, these assumptions clearly lack biological relevance. For instance, assuming that the function ψ is constant means that any cytotoxic T cell acts the same way on the tumour. However, this simplified version (3.3) sheds some light on the role of the parameters in the dynamics and may provide useful hints on the qualitative features of the original IDEs system (3.1). All parameters present in the model are non-negative and are described in the following table

Parameter	Description
r	tumor proliferation rate
d	death rate of tumour cells
ν	immunotolerance of T cells induced by tumor cells
k	carrying capacity of naive T cells

Table 3.1: **Summary of the biological parameters used in system** (3.3)**.**

In this simplified version of (3.1), we do not take into account the heterogeneity in cell populations.

3.3 Qualitative analysis of the model

In this section, we first identify and characterize the steady-state solutions. We then, linearize about the steady-state solutions to determine their local asymptotic stability. Finally, using a suitable Lyapunov function, we can show the global asymptotic stability.
We note that, from classical Cauchy-Lipschitz arguments ([43]), it is easy to check that system (3.3) admits a unique solution in $\mathbb{R}^3_+$ which remains bounded for all $t > 0$. Furthermore, we mention that, with positive initial conditions $(\rho_0, \sigma_0, \gamma_0)$, every solution (ρ, σ, γ) of the system (3.3) remains positive for all $t > 0$.

3.3.1 Steady state analysis

Setting the time derivatives to be zero in system (3.3) yields three steady states, which are

- The trivial equilibrium $E_0 = (0, 0, 0)$,
- The tumor equilibrium $E_1 = \left(\frac{r}{d}, 0, 0\right)$,
- The interior equilibrium that provides the coexistence between tumour and immune cells: $E^\star = (\rho^\star, \sigma^\star, \gamma^\star)$ that lies at the intersection of the following three surfaces

$$r - d\rho^\star = \sigma^\star, \tag{3.5}$$

$$\sigma^\star = \frac{\gamma^\star}{\nu\,(1+\rho^\star)}, \tag{3.6}$$

$$\gamma^\star = \frac{\rho^\star}{k}. \tag{3.7}$$

Substituting (3.7) and (3.6) into (3.5), we obtain the following quadratic equation

$$-d\rho^{\star 2} + \left(r - d - \frac{1}{\nu k}\right)\rho^\star + r = 0, \tag{3.8}$$

The equation (3.8) has one positive root $(\rho^\star, \sigma^\star, \gamma^\star)$ given by:

$$\begin{cases} \rho^\star = \frac{1}{2d}\left[r - d - \frac{1}{\nu k} + \sqrt{\left(r - d - \frac{1}{\nu k}\right)^2 + 4dr}\right], \\ \sigma^\star = \frac{1}{2}\left[r + d + \frac{1}{\nu k} - \sqrt{\left(r - d - \frac{1}{\nu k}\right)^2 + 4dr}\right], \\ \gamma^\star = \frac{1}{2dk}\left[r - d - \frac{1}{\nu k} + \sqrt{\left(r - d - \frac{1}{\nu k}\right)^2 + 4dr}\right]. \end{cases} \tag{3.9}$$

3.3.2 Local stability analysis

To determine the stability of both the trivial equilibrium and the tumour equilibrium, we define the Jacobian matrices at E_0 and E_1 respectively by

$$J(E_0) = \begin{pmatrix} r & 0 & 0 \\ 0 & -\nu & 1 \\ 0 & 0 & 0 \end{pmatrix} \quad \text{and} \quad J(E_1) = \begin{pmatrix} -r & 0 & 0 \\ 0 & -\nu(1+\frac{r}{d}) & 1 \\ 0 & 0 & \frac{r}{d} \end{pmatrix}.$$

Since $\lambda = r$ (resp. $\lambda = \frac{r}{d}$) is positive eigenvalue of $J(E_0)$ (resp. of $J(E_1)$), then both trivial equilibrium E_0 and the tumor equilibrium E_1 are unstable. We have the following theorem.

Theorem 3.3.1. *[41]*

- *The trivial equilibrium E_0 is unstable.*
- *The tumor equilibrium E_1 is unstable.*

For the equilibrium $E^\star$, the Jacobian matrix $J(E^\star)$ is given by

$$J(E^\star) = \begin{pmatrix} -d\rho^\star & -\rho^\star & 0 \\ -\nu\left(r - d\rho^\star\right) & -\nu\left(1 + \rho^\star\right) & 1 \\ \frac{\rho^\star}{k} & 0 & -\rho^\star \end{pmatrix}.$$

To compute the eigenvalues $\lambda_i \quad (i = 1, 2, 3)$ satisfying $\det(J^\star - \lambda Id) = 0$, one need to solve the following auxiliary equation

$$P(\lambda) = -\left[\lambda^3 + a_2\lambda^2 + a_1\lambda + a_0\right], \tag{3.10}$$

where, a_i for $i = 0, 1, 2$ are defined as follow

$$\begin{cases} a_2 = \nu + (d + \nu + 1)\,\rho^\star > 0, \\ a_1 = \left[\nu\,(1 + d - r) + (2d\nu + \nu + d)\,\rho^\star\right], \\ a_0 = \nu\rho^{\star 2}\sqrt{\left(r - d - \frac{1}{\nu k}\right)^2 + 4dr} > 0. \end{cases} \tag{3.11}$$

It is easy to see that the first term and the last one of (3.11) are positive. Then, from the Routh-Hurwitz criterion as in [19], the steady state $E^\star$ is locally asymptotically stable if $a_1a_2 - a_0 > 0$. We have,

$$\begin{aligned} a_1a_2 - a_0 &= [-\nu(r - d - 1) + (2d\nu + \nu + d)\rho^\star][\nu + (\nu + d + 1)\rho^\star]\rho^\star - \nu\rho^{\star 2}\sqrt{\left(r - d - \frac{1}{\nu k}\right)^2 + 4dr} \\ &= ([-\nu(r - d - 1) + (2d\nu + \nu + d)\rho^\star][\nu + (\nu + d + 1)\rho^\star] - [\nu(2d\rho^\star + d - r) + 1/k]\rho^\star)\,\rho^\star \\ &= \left(A\rho^{\star 2} + B\rho^\star + C\right)\rho^\star, \end{aligned}$$

with

$$\begin{cases} A = (\nu + d)\,(2d\nu + \nu + d + 1) > 0, \\ B = (\nu + d)\,\nu\,(1 + d - r) + \nu\,(2d\nu + \nu + d + 1) - \frac{1}{k}, \\ C = \nu^2\,(1 + d - r)\,. \end{cases} \tag{3.12}$$

Then, the inequality $a_1 a_2 - a_0 > 0$ is equivalent to

$$A\rho^{\star 2} + B\rho^{\star} + C > 0. \tag{3.13}$$

Thus, the solutions to the inequality (3.13) depend heavily on the sign of the discriminant Δ given by

$$\Delta = \left[(\nu + d)\,\nu\,(1 + d - r) + \nu\,(2d\nu + \nu + d + 1) - \frac{1}{k}\right]^2 - 4\nu^2 A\,(1 + d - r)\,. \tag{3.14}$$

In order to establish the local asymptotic stability results of the coexistence equilibrium $E^{\star}$, we define the critical thresholds of the parameters $\rho^{\star}$, r and k as follow,

$$\begin{cases} \rho_1 := \frac{-(\nu+d)\nu(1+d-r)-\nu(2d\nu+\nu+d+1)+\frac{1}{k}-\sqrt{\Delta}}{2A}, \\ \rho_2 := \frac{-\nu(\nu+d)(1+d-r)-\nu(2d\nu+\nu+d+1)+\frac{1}{k}+\sqrt{\Delta}}{2A}, \\ \rho_3 := \frac{-\nu[(2d\nu+\nu+d+1)]+\frac{1}{k}}{A}, \end{cases} \tag{3.15}$$

$$\begin{cases} r_0 := \frac{\nu(d+1)}{(1+\nu)}, \\ r_1 := \frac{\nu(d+1)(2A+\nu d)}{[A(1+2\nu)+\nu^2 d]}, \end{cases} \tag{3.16}$$

$r_1 < r_2 < d + 1$ is the unique positive solution of equation $F(r) = 0$, where

$$\begin{aligned} F(r) \;:=\; & \nu(\nu + d + 1)\sqrt{A}\left[\sqrt{-(r - d - 1)}\right]^3 + (d\nu^2 + (2\nu + 1)A)\left[\sqrt{-(r - d - 1)}\right]^2 \\ & + \nu(2\nu d + \nu + d)\sqrt{A}\sqrt{-(r - d - 1)} - A(d + 1). \end{aligned} \tag{3.17}$$

$$\begin{cases}
\frac{1}{k_1} &:= \frac{1}{k_3} - 2\nu\sqrt{A\,(1+d-r)}, \\
\frac{1}{k_2} &:= \frac{1}{k_3} + 2\nu\sqrt{A\,(1+d-r)}, \\
&:= \frac{1}{k_6} + 2\nu\sqrt{-A(r-d-1)} + \frac{A}{\nu\left(d+\frac{A}{\nu}\right)}\left(\frac{1}{k_3} - \nu(r-d)\right), \\
\frac{1}{k_3} &:= \nu\left[(\nu+d)\,(1+d-r) + (2d\nu+\nu+d+1)\right], \\
\frac{1}{k_4} &:= \frac{1}{k_3} + \frac{-A\left[\frac{1}{k_3}-(r-d)\nu\right]+A\sqrt{\left[\frac{1}{k_3}-(r-d)\nu\right]^2+4r\nu(d\nu+2A)}}{(d\nu+2A)}, \\
&:= \frac{1}{k_6} + \frac{\frac{A^2}{\nu^2}\left[\frac{1}{k_6}-\nu(r-d)\right]+\frac{A}{\nu}\sqrt{\left(d+\frac{A}{\nu}\right)^2\left[\frac{1}{k_6}-\nu(r-d)\right]^2+4rd^2\nu^2\left(d+2\frac{A}{\nu}\right)}}{d\left(d+2\frac{A}{\nu}\right)}, \\
\frac{1}{k_5} &:= \frac{1}{k_3} + \frac{-\left[\frac{A}{\nu}r-\frac{C}{\nu}\left(2\frac{A}{\nu}+d\right)\right]\left[\frac{1}{k_3}-(r-d)\nu\right]+\left[\frac{A}{\nu}r+d\frac{C}{\nu}\right]\sqrt{\left[\frac{1}{k_3}-(r-d)\nu\right]^2+4\nu^2\left(d+\frac{A}{\nu}\right)\left(r-\frac{C}{\nu}\right)}}{2\left(d+\frac{A}{\nu}\right)\left(r-\frac{C}{\nu}\right)}, \\
&:= \frac{1}{k_6} + \frac{(Ar+Cd)\left[\frac{1}{k_3}-\nu(r-d)\right]+(Ar+Cd)\sqrt{\left[\frac{1}{k_3}-\nu(r-d)\right]^2+4(d\nu+A)(r\nu-C)}}{2(d\nu+A)\left(r-\frac{C}{\nu}\right)}, \\
\frac{1}{k_6} &:= \frac{1}{k_3} + \frac{A\left[(\nu+d+1)(r-d-1)-(2d\nu+\nu+d)\right]}{\left(d+\frac{A}{\nu}\right)} \\
&:= \frac{(d\nu+\nu+d+1)(\nu+d)(r-d-1)+d\nu(2d\nu+\nu+d+1)+A}{\left(d+\frac{A}{\nu}\right)},
\end{cases} \tag{3.18}$$

We denote also

$$\begin{cases}
\alpha_0 := \nu^2\left[(\nu+d)\,(1+d-r) - (2d\nu+d+\nu+1)\right]^2, \\
\alpha_1 := \frac{1}{k_3}.
\end{cases} \tag{3.19}$$

According to the sign of C, we have the following three cases.

- Case 1: When $r < d+1$, the stability of the interior equilibrium $E^\star$ can therefore change according to the thresholds k_2, ρ_1 and ρ_2 described by (3.18) and (3.15). Thus, we have the following theorem.

  Theorem 3.3.2. *[41] Let $r < 1+d$. We have the following results.*

  - *If $k > k_2$, then the interior equilibrium $E^\star$ is locally asymptotically stable.*
  - *If $k = k_2$, then the interior equilibrium $E^\star$ is locally asymptotically stable for all $\rho^\star \neq \rho_1$.*
  - *If $k < k_2$, then the interior equilibrium $E^\star$ is locally asymptotically stable when either $0 < \rho^\star < \rho_1$ or $\rho^\star > \rho_2$, and unstable when $\rho_1 < \rho^\star < \rho_2$.*

Proof. The discriminant Δ given by (3.14) can be written as follows

$$\Delta = \frac{1}{k^2} - 2\alpha_1 \frac{1}{k} + \alpha_0,$$

where α_0 and α_1 are given by (3.19). Then, the equation $\Delta = 0$ has two distinct real roots k_i where k_i, $i = 1, 2$ are given by (3.18).
Hence, the stability of the interior equilibrium $E^\star$ can be deduced from the sign of Δ and B. This is summarized on the following table

k	$k \leq k_2$	$k_2 < k \leq k_3$	$k_3 < k < k_1$	$k \geq k_1$
Signs of Δ and B	$\Delta \geq 0$ and $B < 0$	$\Delta < 0$ and $B \leq 0$	$\Delta < 0$ and $B > 0$	$\Delta \geq 0$ and $B > 0$

Table 3.2: **Signs of Δ and B when $r < 1 + d$.**

From table 3.2, when $k > k_2$, the interior equilibrium $E^\star$ is locally asymptotically stable and when $k = k_2$, the inequality (3.13) is equivalent to

$$A(\rho^\star - \rho_1)^2 > 0,$$

since $\Delta = 0$. Hence, the interior equilibrium $E^\star$ is locally asymptotically stable for all $\rho^\star \neq \rho_1$.
Moreover, if $k < k_2$, then the interior equilibrium $E^\star$ is locally asymptotically stable when either $0 < \rho^\star < \rho_1$ or $\rho^\star > \rho_2$, and unstable when $\rho_1 < \rho^\star < \rho_2$. □.

- Case 2: When $r = d + 1$, the stability of the interior equilibrium $E^\star$ can therefore change according to the thresholds k_3 and ρ_3. Thus, we have the following theorem.

  Theorem 3.3.3. *Suppose that $r = 1 + d$. Then we have the following results.*

  - *If $k \geq k_3$, then the interior equilibrium $E^\star$ is locally asymptotically stable.*
  - *If $k < k_3$, then the interior equilibrium $E^\star$ is locally asymptotically stable if $\rho^\star > \rho_3$ and unstable if $\rho^\star < \rho_3$.*

  Proof. If $r = d + 1$, then the inequality (3.13) is equivalent to

$$(\nu + d)(2d\nu + \nu + d + 1)\rho^2 + \left[\nu(2d\nu + \nu + d + 1) - \frac{1}{k}\right]\rho > 0. \tag{3.20}$$

That is, $\rho > \rho_3$.

Hence, if $k < k_3$ and $\rho^\star > \rho_3$, the interior equilibrium $E^\star$ is locally asymptotically stable. When $k \geq k_3$, it is easy to show that the interior equilibrium $E^\star$ is locally asymptotically stable for all $\rho^\star > 0$. □

- Case 3: When $r > d + 1$, the stability of the interior equilibrium $E^\star$ can therefore change according to the threshold ρ_2. Thus, we have the following theorem.

  Theorem 3.3.4. *[41] Assume that $r > 1 + d$. Then the interior equilibrium $E^\star$ is locally asymptotically stable if $\rho^\star > \rho_2$ and unstable if $\rho^\star < \rho_2$.*

  Proof. When $r > 1 + d$, if is obviously to show that $\Delta > 0$, since $C < 0$. Hence, there are two distinct roots $\rho_1 < 0$ and $\rho_2 > 0$. Then, the interior equilibrium $E^\star$ is locally asymptotically stable if $\rho^\star > \rho_2$ and unstable if $0 < \rho^\star < \rho_2$. □

To establish the local stability according to the parameters of our model, it remains to solve the inequalities

$$\rho^\star < \rho_i, \tag{3.21}$$

$i = \overline{1,3}$ (see Appendix, Subsection A.2).

We need the following lemma.

Lemma 3.3.1. *(see Appendix, Subsection A.1)*

1. *If $0 < r \leq r_0$, then $k_2 < k_4$.*
2. *If $r_0 < r < r_2$, then $k_5 < k_2 < k_4$.*
3. *If $r = r_2$, then $k_2 = k_4 = k_5$.*
4. *If $r_2 < r < d + 1$, then $k_4 < k_5 < k_2$.*
5. *If $r \geq d + 1$, then $k_4 < k_5$.*

We have the following theorems (see Appendix, Subsection A.2).

Theorem 3.3.5. *[41] Let $r_0 < r \leq r_2$, then we have the following results.*

1. *If $k < k_5$, then $\rho_1 < \rho^\star < \rho_2$ and the interior equilibrium $E^\star$ is locally asymptotically stable.*
2. *If $k = k_5$, then we have an undetermined case since $\rho^\star = \rho_1 < \rho_2$.*
3. *If $k_5 < k < k_2$, then $\rho^\star < \rho_1 < \rho_2$ and the interior equilibrium $E^\star$ is unstable.*

4. *If $k > k_2$, then the interior equilibrium $E^\star$ is locally asymptotically stable.*

Theorem 3.3.6. *[41] Let $r_2 < r < d+1$. We have the following results.*

1. *If $k < k_5$, then $\rho_1 < \rho^\star < \rho_2$ and the interior equilibrium $E^\star$ is unstable.*
2. *If $k = k_5$, then we have an undetermined case since $\rho^\star = \rho_2 > \rho_1$.*
3. *If $k_5 < k < k_2$, then $\rho_1 < \rho_2 < \rho^\star$ and the interior equilibrium $E^\star$ is locally asymptotically stable.*
4. *If $k \geq k_2$, then the interior equilibrium $E^\star$ is locally asymptotically stable.*

Theorem 3.3.7. *[41] Let $r \geq d+1$. We have the following results.*

1. *If $k < k_5$, then $\rho^\star < \rho_2$ and the interior equilibrium $E^\star$ is unstable.*
2. *If $k = k_5$, then we have an undetermined case since $\rho^\star = \rho_2$.*
3. *If $k > k_5$, then $\rho^\star > \rho_2$ and the interior equilibrium $E^\star$ is locally asymptotically stable.*
4. *If $k \geq k_2$, then the interior equilibrium $E^\star$ is locally asymptotically stable.*

Remark 3.3.1. *Note that when $k = k_2$ (in theorem 3.3.5), the interior equilibrium $E^\star$ is locally asymptotically stable when $r_0 < r < r_2$ (since $\rho^\star < \rho_1 < \rho_2$), and we have undeterminate case when $r = r_2$ (since $\rho_1 = \rho^\star = \rho_2$).*

3.3.3 Global stability of interior equilibrium $E^\star$

Now, using a suitable Lyapunov function and LaSalle's Invariance Principle (see, [43]), we investigate the global asymptotic stability of interior equilibrium $E^\star$. We state the following theorem (see Appendix, Subsection A.3).

Theorem 3.3.8. *[41] The interior equilibrium $E^\star$ is globally asymptotically stable in $\mathbb{R}^3_+/M$ if either*

1. *$d < r < 2d$ with $k \geq \frac{1}{2\nu(r-d)}$, or*
2. *$r \geq 2d$ with $k > \frac{(r-d)}{d\nu r}$.*

where $M = \{0\} \times \mathbb{R}^2_+ \bigcup \mathbb{R}^2_+ \times \{0\}$.

Remark 3.3.2.

1. *If the initial conditions $(\rho_0, \sigma_0, \gamma_0) \in \{0\} \times \mathbb{R}^2_+$, then the solution of (3.3) converges to the trivial equilibrium $E_0 = (0,0,0)$.*

2. *If the initial conditions* $(\rho_0, \sigma_0, \gamma_0) \in \mathbb{R}^2_+ \times \{0\}$, *then the solution of (3.3) converges either to the trivial equilibrium* $E_0 = (0, 0, 0)$ *or to the tumor equilibrium* $E_1 = \left(\frac{r}{d}, 0, 0\right)$.

3.4 Hopf bifurcation analysis

In this section, we will investigate the existence of periodic solutions and this amounts to prove that a Hopf bifurcation exists.

According to theorems 3.3.5-3.3.7, when $\rho^\star = \rho_i$ (*i.e.* $k = k_5$), we have an undetermined case, then it is possible to show a periodic solution (Hopf bifurcation) since the equilibria E_0 and E_1 are unstable.

We recall that the characteristic equation corresponding to the Jacobian matrix at $E^\star$ is given by

$$P(\lambda) = \lambda^3 + a_2\lambda^2 + a_1\lambda + a_0, \tag{3.22}$$

where

$$\begin{cases} a_2 = \rho^\star (d + \nu + 1) + \nu > 0, \\ a_1 = \left[\nu (1 + 2d\rho^\star + d - r) + (\nu + d)\rho^\star\right]\rho^\star, \\ a_0 = \nu\rho^{\star 2}\sqrt{\left(r - d - \frac{1}{\nu k}\right)^2 + 4dr} > 0. \end{cases} \tag{3.23}$$

Periodic solutions emerge when two roots of Equation (3.22) are purely imaginary, of the form $\lambda_{2,3} = \pm i\omega$.

The discriminant of the above equation can be expressed as:

$$D = \frac{4}{27}\left(a_1 - \frac{a_2^2}{3}\right)^3 + \left(a_0 - \frac{a_1 a_2}{3} + \frac{2a_2^3}{27}\right)^2, \tag{3.24}$$

Hence, if $D > 0$ then the characteristic equation (3.22) has three distinct roots given as follows

$$\begin{aligned}
x_1 + y_1 - \frac{a_2}{3} &= t_1^{\frac{1}{3}} + t_2^{\frac{1}{3}} - \frac{a_2}{3}, \\
x_2 + y_2 - \frac{a_2}{3} &= t_1^{\frac{1}{3}}\left(-\frac{1}{2} + i\frac{\sqrt{3}}{2}\right) + t_2^{\frac{1}{3}}\left(-\frac{1}{2} - i\frac{\sqrt{3}}{2}\right) - \frac{a_2}{3}, \\
x_3 + y_3 - \frac{a_2}{3} &= t_1^{\frac{1}{3}}\left(-\frac{1}{2} - i\frac{\sqrt{3}}{2}\right) + t_2^{\frac{1}{3}}\left(-\frac{1}{2} + i\frac{\sqrt{3}}{2}\right) - \frac{a_2}{3},
\end{aligned}$$

where

$$\begin{aligned}
t_1 &= \frac{-\left(a_0 - \frac{a_1 a_2}{3} + \frac{2a_2^3}{27}\right) - \sqrt{D}}{2} = x^3, \\
t_2 &= \frac{-\left(a_0 - \frac{a_1 a_2}{3} + \frac{2a_2^3}{27}\right) + \sqrt{D}}{2} = y^3.
\end{aligned}$$

It is obvious that the first root is real, while the last two roots are complex conjugates. Therefore, we locate the Hopf bifurcation point by seeking solutions to equation (3.22) which are purely imaginary, which means that one had to determine conditions on model parameters satisfying $Re(\lambda_2) = Re(\lambda_3) = 0$, *i.e.*, $Re(x_2 + y_2 - \frac{a_2}{3}) = 0$. It follows that $Re(x_2 + y_2 - \frac{a_2}{3}) = 0$ if and only if $a_0 = a_1 a_2$ (see Appendix, Subsection A.4), *i.e.*,

$$A\rho^{\star 2} + B\rho^{\star} + C = 0.$$

Moreover, when $a_0 = a_1 a_2$ (*i.e.* $k = k_c$), we have

$$\frac{\partial Re(x_2 + y_2 - \frac{a_2}{3})}{\partial k} = \frac{\partial Re(x_2 + y_2 - \frac{a_2}{3})}{\partial \rho^{\star}} \frac{\partial \rho^{\star}}{\partial k},$$

$$\frac{\partial \rho^{\star}}{\partial k} = \frac{1}{\nu k^2}\left[\frac{\rho^{\star}}{\sqrt{(r - d - \frac{1}{k\nu})^2 + 4rd}}\right] > 0,$$

and

$$\begin{aligned}\frac{\partial Re(x_2+y_2-\frac{a_2}{3})}{\partial \rho^\star} &= \frac{1}{2\left(a_1+a_2^2\right)}\left[-(\nu+d+2d\nu)(\nu+d+1)\rho_\star^2+\nu^2(1+d-r)\right] \\ &= \frac{1}{\left(a_1+a_2^2\right)}\left[\frac{-(A+2d\nu)B^2+4AC(A+d\nu)+B(A+2d\nu)\sqrt{B^2-4AC}}{4A^2}\right],\end{aligned}$$

(see Appendix, Subsection A.4).

Proposition 3.4.1. 1. *From (3.25), if* $r \geq d+1$, *then* $\frac{\partial Re(x_2+y_2-\frac{a_2}{3})}{\partial \rho_\star} < 0$.

2. *From (3.25), if* $r < d+1$ *and* $k < k_2$, *then* $\frac{\partial Re(x_2+y_2-\frac{a_2}{3})}{\partial \rho_\star} < 0$ *since* $B < 0$ *and* $(A+2d\nu)B^2 > 4AC(A+d\nu)$ $(B^2 > 4AC)$.

Hence, at $k = k_c$, *we have*

$$\frac{\partial Re(x_2+y_2-\frac{a_2}{3})}{\partial k} = \frac{\partial Re(x_2+y_2-\frac{a_2}{3})}{\partial \rho^\star}\frac{\partial \rho_\star}{\partial k} < 0$$

for all $r > 0$.

We have the following theorem.

Theorem 3.4.1. *[41] Assume that* $r > r_0$. *Then there exists* $k_c > 0$, *such that the system (3.3) undergoes Hopf bifurcation near the interior equilibrium* $E^\star$ *when* $k = k_c$.

Remark 3.4.1. *Not that when* $r \leq r_0$, *then the interior equilibrium* $E^\star$ *is locally asymptotically stable. Hence, there is no Hopf bifurcation since* $\rho^\star < \rho_1 < \rho_2$ *for all* $r \leq r_0$ *and* $k \leq k_2$ *(see Appendix, Subsection A.2).*

3.5 Numerical simulations

In this section, we present some numerical simulations of system (3.3), to illustrate the results obtained in Sections 3.3 and 3.4. We choose the following parameter values: $d = 0.25$, $\nu = 0.4$ and $r = 1.3$. For all plots the initial conditions are $(\rho_0, \sigma_0, \gamma_0) = (1.5, 0.5, 3)$.

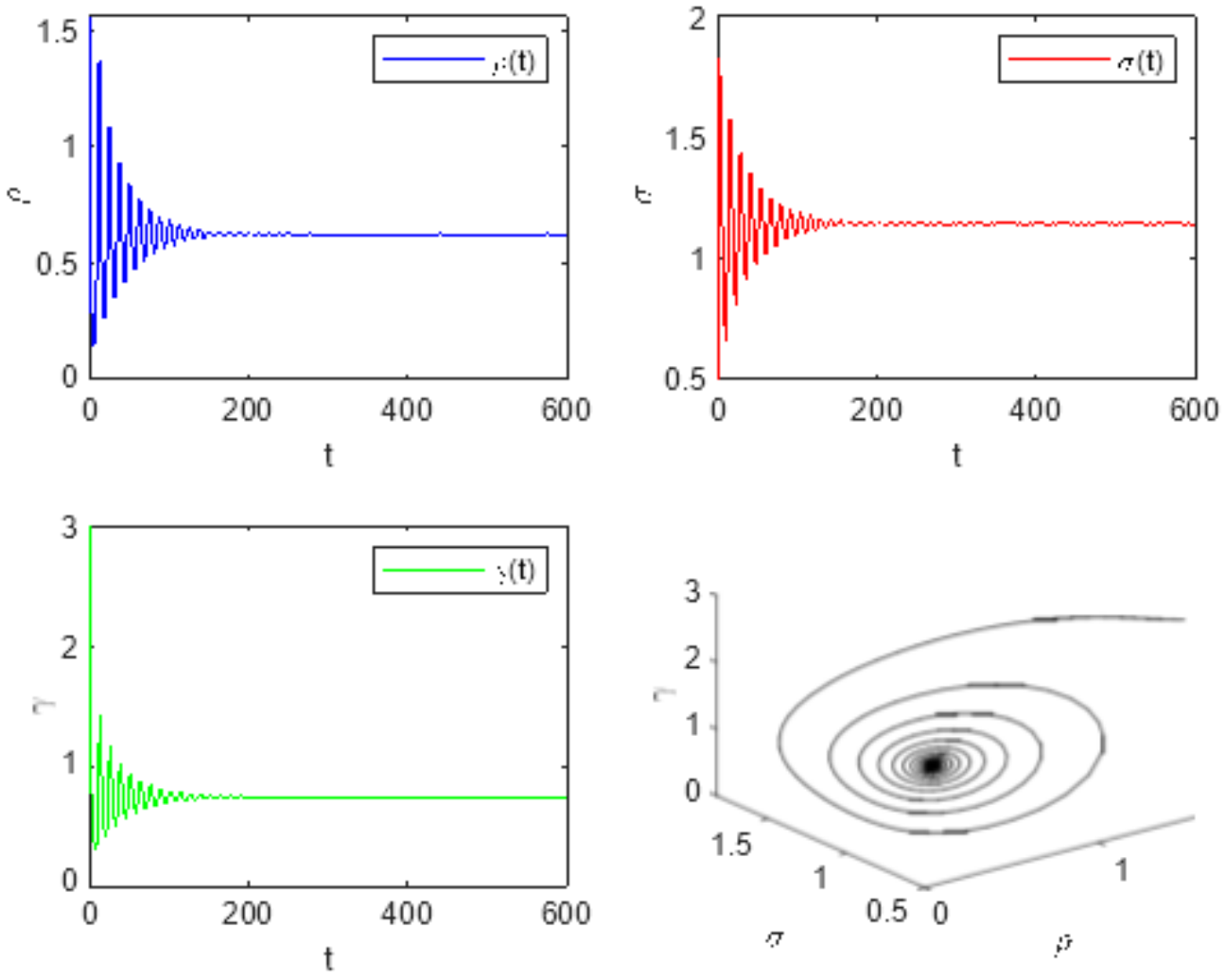

Figure 3.2: **The solution is drawn for the stability of the interior equilibrium** $E^{\star} = (0.6257, 1.1436, 0.7436)$**, for** $k = k_5 + 0.1 = 0.7414 + 0.1 = 0.8414$**.**

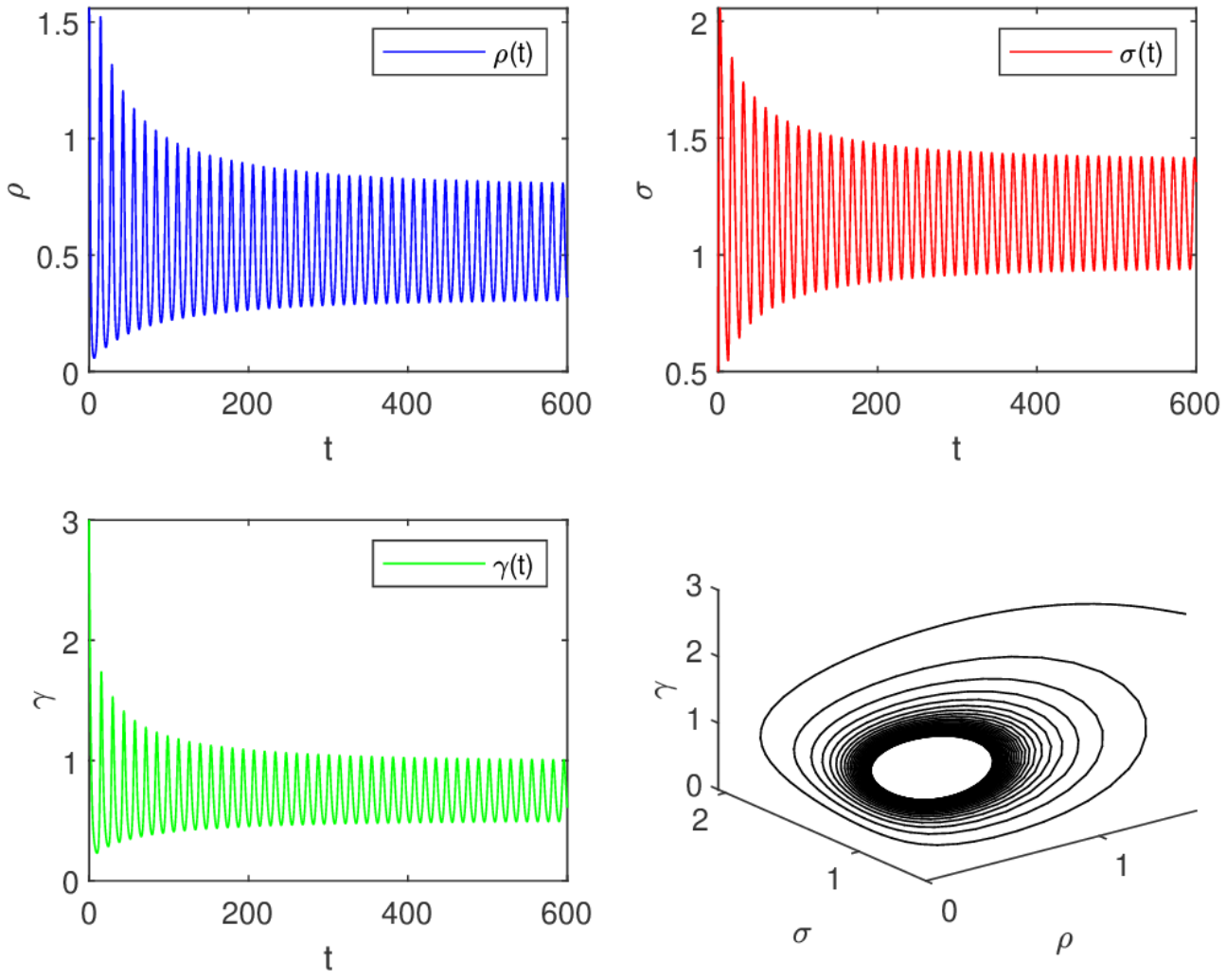

Figure 3.3: **The solution is drawn for the instability of the interior equilibrium** $E^\star = (0.5204, 1.1699, 0.7115)$ **with limit cycle (Hopf bifurcation), for** $k = k_5 - 0.01 = 0.7414 - 0.01 = 0.7314$**.**

3.6 Discussion and conclusions

In this chapter, we have established a new mathematical model for tumour-immune response interactions. Let us stress that the analysis developed in this chapter is limited to a simplified model where the outset of tumour-immune response interactions is not yet relevant. In spite of this limitation, the model is able to capture the second phase of the immunoediting process, depending on the model's parameters. However, this modelling approach allows

for the characterization of both local and global stability of steady states, as well as the identification of the model parameters that have an important issue on tumour development. The existence of the steady states has been characterized and analyzed with respect to their local asymptotic stability. Regions of the parameter space have also been identified, in which a Hopf bifurcation exists. The ODE model reproduces a tumour equilibrium (second situation of the immunoediting process), which corresponds either to a stable steady state or to a stable limit cycle, characterized by a sustained periodic behaviour of alternating growth and decay (without extinction) of both tumour and immune T cells. For particular choices of initial conditions, the ODE model also captures either tumour eradication or tumour immune escape.

In future work, it would be interesting to introduce different time scales for (fast) activation by APCs of naïve T cells in lymphoid organs and (slow) tumour-immune interactions at the tumour site. The model might include a constant delay in the recruitment term of the immune cells to illustrate the time lag between the stimulated accumulations of immune cells in the vicinity of cancer cells.

Chapter 4

A phenotype structured model for the tumour-immune response

The work presented in this chapter is the result of a fruitful collaboration with Jean Clairambault and Camille Pouchol that took place during my internship at the Laboratoire Jacques-Louis-Lions (LJLL). It is the subject of an article recently published in Mathematical Modelling of Natural Phenomena, entitled *A phenotype-structured model for the tumour-immune response.*

4.1 Biological background

When a cancer cell population thrives, the immune response, and essentially its part that is constituted of CD8+ T-lymphocytes (for the adaptive response) and NK-lymphocytes (for the innate response), consists of recognising as foe elements and killing these cancer cells. This has been called immunosurveillance, later immunoediting ([8], [67], [71]), which may consist of three different configurations: eradication, equilibrium or escape (see Figure 1.1). If this process is performed during the early stages of tumour initiation, the tumour is quickly and successfully eradicated. However, cancer cells can escape these innate NK-cell and adaptive specific T-cell immune responses in the course of genetic and phenotypic evolution at the time scale of a cancer disease. More precisely, phenotypic heterogeneity in the cancer cell population, involving its possible internal invasion by secondarily mutated, robust, cells,

may be responsible for both tumour escape and treatment failure. Here, a focus is set on immunotolerance ([67], [71]), which renders cancer cells able to evade immune detection and elimination. Indeed, cancer cells have the resource to weaken the immune response by emitting molecules such as PD-L1 (i.e., PD-1 ligand) and CTLA-4, which can respectively bind to the PD-1 and B7 receptors on activated T-cells, inhibiting their cytotoxic activity and reducing their own immunogenicity. This is represented in the model by direct competition between cancer cells and T-lymphocytes. As regards innate immunity, the role of NK-lymphocytes (readily effective on cancer cells with lacking MHC-I surface antigens [59], not the same mechanism as in the case of CD8+ T-cells, that are activated by tumour antigen-presenting cells, APCs), has recently gained more consideration, in particular, because a role for anti-PD1/anti-PDL1 has been suspected for them in cancer immunotherapies [62].

Immunotherapy with immune checkpoint inhibitors [71] (hereafter noted *ICI*s) is a recently introduced class of drugs that inhibit such cancer cell-produced inactivation of T- and NK-lymphocytes, either at the receptor sites on lymphocytes or by inhibiting the ligands themselves. The clinical use, firstly of anti-CTLA4 drug Ipilimumab, which has been shown to mainly target the priming lymphocyte response at the level of lymphoid organs [82], and later of direct (at the tumour site) antagonisers of PD-L1 to PD-1 binding, drugs Nivolumab and Pembrolizumab [34] [1], has drastically modified the prognosis of several advanced cancers that were until recently out of reach (e.g., melanoma, a skin cancer with very bad prognosis [68]), offering sustained positive responses (about 20% of complete cures, the remaining 80% consisting of non- or partial responders with relapse). However, not all cancer types respond as well as melanoma. To the best of our knowledge, the reasons for successes or failures are still unknown. Moreover, there is no clear dose-response relationship and a maximum tolerated dose, for checkpoint inhibitors, has not been identified as yet [50].

[1] Note that in the sequel, as our model aims at representing direct tumour-immune interactions and their possible enhancing by immunotherapy, the term *ICI*s should be thought of as representing this second class of drugs.

4.2 The model

4.2.1 The cell populations

To describe tumour-immune interactions, we consider three different cell population densities:

- a heterogeneous cancer cell population $n(t,x)$ with continuous aggressiveness (or malignancy) trait $x \in [0,1]$ linked to their stemness (i.e., their ability to de-differentiate, allowing them to re-differentiate with adapted phenotypes);
- a heterogeneous population of mixed competent T-lymphocytes and NK-lymphocytes $\ell(t,y)$ endowed with continuous anti-tumour aggressiveness trait y ranging from 0 (exhausted) to 1 (highly aggressive) interacting with cancer cells $n(t,x)$ at the tumour site;
- a heterogeneous population of naïve T-lymphocytes and patrolling NK-lymphocytes $p(t,y)$, either resident and present at the tumour site (for NK-cells, particularly activated by their sensing lack of MHC-I surface antigens in tumour cells, so-called "loss-of-self"), or present in distant lymphoid organs, informed there by **APCs** (antigen-presenting cells, here represented by a weighted integral of the cancer cell population involving a localisation kernel coupling x and y) of the number and malignancy x of the cancer cell population. Both "naïve" cell populations are represented by the lumped population density $p(t,y)$. Note that in simulations, we will consider separately the three cases: innate, adaptive, and a combination of the two immune responses.

Our model is given by the following system of integro-differential equations (IDEs):

$$\begin{cases} \dfrac{\partial n}{\partial t}(t,x) = \left[r(x) - d(x)\rho(t) - \mu(x)\varphi(t)\right] n(t,x), \\ \dfrac{\partial \ell}{\partial t}(t,y) = p(t,y) - \left(\dfrac{\nu(y)\rho(t)}{1+hICI(t)} + k_1\right)\ell(t,y), \\ \dfrac{\partial p}{\partial t}(t,y) = \chi(t,y)p(t,y) - k_2 p^2(t,y). \end{cases} \tag{4.1}$$

with the total number of cancer cells at time t

$$\rho(t) := \int_0^1 n(t,x)dx. \tag{4.2}$$

The initial value function $n(0,x)$ is chosen to represent the assumed initial malignancy of the tumour, and in the same way, the initial value functions $\ell(0,y)$ and $p(0,y)$ will be chosen to represent the initial host's immune response.

4.2.2 Biological motivations

In the above model:

- For the tumour cell population of density $n(t,x)$, a cell of phenotype x is all the more malignant, i.e., able to thrive, as x is closer to 1, and conversely less malignant when x is close to 0. More particularly, the malignancy trait x represents a progression potential towards stemness (ability to differentiate).
  Let us mention that the malignancy trait x might in principle be measured in single cells by assessing the expression of genes like the Yamanaka factors, a group of transcription factors, Oct3/4, Sox2, Klf4, c-Myc, identified in 2006 by Nobel prize winner Shinya Yamanaka, that enable dedifferentiation [76] from differentiated cells into so-called IPSCs (induced pluripotent stem cells). More recently, a de-differentiated phenotype MIT^{low}/AXL^{high} phenotype, defined by the concomitant downregulation of the transcription factor MIT and accumulation of the tyrosine kinase receptor AXL has been evidenced in immunotherapy-resistant melanoma cells [48], which could provide a measurable basis for such continuous malignancy trait x identified as a potential for tumour cells to de-differentiate in response to deadly attacks coming from the immune response or more generally from the tumour microenvironment, including drugs. Importantly, we assume in this model that both the density of a loss-of-self sensed by NK-cells in tumour cells (recalled in next paragraph) and the density of tumour antigens sensed by APCs reflect the level of the *hidden* tumour aggressivity phenotype x in the tumour cell population, even though the anti-tumour action of lymphocytes will be directed towards the *manifest* loss-of-self and tumour antigen-bearing cells.
- For the T-lymphocyte population and for the non-adaptive NK-lymphocyte population, in a similar way, we structure it by a phenotype y of anti-tumour aggressiveness, which may be defined as the reverse of the 'dysfunction' or 'exhaustion' phenotype that has been observed in $CD8^+$ T-cells exhibiting incapacity to efficaciously fight tumour cells. In our model, the difference between NK-lymphocytes and effector (CD8+)

T-cells consists in the nature of their action on tumour cells, either independent of the tumour phenotype x for NK-cells represented below by a function $\varphi(t)$, or highly dependent on it for T-cells, represented by a function $\varphi(t, x)$. In the analysis of our model, we will study separately the case of innate (function $\varphi(t)$) and adaptive (function $\varphi(t, x)$) immune response (and also a mix of these two cases in our simulations). To identify and measure in single cells such dysfunction or exhaustion in T-cells, different biological markers have been proposed; they have been recently reviewed in [78] (an article in which it is, in particular, noted that *"T cell dysfunctionality is a gradual, not a binary, state"*, which fully justifies the continuous character of our structure variable y). The closer the phenotype y approaches 0, the less aggressive are T- and NK-lymphocytes, i.e., less competent to kill cancer cells (complete exhaustion), whereas if y approaches 1, they are highly aggressive (full competence) against the targeted tumour cells, as identified by their competence as immune cells due to the tumour antigen recognition performed by the APCs, or to the absence of MHC-I antigens (loss-of-self) in tumour cells directly sensed by NK-cells. The principle of immune checkpoint inhibition (*ICI*) immunotherapy is to boost CD8+ T-lymphocytes and NK-lymphocytes in their efficacy by antagonising such tumour-emitted inhibitory mechanisms, mainly in the modelling framework presented here, PD-L1 to PD-1 binding on T-cells and NK-cells.

4.2.3 Modelling choices for the mathematical functions of phenotypes

In the absence of experimental data, the precise choices for functions r, d, μ, ν, ψ are largely arbitrary, only guided by physiological considerations on an assumed monotonicity. They are listed in Table 4.1 of Section 4.4 for simulations, reflecting such monotonicity: non-increasing for r, d, μ, ν, non-decreasing for ψ. The biological background for these functions is as follows.

- We assume that in the absence of immune response, tumour cells undergo logistic growth, with a net growth rate (aka fitness) defined by

$$r(x) - d(x)\rho(t). \tag{4.3}$$

Here, the function $r(x)$ stands for the intrinsic proliferation rate. As x stands for a de-differentiation, stem-like, cell phenotype, admitting that a stem-like status does not favour replication velocity, r will typically be assumed to be a positive, decreasing function of x on $[0,1]$, e.g., of the form

$$r(x) = r_0 - \eta x^2, \tag{4.4}$$

where the parameter $r_0 > 0$ corresponds to the maximum fitness of cancer cells, while $\eta > 0$ provides a measure of the strength of natural selection in the absence of the immune response. The term $d(x)\rho(t)$ models the intrinsic death rate due to within-population competition for space and resources, assumed to be proportional to the total population number of tumour cells $\rho(t)$. The function d will typically be taken to be positive, decreasing function of x on $[0,1]$ (in the same way as for the replication function r, a de-differentiated, stem-like, status is admitted to protect cells from the natural death term represented by the function d).

The fitness structure chosen here for the tumour and for the immune cell population is of the nonlocal Lotka-Volterra type. It has been in particularly used in [63] to model the adaptation of individuals to their environment.

- We assume that, once an immune response has been activated, the tumour cells interact with competent T-cells and NK-cells at a rate which is proportional to the product of the tumour cell population density by a weighted integral $\varphi(t)$ given by

$$\varphi(t) = \int_0^1 \psi(y) l(t,y) dy, \tag{4.5}$$

where ψ is a positive function, which we will typically take to be increasing on $[0,1]$. The term $\mu(x)\varphi(t)$ models an additional death rate for tumour cells due to their interactions with NK-cells ℓ. We note that in this formulation, the immune response $\varphi(t)$, emitted by NK-cells present at the tumour site, is non-specific, only the tumoral sensitivity function $\mu(x)$ makes it somehow specific; the function $\varphi(t)$ then stands for a response in which the phenotype y in lymphocytes is averaged over all the population of activated NK-cells, $\varphi(t)$ representing a sort of "mass immune response".

- In order to account for an adaptive, specific, immune response which is the one of T-cells, we more generally consider φ to be of the form

$$\varphi(t,x) = \int_0^1 \Psi(x,y)\ell(t,y)dy. \tag{4.6}$$

Here, the weight function $\psi(y)$ of the innate response is replaced by $\Psi(x,y)$, which we typically take to be the product of a function $\psi(y)$ by a localisation kernel, e.g.,

$$\Psi(x,y) = \frac{\psi(y)}{v} e^{-|x-y|/v}, \tag{4.7}$$

in which ψ will again be a positive function, non-decreasing on $[0,1]$, assumed for simplicity to be the same as in the innate, non-adaptive case. One can see parameter v as the precision with which the immune response targets the cancer cell population (as identified by its malignancy trait x).
We will in fact in simulations consider separately these two cases, native non-specific (NK-cells: $\varphi(t)$ given by (4.5)) and adaptive specific (T-cells: $\varphi(t,x)$ given by (4.7)) anti-tumour immune response, and also a mixed case, convex combination of the two immune responses, non-specific (NK-cells) and specific (T-cells):

$$\Psi_\lambda(x,y) = \left((1-\lambda) + \lambda\frac{1}{v}e^{-|x-y|/v}\right)\psi(y), \quad \lambda \in [0,1], \tag{4.8}$$

corresponding to a simultaneous and independent activation of NK-cells and T-cells by loss-of-self (NK-cells) and specific tumour antigen (T-cells) stimuli. This choice interpolates (for a given fixed ψ) between (4.5) obtained with $\lambda = 0$, and (4.6) with the choice (4.7) obtained with $\lambda = 1$.

- The function $\mu(x)$ represents a factor of sensitivity to the effects of the immune response. As de-differentiation is supposed to protect tumour cells from these effects (e.g., by hiding tumoral antigens, targets of lymphocytes), μ is chosen to be a positive, decreasing function of x.
- The amplification of the naïve T-lymphocytes $p(t,y)$ at lymphoid organs is related to the mean x malignancy value through a weighted integral $\chi(t,y)$ of the tumour cell population, representing the message borne by APCs to initiate the adaptive anti-tumour immune response produced in the lymphoid organs. When an APC detects a

tumour cell, the related antigen is presented to naïve T-cells. Thus, naïve T-cells that recognise this antigen as their cognate one become activated. Activated T cells start to proliferate and, through a complex process chain, they become able to recognise and attack tumour cells that express the cognate antigen. The function $\chi(t, y)$ is defined as

$$\chi(t, y) = \int_0^1 \omega(x, y) n(t, x) dx, \tag{4.9}$$

where ω is another localisation kernel such as $\omega(x, y) = \alpha \frac{1}{s} e^{-|x-y|/s}$, so as to represent a more or less faithful message transmitted by the APCs (activating naive T-lymphocytes) to the lymphoid organs about both the size and malignancy of the tumour. The efficacy of activated T-lymphocytes in killing tumour cells depends on the initial size of the tumour and on how localised the kernel is (i.e., on the width of the range of phenotypes y concerned by their detected tumour cognates x, which can be measured by the value of the parameter s in the proposed function $\omega(x, y)$). The parameter α represents the strength of the immune response (i.e., a good transmission by APCs, and a good synthesis of the expansion). In the present model, communication between recognition at the contact of tumour cells and activation of naive T-lymphocytes at the site of lymphoid organs is represented, for the sake of simplicity without taking communication time into consideration, by the shortcut of the function $\omega(x, y)$. In this localisation kernel function, the parameter s may be seen as the precision of the detection of the malignancy trait x in the cancer cell population by APCs or circulating NK-cells.

- We consider a similar mechanism for NK-lymphocytes, that are known to proliferate and amplify not only in the bone marrow but also in lymphoid organs, like T-lymphocytes [1]. In the case of this innate immune response, there are no APCs, but the message from sensor patrolling NK-lymphocytes to proliferating NK-lymphocytes is assumed to be of (coarse, quantitative) humoral nature.
- In the second equation of (4.1) for the competent T-lymphocytes $\ell(t, y)$, the function ν of the anti-tumour aggressiveness phenotype y represents the weakening (immunotolerance) of T-lymphocytes induced by PD-1 ligands; note that it is assumed to be decreased by *ICI*s. As the function ν stands for a sensitivity factor in lymphocytes to the weakening reaction molecules (in this model, mainly PD-L1) emitted by tumour cells or produced in the tumour microenvironment, it will typically be chosen to be a

positive, decreasing function of y, which in this case reflects the fact that cells in the phenotypic state $y = 1$ are fully aggressive on contact with tumour cells and, for cells in phenotypic states other than the most aggressive one, the inhibition term induced by the tumour cells decreases with the drug dose.

- The parameter k_1 stands for the natural death rate of the population of competent T- and NK-lymphocytes.
- The input of external control targeting immune checkpoints inhibitors is represented by the function $ICI(t)$ that enhances anti-tumour CD8+ T-lymphocyte and NK-lymphocyte responses by boosting the exhausted immune cells, which helps them to respond more strongly to the presence of the tumour, by "weakening the weakening" due to immunotolerance induced by the tumour cells. We assume that

$$0 \leq ICI(t) \leq ICI^{max}. \tag{4.10}$$

for some maximum tolerated dose ICI^{max}. The factor $\frac{1}{1+hICI(t)}$, with $h > 0$, models the decrease in the immunotolerance rate due to the immune checkpoints inhibitors therapy. We note that fine details of clinical administration protocols are not meant to be described here. We also mention that ICI is a quantitative dose function, and is APC-independent.

- The term $-k_2 p(t, y)$ with the positive constant k_2 stands for the self-limitation on population growth imposed by carrying capacity constraints (e.g., limited availability of space and resources in lymphoid organs).

4.2.4 Goals of the present study

Our goals in this study are

- to study the asymptotic properties of the model, as we want to understand how the interaction between tumour cells and T cells leads to the selection (or not) of some traits, which are considered as dominant traits by the environment;
- to numerically investigate if and how our model captures the three Es of immunoediting, i.e., eradication, equilibrium and escape.

4.3 Asymptotic analysis

4.3.1 Asymptotics in the absence of treatment

We study the asymptotic properties of the system (4.1) in the absence of treatment, i.e., with $ICI(t) = 0$. Of course, upon changing the function ν, our study also encompasses the case where the dose ICI is taken to be constant with time.
The evolution of the population densities is then governed by the following integro-differential system:

$$\begin{cases} \frac{\partial n}{\partial t}(t,x) = [r(x) - d(x)\rho(t) - \mu(x)\varphi(t)]\, n(t,x), \\ \frac{\partial \ell}{\partial t}(t,y) = p(t,y) - (\nu(y)\rho(t) + k_1)\, \ell(t,y), \\ \frac{\partial p}{\partial t}(t,y) = \chi(t,y)p(t,y) - k_2 p^2(t,y), \end{cases} \tag{4.11}$$

the above system starting from initial conditions

$$n(0,x) = n^0(x) \geq 0, \quad \ell(0,y) = \ell^0(y) \geq 0, \quad p(0,y) = p^0(y) \geq 0. \tag{4.12}$$

Main assumptions on the functions and initial conditions. For the remaining part of this paper, we assume that the initial conditions n^0, ℓ^0 and p^0 are all in $\mathcal{C}([0,1])$, and whenever necessary, we will assume that

$$n^0 > 0 \quad \text{and} \quad p^0 > 0 \quad \text{on } [0,1], \tag{4.13}$$

and we will work with the following regularity assumptions:

$$r, d, \mu, \psi, \nu \in \mathcal{C}([0,1]), \quad \text{and} \quad \omega \in \mathcal{C}\left([0,1] \times [0,1]\right), \tag{4.14}$$

all the above functions are assumed to be positive.

The existence and uniqueness of global classical (nonnegative) solutions in $C^0([0,+\infty), L^1(0,1)^3)$ is standard and follows from the Banach fixed point theorem, see [63].

Notations. For the rest of the article, we will when needed denote

$$\limsup_{t\to+\infty} g(t) = \overline{\lim_{t\to+\infty}}\, g(t), \quad \liminf_{t\to+\infty} g(t) = \underline{\lim_{t\to+\infty}}\, g(t), \tag{4.15}$$

For a continuous real-valued function f defined on a compact set, we denote f^m and f^M its minimum and maximum. Finally, δ_x denotes the Dirac mass at the position x.

4.3.1.1 Asymptotics for tumour cells alone

In the absence of immune response (for instance, assuming either that there are no competent immune cells initially, i.e., $\ell^0 = 0$, or that immune cells are inefficient in interacting with cancer cells through either $\psi = 0$ or $\mu = 0$), the first equation of (4.11) boils down to a standard logistic integro-differential model, namely

$$\begin{cases} \frac{\partial n}{\partial t}(t,x) = [r(x) - d(x)\rho(t)]\, n(t,x), \quad n(t=0,x) = n^0(x) \geq 0, \\ \rho(t) = \int_0^1 n(t,x)dx. \end{cases} \tag{4.16}$$

For any positive continuous initial condition n^0, the total population of tumour cells $\rho(t)$ converges to $\rho^\star := \left(\max_{[0,1]} \frac{r(x)}{d(x)}\right)$ as $t \to +\infty$.
This asymptotic cell population number, which is its maximal value, is readily interpreted, as for all logistic models of tumour growth, as the tumour *carrying capacity*. Furthermore, the density $n(t,\cdot)$ viewed as a Radon measure supported on $[0,1]$ concentrates on the set

$$A := \{x \in [0,1], r(x) - d(x)\rho^\star = 0\} \tag{4.17}$$

as $t \to +\infty$. If A is reduced to a singleton $x^\star$, then in particular $n(t,\cdot) \rightharpoonup \rho^\star \delta_{x^\star}$. As $t \to +\infty$ in $\mathcal{M}([0,1])$. As stated in chapter 2- Theorem 2.1.1, a direct proof of convergence based on proving that $\rho(t)$ is BV on $[0,\infty)$, from which concentration follows from exponential growth.

4.3.1.2 A priori bounds

We first indicate the derivation of an upper bound for ρ. Integrating the first equation of system (4.11) with respect to x, we find using $\varphi \geq 0$:

$$\frac{d\rho}{dt} = \int_0^1 \left[r(x) - d(x)\rho - \mu(x)\varphi(t)\right] n(t,x)\, dx \leq \max_{x\in[0,1]} \left(r(x) - d(x)\rho\right) \rho.$$

The right-hand side is negative as soon as $\max_{x\in[0,1]} \left(r(x) - d(x)\rho\right) < 0$, i.e., as soon as $\rho > \max \frac{r}{d}$. Hence

$$\rho(t) \leq \rho^M =: \max\left(\rho(0), \max_{x\in[0,1]} \frac{r(x)}{d(x)}\right), \quad \forall t > 0. \tag{4.18}$$

Consequently, we have

$$\forall y \in [0,1], \quad \chi(t,y) \leq \omega^M \rho^M \quad \forall t \in [0,+\infty). \tag{4.19}$$

Let us fix $y \in [0,1]$. From the bounds (4.18) and (4.19), we have

$$\frac{d}{dt} p(t,y) \leq \left[\omega^M \rho^M - k_2 p(t,y)\right] p(t,y). \tag{4.20}$$

By the comparison principle, we find

$$p(t,y) \leq p^M(y) =: \max\left(p^0(y), \frac{\omega^M \rho^M}{k_2}\right), \quad \forall t > 0. \tag{4.21}$$

Using the same arguments, one can prove that the population density ℓ is bounded from above. Indeed,

$$\frac{d}{dt}\ell(t,y) = p(t,y) - \left(\nu(y)\rho(t) + k_1\right)\ell(t,y) \leq p(t,y) - k_1 \ell(t,y) \leq p^M(y) - k_1 \ell(t,y). \tag{4.22}$$

Applying the comparison principle, we have

$$\ell(t,y) \leq \ell^M(y) := \max\left(\ell^0(y), \frac{p^M(y)}{k_1}\right), \quad \forall t > 0. \tag{4.23}$$

As a result, we obtain

$$\varphi(t) \leq \varphi^M := \int_0^1 \psi(y)\ell^M(y) dy, \quad \forall t > 0. \tag{4.24}$$

Finally, we may argue as above for a lower bound for ρ (on top of nonnegativity $\rho \geq 0$). Indeed, from

$$\frac{d\rho}{dt} \geq \min_{x\in[0,1]} \left(r(x) - d(x)\rho - \mu(x)\varphi^M\right)\rho, \tag{4.25}$$

it follows that

$$\rho(t) \geq \rho^m := \min\left(\rho(0), \min_{x\in[0,1]}\left(\frac{r(x) - \mu(x)\varphi^M}{d(x)}\right)\right), \quad \forall t > 0. \tag{4.26}$$

We accordingly consider an assumption ensuring non-extinction, given by

$$\min_{x\in[0,1]}\left(\frac{r(x) - \mu(x)\varphi^M}{d(x)}\right) > 0. \tag{4.27}$$

4.3.1.3 Asymptotics for the complete model, non-adaptive immune response case

This section is devoted to analysing the asymptotic behaviour of the model (4.11) in the non-adaptive case, particularly represented by NK-lymphocytes rather than by T-lymphocytes, where φ does not depend on x.

As already mentioned in Section 3.3, assuming all functions to be constant, the IDE system has the ODE (3.3) as a particular case. For that ODE, it has been proved that all three behaviours can occur: convergence to a (unique) trivial stable point (extinction or escape), convergence to a (unique) non-trivial stable point (equilibrium) and convergence to a limit cycle. The existence of such periodic solutions means that there is no hope of deriving any unconditional result of convergence to steady states for the IDE model.

In what follows, we prove a partial result, which makes the strong *a priori* assumption that n converges. Then we prove that the limit either equals 0 or can precisely be characterised, see Theorem 4.3.1.

Proposition 4.3.1. *Suppose that the density n weakly converges in $\mathcal{M}([0,1])$, and denote n^∞ the limit measure. Setting $\rho^\infty := \int_0^1 dn^\infty(x)$, and under the assumptions (4.13)- (4.14),*

both densities ℓ and p converge respectively to $\ell^\infty, p^\infty \in C^0([0,1])$ given by

$$\begin{aligned} \ell^\infty(y) &= \tfrac{p^\infty(y)}{\nu(y)\rho^\infty + k_1}, \\ p^\infty(y) &= \tfrac{1}{k_2}\int_0^1 \omega(x,y)\, dn^\infty(x). \end{aligned} \tag{4.28}$$

Proof. We let $y \in [0,1]$ be fixed. First remark that $\chi(t,y)$ converges to $\bar{\chi}(y)$ given by

$$\bar{\chi}(y) := \int_0^1 \omega(x,y)\, dn^\infty(x). \tag{4.29}$$

Hence $p(\cdot, y)$ satisfies a non-autonomous logistic ODE, given by

$$\frac{dp(t,y)}{dt} = [\chi(t,y) - k_2 p(t,y)]\, p(t,y). \tag{4.30}$$

For a given $\varepsilon > 0$ and t large enough (say $t \geq t_0$) such that $\chi(t,y) \leq \bar{\chi}(y) + \varepsilon$, we can write

$$\frac{dp(t,y)}{dt} \leq [\bar{\chi}(y) + \varepsilon - k_2 p(t,y)]\, p(t,y), \tag{4.31}$$

p is thus a sub-solution of the equation

$$\frac{du}{dt}(t) = [\bar{\chi}(y) + \varepsilon - k_2 u(t)]\, u(t), \tag{4.32}$$

with initial condition chosen to be $u(t_0) = p(t_0, y)$. The solution of the latter logistic autonomous equation converges to $\frac{\bar{\chi}(y)+\varepsilon}{k_2}$ as $t \to +\infty$, since $p(t_0, y) > 0$ by the assumption (4.13). We conclude by the comparison principle that

$$\forall \varepsilon > 0, \quad \overline{\lim_{t\to+\infty}}\, p(t,y) \leq \lim_{t\to+\infty} u(t) = \frac{\bar{\chi}(y) + \varepsilon}{k_2}. \tag{4.33}$$

Therefore, we may pass to the limit $\varepsilon \to 0$ in inequality (4.33) to obtain

$$\overline{\lim_{t\to+\infty}}\, p(t,y) \leq \frac{\bar{\chi}(y)}{k_2}. \tag{4.34}$$

Using the same reasoning from below, we have proved

$$\forall y \in [0,1], \quad \lim_{t\to+\infty} p(t,y) = \frac{\bar{\chi}(y)}{k_2} = \frac{1}{k_2}\int_0^1 \omega(x,y)\, dn^\infty(x) = p^\infty(y). \tag{4.35}$$

Turning to the limit for ℓ, we fix y in $[0,1]$. Letting $L_y(t) := l(t,y)$, we have

$$\frac{dL_y(t)}{dt} = A_y(t) - B_y(t)L_y(t), \tag{4.36}$$

which is a non-autonomous linear differential equation, with

$$\begin{cases} \lim\limits_{t\to+\infty} A_y(t) = \lim\limits_{t\to\infty} p(t,y) = p^\infty(y) =: \bar{A}_y, \\ \lim\limits_{t\to+\infty} \left(\nu(y)\rho(t) + k_1\right) = \nu(y)\rho^\infty + k_1 =: \bar{B}_y. \end{cases} \tag{4.37}$$

For $\varepsilon > 0$ small enough and t large enough (say $t \geq t_0$) such that $A_y(t) \leq \bar{A}_y + \varepsilon$ and $B_y(t) \geq \bar{B}_y - \varepsilon$, we can write

$$\frac{dL_y}{dt} \leq \left(\bar{A}_y + \varepsilon\right) - \left(\bar{B}_y - \varepsilon\right) L_y, \tag{4.38}$$

L_y is thus a sub-solution of the autonomous equation given by

$$\frac{dv}{dt} = \left(\bar{A}_y + \varepsilon\right) - \left(\bar{B}_y - \varepsilon\right) v, \tag{4.39}$$

with $v(t_0) = L_y(t_0)$, the comparison principle allows us to conclude that

$$\forall > 0, \quad \overline{\lim_{t\to+\infty}} L_y(t) \leq \lim_{t\to+\infty} v(t) = \frac{\bar{A}_y + \varepsilon}{\bar{B}_y - \varepsilon}. \tag{4.40}$$

We then let ε go to 0 to get

$$\forall y \in [0,1], \quad \overline{\lim_{t\to+\infty}} L_y(t) \leq \frac{\bar{A}_y}{\bar{B}_y} = \frac{p^\infty(y)}{\nu(y)\rho^\infty + k_1}. \tag{4.41}$$

Arguing in a similar manner to get a lower bound, we find

$$\forall y \in [0,1], \quad \lim_{t\to+\infty} \ell(t,y) = \frac{p^\infty(y)}{k_1 + \nu(y)\rho^\infty} = \ell^\infty(y). \tag{4.42}$$

□

Let us now explain how to determine possible limits for the system, still making the strong *a priori* assumption that $n(t,\cdot)$ converges. We shall need a technical (but rather weak)

assumption, namely

$$\forall \bar{\rho} > 0,\ \forall \bar{\varphi} > 0, \quad \arg\max_{x\in[0,1]} \left(r(x) - d(x)\bar{\rho} - \mu(x)\bar{\varphi}\right) =: \{x(\bar{\rho}, \bar{\varphi})\}. \tag{4.43}$$

From the proof and by the *a priori* bounds, one can see that this can be weakened by restricting the above assumption to the values $0 < \bar{\rho} \leq \rho^M$, $0 < \bar{\varphi} \leq \varphi^M$ such that the function $x \mapsto r(x) - d(x)\bar{\rho} - \mu(x)\bar{\varphi}$ has maximum zero.

Theorem 4.3.1. *[42] Suppose that the density n weakly converges in $\mathcal{M}([0,1])$, and denote n^∞ the limit measure. Under the assumptions (4.13)-(4.14)-(4.43), then either $n^\infty = 0$ or n^∞ is of the form*

$$n^\infty = \rho^\infty \delta_{x^\infty},$$

where $x^\infty = x(\rho^\infty, \varphi^\infty)$ and $(\rho^\infty, \varphi^\infty)$ solves the following system over $(\rho, \varphi) \in \mathbb{R}^2$

$$\begin{cases} \rho = \max\limits_{x\in[0,1]} \left(\dfrac{r(x) - \mu(x)\varphi}{d(x)}\right), \\ \varphi = \dfrac{\rho}{k_2} \displaystyle\int_0^1 \frac{\psi(y)\,\omega(x(\rho,\varphi), y)}{\nu(y)\rho + k_1}\, dy. \end{cases} \tag{4.44}$$

Remark 4.3.1. *If one makes the additional assumption (4.27), ρ is bounded away from 0 and hence we must have $n^\infty \neq 0$. In other words, the only possible limits are of the form given by the above result if (4.27) holds.*

Proof. We assume that $n^\infty \neq 0$.

According to Proposition 4.3.1, both $t \mapsto \ell(t, \cdot)$ and $t \mapsto p(t, \cdot)$ converge pointwise to ℓ^∞ and p^∞ implicitly given by formulae (4.28).

Let us justify that φ converges. The bound (4.23) shows that the function $(t, y) \mapsto \psi(y)\ell(t, y)$ is dominated by the continuous function $y \mapsto \psi(y)\ell^M(y)$, hence by the dominated convergence theorem, we have

$$\lim_{t\to+\infty} \varphi(t) = \varphi^\infty := \int_0^1 \psi(y)\ell^\infty(y)\, dy = \frac{1}{k_2} \int_0^1 \left[\frac{\psi(y)}{\nu(y)\rho^\infty + k_1} \int_0^1 \omega(x, y)\, dn^\infty(x)\right] dy. \tag{4.45}$$

The asymptotic behaviour of n is exponential, governed by $r(x) - d(x)\rho^\infty - \mu(x)\varphi^\infty$, a quantity whose sign we now analyse.

In fact, for a fixed $x \in [0,1]$, $t \mapsto n(t,x)$ solves an exponential ODE (*i.e*, of the form $z'(t) = a(t)z(t)$), whose time-dependent rate asymptotically approaches $r(x) - d(x)\rho^\infty - \mu(x)\varphi^\infty$. We may hence analyse its sign as follows.

i) If $r(x_0) - d(x_0)\rho^\infty - \mu(x_0)\varphi^\infty > 0$ for some $x_0 \in [0,1]$, then by continuity there exists an nontrivial interval $I \subset [0,1]$ containing x_0, along which $r(x) - d(x)\rho^\infty - \mu(x)\varphi^\infty \geq 2\varepsilon$ for small enough. Since the convergence of $r(x) - d(x)\rho(t) - \mu(x)\varphi(t)$ towards $r(x) - d(x)\rho^\infty - \mu(x)\varphi^\infty$ as $t \to \infty$ is uniform with respect to $x \in [0,1]$, there exists $t_0 > 0$ such that $r(x) - d(x)\rho(t) - \mu(x)\varphi(t) \geq \varepsilon$ for all $t \geq t_0$ and $x \in I$. Writing the solution (4.11) in implicit form gives for all $t \geq 0$

$$n(t,x) = n(t_0,x)\, e^{\int_{t_0}^t (r(x) - d(x)\rho(s) - \mu(x)\varphi(s))\, ds},$$

which after integration over $[0,1]$ leads to

$$\rho(t) = \int_0^1 n(t,x)\, dx \geq \int_I n(t_0,x)\, e^{\int_{t_0}^t (r(x) - d(x)\rho(s) - \mu(x)\varphi(s))\, ds}\, dx \geq |I| \inf_{x\in I} n(t_0,x)\, e^{\varepsilon(t-t_0)}.$$

with $|I|$ the Lebesgue measure of I. Recalling the assumption (4.13), the continuous function $n(t_0,\cdot)$ is also positive, which shows that $\inf_{x\in I} n(t_0,x) > 0$. Since the right-hand side goes to $+\infty$, we obtain a contradiction with the convergence of ρ.

ii) If $r - d\rho^\infty - \mu\varphi^\infty < 0$ on the whole of $[0,1]$, one readily proves that ρ converges to 0 which is incompatible with the convergence of ρ to a positive limit (since $n^\infty \neq 0$).

The function $r - d\rho^\infty - \mu\varphi^\infty$ is thus non positive on $[0,1]$, and its maximum equals 0. This is equivalent to saying that $\rho^\infty = \max(\frac{r-\mu\varphi^\infty}{d})$. Assumption (4.43) ensures that the maximum point $x^\infty := x(\rho^\infty, \varphi^\infty)$ is unique. Furthermore, the first bullet further shows that $n(t,x)$ vanishes at any other point x than $x \neq x^\infty$. We have thus proved that n concentrates at x^∞, hence $n^\infty = \rho^\infty \delta_{x^\infty}$.

Finally, inserting $n^\infty = \rho^\infty \delta_{x^\infty}$ into the formula (4.45), we obtain the second equation, concluding the proof. □

Remark 4.3.2. *In general, there is no close formula for the solutions of (4.44), which may not be unique. In practice, this system is easily solved numerically, for instance by a fixed point method. Hence, assuming convergence of n, this theorem does provide a rather complete picture of the possible non-trivial limits the system may reach. When there exists a unique solution to (4.44), a single such limit is hence characterised.*

4.3.1.4 Asymptotics in the adaptive case

We now sketch the extension of Theorem 4.3.1 to the (more general) case where φ depends on x. In this case, we may obtain a result similar to Theorem 4.3.1, but at the expense of an assumption stronger than (4.43) and a more intricate system solved by the stationary state.

Indeed, keeping the same notations, we make the assumption that for all $0 < \bar{\rho} \leq \rho^M$ and for all functions $\bar{\ell} \in \mathcal{C}([0,1])$ satisfying $0 \leq \bar{\ell}(y) \leq \ell^M(y)$,

$$\arg\max_{x\in[0,1]} \left(r(x) - d(x)\bar{\rho} - \mu(x) \int_0^1 \psi(x,y)\bar{\ell}(y)\, dy \right) =: \{x(\bar{\rho}, \bar{\ell})\}. \tag{4.46}$$

Following the proof of Theorem 4.3.1, one can then prove in exactly the same way:

Theorem 4.3.2. *[42] Under the assumptions (4.13)-(4.14)-(4.46), supposing that n converges weakly in $\mathcal{M}([0,1])$ to some n^∞, then either $n^\infty = 0$ or n^∞ is of the form*

$$n^\infty = \rho^\infty \delta_{x^\infty},$$

where $x^\infty = x(\rho^\infty, \ell^\infty)$ and $(\rho^\infty, \ell^\infty)$ solves the following system over $(\rho, \ell) \in \mathbb{R} \times \mathcal{C}([0,1])$

$$\begin{cases} \rho = \max\limits_{x\in[0,1]} \left(\dfrac{r(x) - \mu(x) \int_0^1 \psi(x,y)\ell(y)\, dy}{d(x)} \right), \\ \ell(y) = \dfrac{\rho}{k_2} \dfrac{\omega(x(\rho,\ell), y)}{\nu(y)\rho + k_1}. \end{cases} \tag{4.47}$$

4.4 Numerical simulations

4.4.1 Simulations in the absence of treatment

4.4.1.1 Numerical approach and parameters

In this section, we present some numerical simulations of system (4.11). The simulations are performed in Matlab using the parameters listed in Table 4.1, which have been chosen arbitrarily in the absence of suitable experimental data, in order to reproduce different biological scenarios. We follow the numerical method given in [66] and we select a discretisation of the phenotype interval $[0,1]$ consisting of 1000 points for the computational domain of the independent variables x and y and let $t \in [0,T]$, unless otherwise specified, we choose the final time $T = 1000$.

To define the initial density of tumour cells, we use a Gaussian profile, and a homogeneous condition for competent immune cells ℓ, while the naïve immune cells p are distributed over the whole interval $[0,1]$ as follows:

$$\begin{cases} n^0(x) = n(0,x) = \frac{C}{\sqrt{2\pi\sigma_0^2}} \exp(\frac{-(x-m)^2}{2e^2}), \\ \ell^0(y) = \ell(0,y) = 0, \\ p^0(y) = p(0,y) = 1 - y^2, \end{cases} \tag{4.48}$$

with $m = 0.5, e = 0.1$, and a normalisation constant $C > 0$ chosen so that $\rho(0) = 1$. Thus, we start with a total mass equal to 1, and the phenotype x is initially concentrated at 0.5.

Remark 4.4.1.

- *For simulations illustrated on Figures 4.2-4.4, 4.6-4.8, 4.10-4.12, and 4.15-4.17:* ***Upper row****. Evolution in time of the densities $x \mapsto n(t,x)$ (left panel); $y \mapsto \ell(t,y)$ (central panel), and $y \mapsto p(t,y)$ (right panel), with the initial conditions in blue, and the final ones in red.* ***Lower row****. Dynamics of the total number of tumour cells $\rho(t)$ (left panel); dynamics of the total number of competent immune cells $\sigma(t)$ (central panel); dynamics of the total number of naïve immune cells $\gamma(t)$ (right panel).*
- *We will assume that the competent T-cells $\ell(t,y)$ are absent at time $t = 0$ and that the most aggressive naïve T-cells $p(t,y)$ have been duly informed by APCs and are already present at the tumour site.*

- *We have explored in simulations separately the innate, adaptive and mixed innate-adaptive cases characterised by different forms of the function φ, which all can lead to the three Es. No treatment with ICIs is considered here, ensured by setting $ICI = 0$. In agreement with Theorems 4.3.1 and 4.3.2, if convergence of the density of cancer cells occurs, we find that tumour cells asymptotically concentrate on a single phenotype, and total masses of cells all converge. Furthermore, the phenotype on which the cancer cell density concentrates as well as the asymptotic masses of cells have been checked to match the specific values uncovered by Theorems 4.3.1 and 4.3.2.*
- *We mention that the final time shown for densities and total numbers of cells might not be the same in a given plot. This is because total numbers of cells rapidly reach equilibrium while densities may converge slowly to their limit, at least when the limit is a Dirac mass.*

Parameter/function	Biological meaning	Value
$r(x)$	Proliferation rate of tumour cells	$0.666 - 0.132x^2$
$d(x)$	Death rate of tumour cells	$0.5(1 - 0.3x)$
$\mu(x)$	Sensitivity to the effects of the immune response	$1 - 0.1x^2$
$\psi(y)$	Efficacy of the immune response	$0.5y^2$
$\nu(y)$	Immunotolerance of immune cells induced by tumour cells	$0.5 - 0.1y$
k_1	Natural death rate of competent immune cells	0.5
k_2	Carrying capacity of naive immune cells	1.5
α	Strength of the immune response	1

Table 4.1: **Values of the model parameters/functions used to carry out numerical simulations.**

4.4.1.2 Tumour development in the absence of the immune response

We begin by establishing a baseline scenario in which tumour cells proliferate and die according to the modelling approach described in Section 4.3, i.e., in the absence of the immune response, the growth of the tumour cell population is of the logistic type.

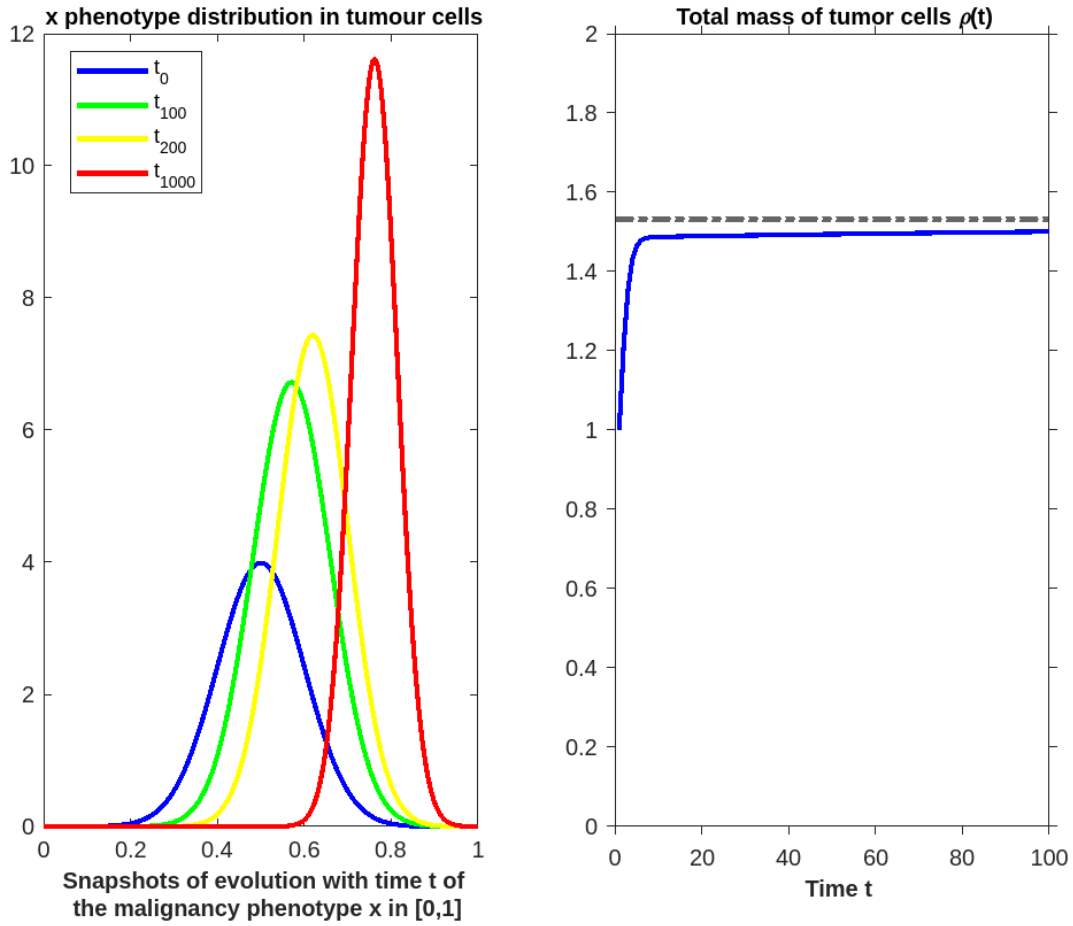

Figure 4.1: Numerical simulation of the solution to (4.16) (*complete absence of immune response*). **Left panel**, plots of cell densities $n(t,\cdot)$ at different times up to $T = 1000$ (in red): the phenotype x evolves towards more and more malignancy. **Right panel**, initial dynamics of the total mass of tumour cells $\rho(t)$ for t between 0 and 100. The black dashed line highlights a numerical estimation of the tumour cell carrying capacity $\rho^\star$ and the parameter values are as listed on Table 4.1, with $\rho(0) = 1$.

According to Section 4.3.1.1, we expect convergence of ρ and weak convergence of n to a weighted Dirac mass. More precisely, the phenotype at which the density of tumour cells concentrates is located at $\arg\max\{\frac{r}{d}\} = \{x^\star\}$, with $x^\star \approx 0.86$, which becomes apparent on Figure 4.1 to the left (and would be seen even more clearly if the simulations were run longer). Moreover, the limit for ρ is $\rho^\star = \max_{[0,1]} \dfrac{r(x)}{d(x)}$, which corresponds to the carrying capacity of the tumour, i.e., the saturation term reached by the total number of tumour cells due to within-population competition for space and resources. Here, $\rho^\star \approx 1.53$ and this is what we observe numerically on Figure 4.1 to the right.

As already mentioned in the introduction, we will from now on, when the immune response is activated, interpret solutions for which the total number of tumour cells approaches this carrying capacity $\rho^\star$ as "tumour escape". This represents one case of the three Es in which the immune cells are present at the tumour site but are inefficient in interacting with the tumour cells.

4.4.1.3 Simulations for the innate-immune response case

In the following subsection, we present numerical results for the *innate* (non-specific) anti-tumour immune response ($\varphi = \varphi(t)$), assumed to be due to the killing action on the tumour site of NK-lymphocytes, that have been activated in tissues and lymphoid organs by messages from circulating NK-cells. Each simulation is carried out by keeping all parameter values fixed as in Table 4.1, and taking three different choices of the parameter s, which is a measure of the precision of the localisation of the phenotype x with respect to the phenotype y at the tumour site: the smaller s is, the sharper the precision.

We also mention that, when the parameter s is small enough, the assumption (4.27) is no longer satisfied. Depending on the parameters and without this assumption, we may have $\rho(t) \to 0$ or convergence to a positive value. In the former case $\rho(t) \to 0$, no control with $ICIs$ would be necessary. According to what is expected from Theorem 4.3.1, the numerical results displayed in Figure 4.3 show that the tumour cell population $n(t, x)$ becomes concentrated as a Dirac mass centred at the point $x^\infty \approx 0.31$: it means that tumour cells become less and less malignant as time goes by. Both total densities $(\rho(t), \varphi(t))$ converge to their asymptotic values given by (4.44), which are numerically equal to $(\rho^\infty, \varphi^\infty) \approx (0.1873, 0.5750)$ (see figure 4.5, middle panel). Of note, the equilibrium situation can be recovered by taking $0 < s < 1$ large enough. As s increases, the equilibrium is reached faster, with less oscillations but it leads to an asymptotic state with a larger tumour mass, which is its apparent carrying (maximum) capacity, representing the "escape" state of the three Es of immunoediting (see Figure 4.4). Let us also mention that there is a perfect match between the asymptotic values given by Theorem 4.3.1 and the ones obtained numerically. As shown in Figure 4.5 in panels **(b)-(c)**, the function $\varphi(t)$ increases or oscillates until it reaches a maximum plateau; on the other hand, $\varphi(t)$ increases in a faster way, and it does not reach a plateau but directly decreases to 0 in panel **(a)** for a small value of s.

Dynamics of tumour cells, effector and naïve lymphocytes with $s = 0.01$

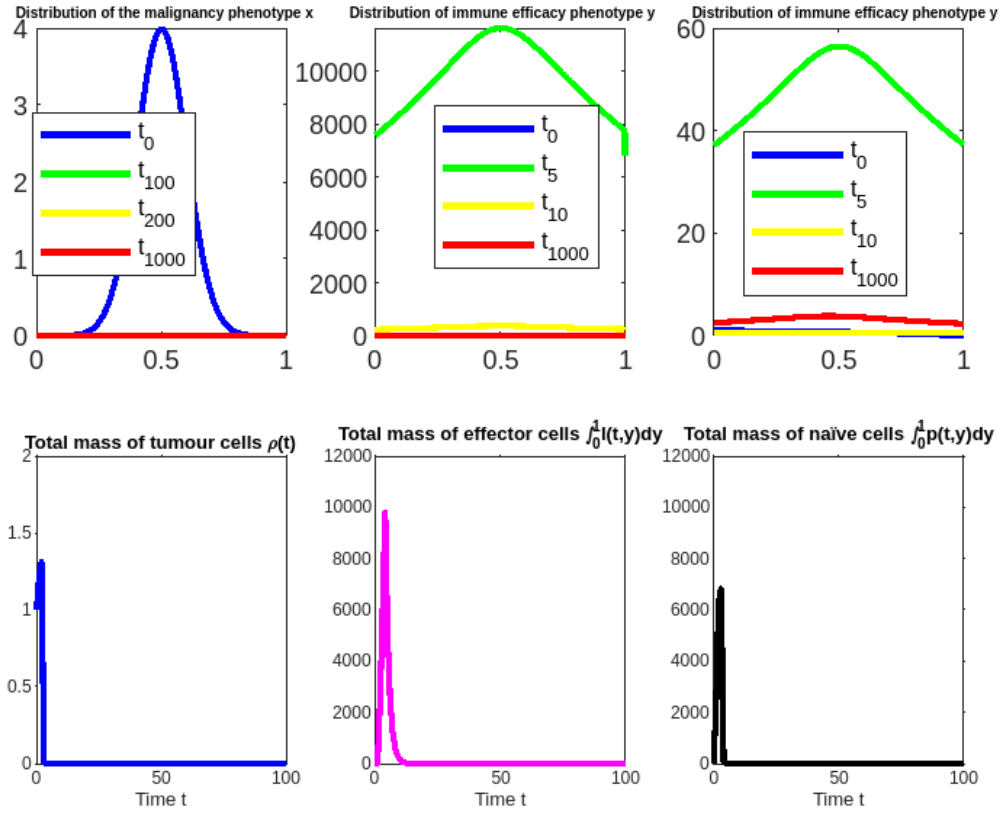

Figure 4.2: **Eradication.** Innate case (i.e., $\lambda = 0$).**Eradication**.Numerical simulations of (4.11) with $s = 0.01$ at different times up to $T = 1000$ in red (**upper row**) and initial evolution with time t from 0 to 100 of the total masses of cells $\int_0^1 n(t,x)\,dx$, $\int_0^1 \ell(t,y)\,dy$, $\int_0^1 p(t,y)\,dy$. The population of tumour cells is Gaussian-shaped, decreasing exponentially to 0, which means that the immune response becomes very effective and leads to the total eradication of tumour cells. Moreover, the phenotypic distribution of the tumour cells population remains unimodal throughout the entire time, with the mean phenotypic state being at the initial point of the distribution, while, both populations of NK cells are uniformly distributed over $[0, 1]$.

4.4.1.4 Simulations for the adaptive (specific) case

In the sequel, we keep the same model and data as in Table 4.1, but we deal with the adaptive specific anti-tumour immune response ($\varphi = \varphi(t,x)$), assumed to be related to the action on tumour cells of CD8+ T lymphocytes, that have been activated in lymphoid organs by APCs. We investigate the way in which the outcomes of the simulations are affected by key parameters whose impacts on the dynamics of tumour cells and T cells are biologically relevant. Such key parameters are the specificity s of the message transmitted by APCs to the lymphoid organs, and the specificity v of the anti-tumour immune response. Moreover,

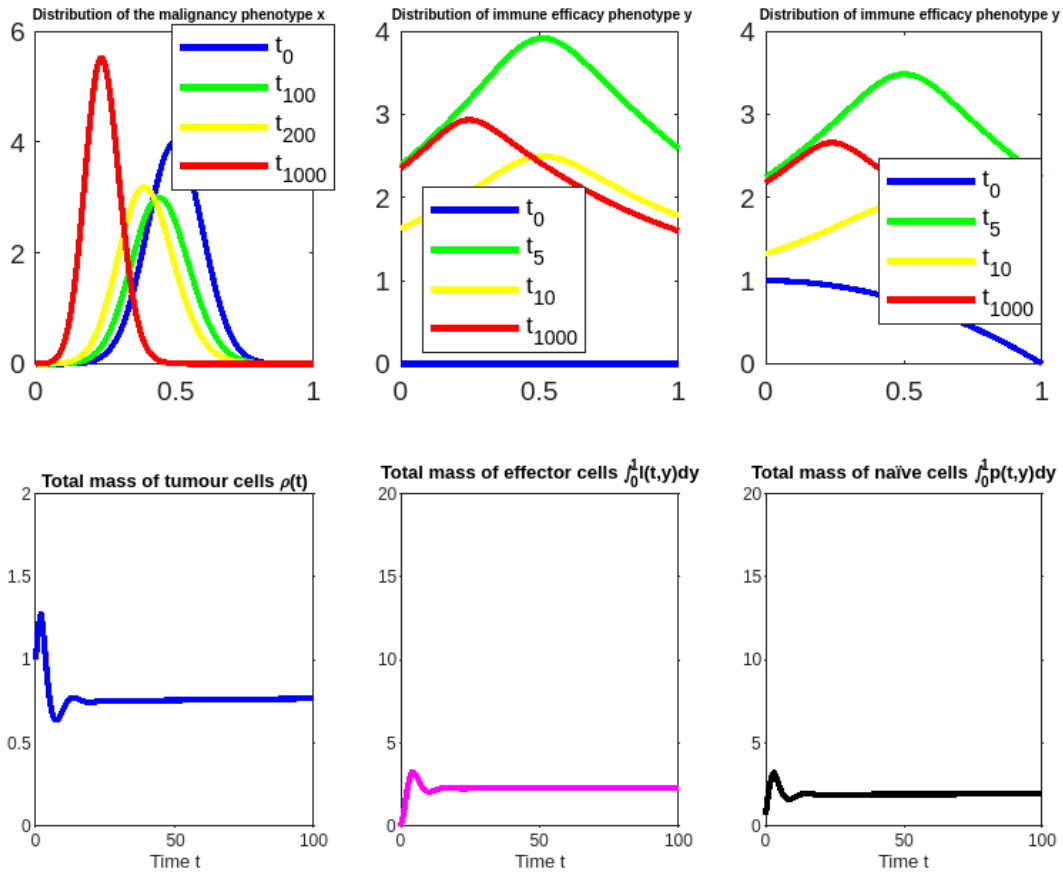

Figure 4.3: **Equilibrium.** Innate case (i.e., $\lambda = 0$). Numerical simulations of (4.11) with $s = 0.2$ at different times up to $T = 1000$ in red (**upper row**) and initial evolution with time t from 0 to 100 of the total masses of cells $\int_0^1 n(t,x)\,dx$, $\int_0^1 \ell(t,y)\,dy$, $\int_0^1 p(t,y)\,dy$. When the parameter s is large enough so that the condition (4.27) is satisfied, the total density of tumour cells decreases over time until it reaches a relatively small value. In the meantime, the population of tumour cells becomes less malignant (upper left panel).

having in mind to explore, further, than the strictly adaptive case in which $\varphi = \varphi(t,x)$, a mixed case representing both the non-adaptive activation (by sensing lacking MHC-I antigens on tumour cells) of the innate immune response ($\varphi = \varphi(t)$) by patrolling NK-lymphocytes, and the activation by APCs of the adaptive specific immune response ($\varphi = \varphi(t,x)$) by CD8+ T-cells, we will in the sequel also consider a convex combination of the two responses, of the form:

$$\varphi(t,x) = \int_0^1 \Psi(x,y)\ell(t,y)dy, \tag{4.49}$$

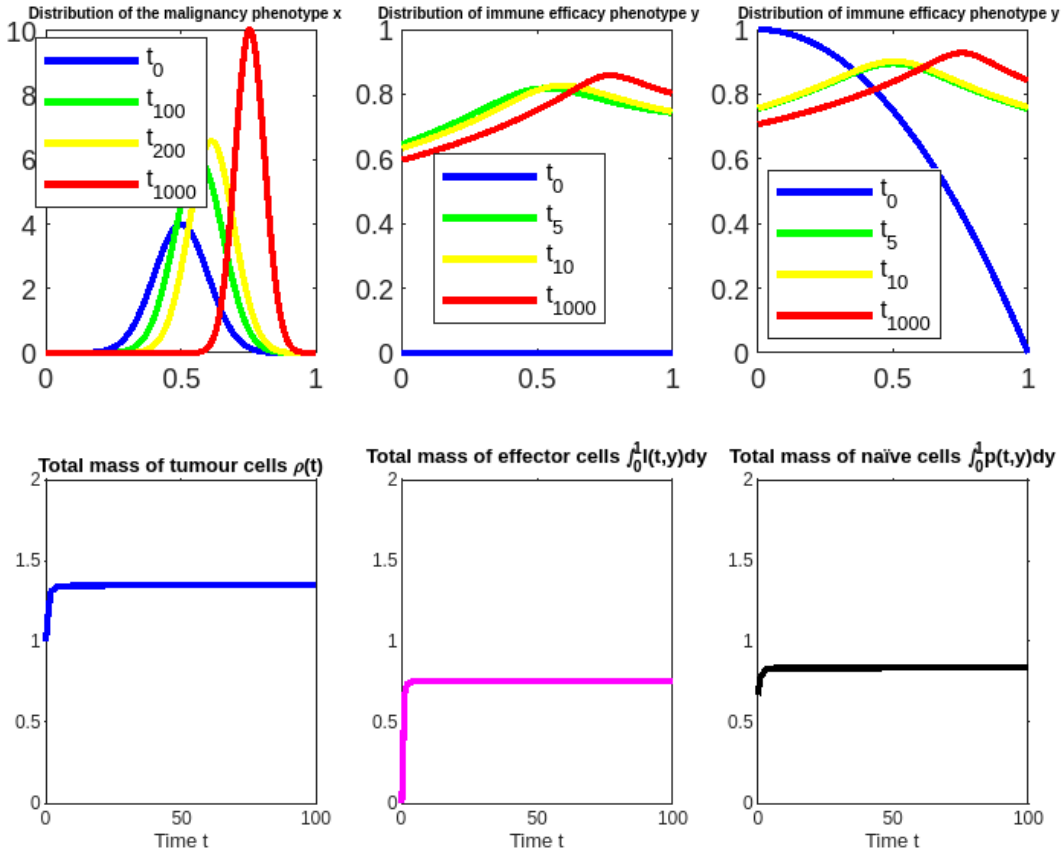

Figure 4.4: **Escape.** Innate case (i.e., $\lambda = 0$). Numerical simulations of (4.11) with $s = 1$ at different times up to $T = 1000$ in red (**upper row**) and initial evolution with time t from 0 to 100 of the total masses of cells $\int_0^1 n(t,x)\,dx$, $\int_0^1 \ell(t,y)\,dy$, $\int_0^1 p(t,y)\,dy$. The total number of tumour cells overtakes the total number of CD8+ T cells and keeps growing until saturation. The asymptotic total number of tumour cells is found to be very slightly below the carrying capacity $\rho^\star = \max_x(\frac{r(x)}{d(x)})$, in agreement with formula (4.44) for a relatively small value of φ^∞. The malignancy phenotype x is on the increase (upper left panel).

where the function Ψ is the following convex combination of the two cases

$$\Psi(x,y) = \left(1 - \lambda + \frac{\lambda}{v} e^{-|x-y|/v}\right) \psi(y), \quad \lambda \in [0,1], \tag{4.50}$$

with the aim to consider the two extreme cases, innate and strictly adaptive, together with a non-trivial convex combination of them. In this representation:

- $\lambda = 0$ corresponds to the *innate non-adaptive* anti-tumour immune response, already explored in section 4.4.1.3, and analysed in section 4.3.1.3;

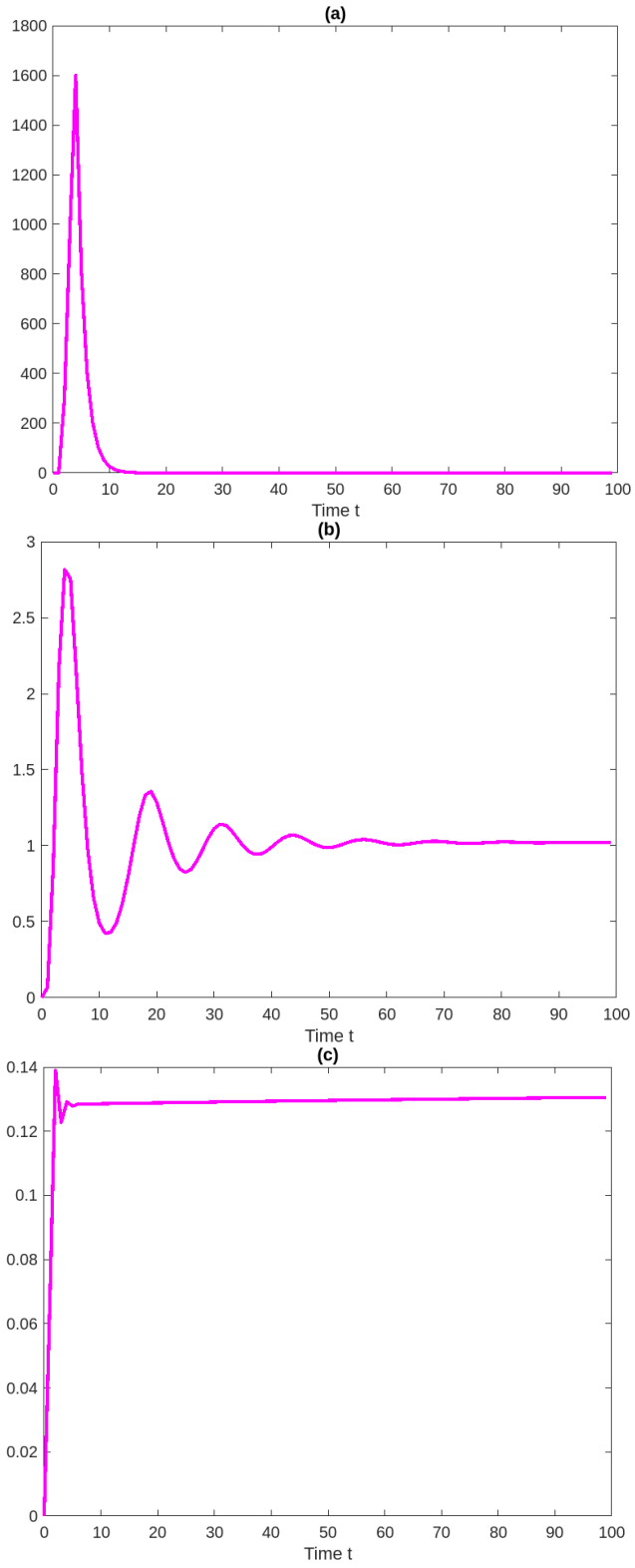

Figure 4.5: **Graphs of $t \mapsto \varphi(t)$: immune response mediated by NK-cells corresponding respectively to simulations of Figures 4.2-4.4. Three values of the parameter s are tested: a,c $s = 0.01$, $s = 0.2$, and $s = 1$ and all other values are reported in Table 4.1. Here the final time is $T = 100$**

.

- $\lambda = 1$ corresponds to the *strictly adaptive* anti-tumour immune response;
- $0 < \lambda < 1$ corresponds to cases for which both anti-tumour immune responses are active.

Note that such a convex combination is a simplified representation of the actual immune response, as we consider the two responses to be independent of one another, which is likely to not be the case of a real immune response. When the parameter s is small enough,

Dynamics of tumour cells, effector and naïve lymphocytes with $(s, v) = (1, 0.1)$

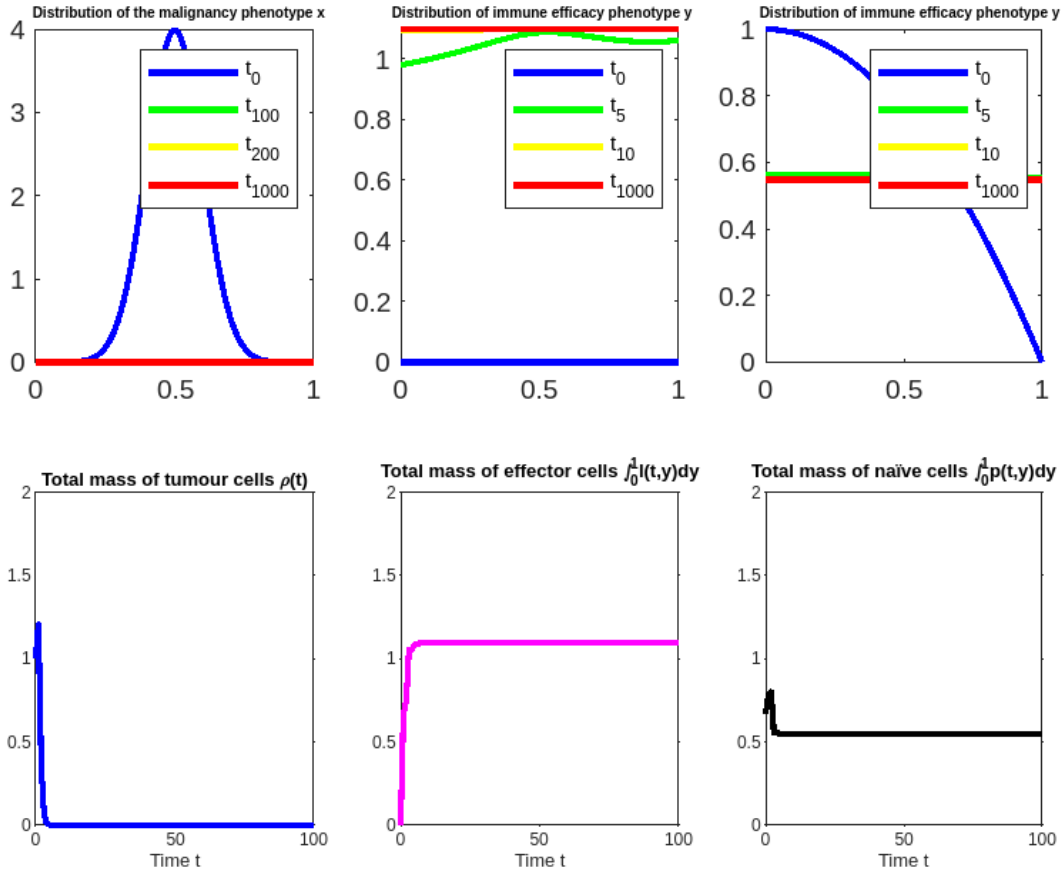

Figure 4.6: **Eradication.** Strictly adaptive case ($\lambda = 1$). Numerical simulations of (4.11) with $(s, v) = (1, 0.1)$ at different times up to $T = 1000$ in red (**upper row**) and initial evolution with time t from 0 to 100 of the total masses of cells $\int_0^1 n(t,x)\,dx$, $\int_0^1 \ell(t,y)\,dy$, $\int_0^1 p(t,y)\,dy$. As one can see on the right panels, with this highly precise value of the targeting parameter v, the total number of tumour cells decreases steadily over time until the tumour cell population is completely eradicated.

and for all considered values of the parameter v, the total number of tumour cells decreases steadily over time until the tumour cell population is completely eradicated (Figure 4.6).

Dynamics of tumour cells, effector and naïve lymphocytes with $(s, v) = (1, 0.5)$

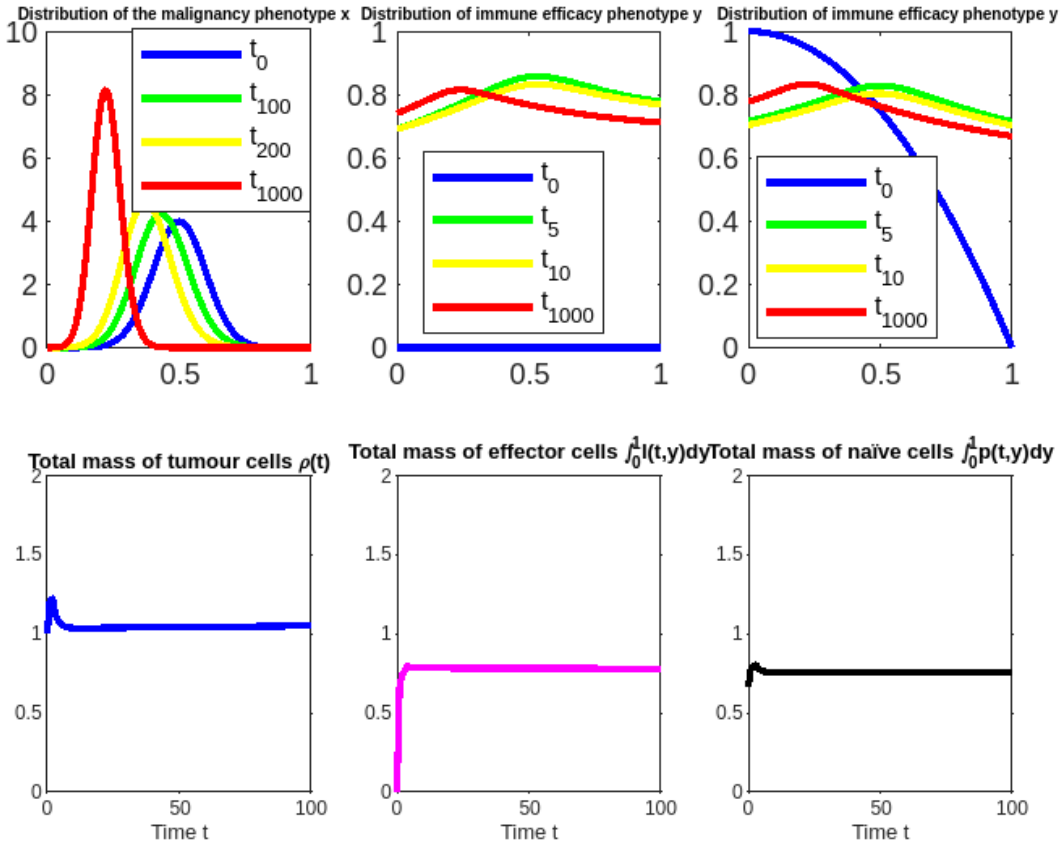

Figure 4.7: **Equilibrium.** Strictly adaptive case ($\lambda = 1$).Numerical simulations of (4.11) with $(s, v) = (1, 0.5)$ at different times up to $T = 1000$ in red (**upper row**) and initial evolution with time t from 0 to 100 of the total masses of cells $\int_0^1 n(t,x)\,dx$, $\int_0^1 \ell(t,y)\,dy$, $\int_0^1 p(t,y)\,dy$.

This is due to the fact that in the case of the strictly adaptive response, good transmission of the malignancy phenotype x by APCs (i.e., small values of the parameter s in the function $\chi(t,y)$) promotes the eradication of tumour cells by CD8+ T-lymphocytes cells. The results displayed on Figure 4.7 show that intermediate values of the parameter s and v facilitate the coexistence between tumour and immune CD8+ T-lymphocytes, while the total number of tumour cells remains at a low level. Finally, Figure 4.8 shows that under the choice of parameters in the computational simulations illustrated on Figure 4.7, increasing the value of the parameter v leads to tumour escape. These results suggest the idea that the efficiency of the anti-tumour immune response is affected by the specificity of the anti-tumour immune response and the specificity of the message transmitted by APCs to the naive T cells. In summary, increasing values of parameters s and v respectively is associated with low numbers

Dynamics of tumour cells, effector and naïve lymphocytes with $(s, v) = (1, 2)$

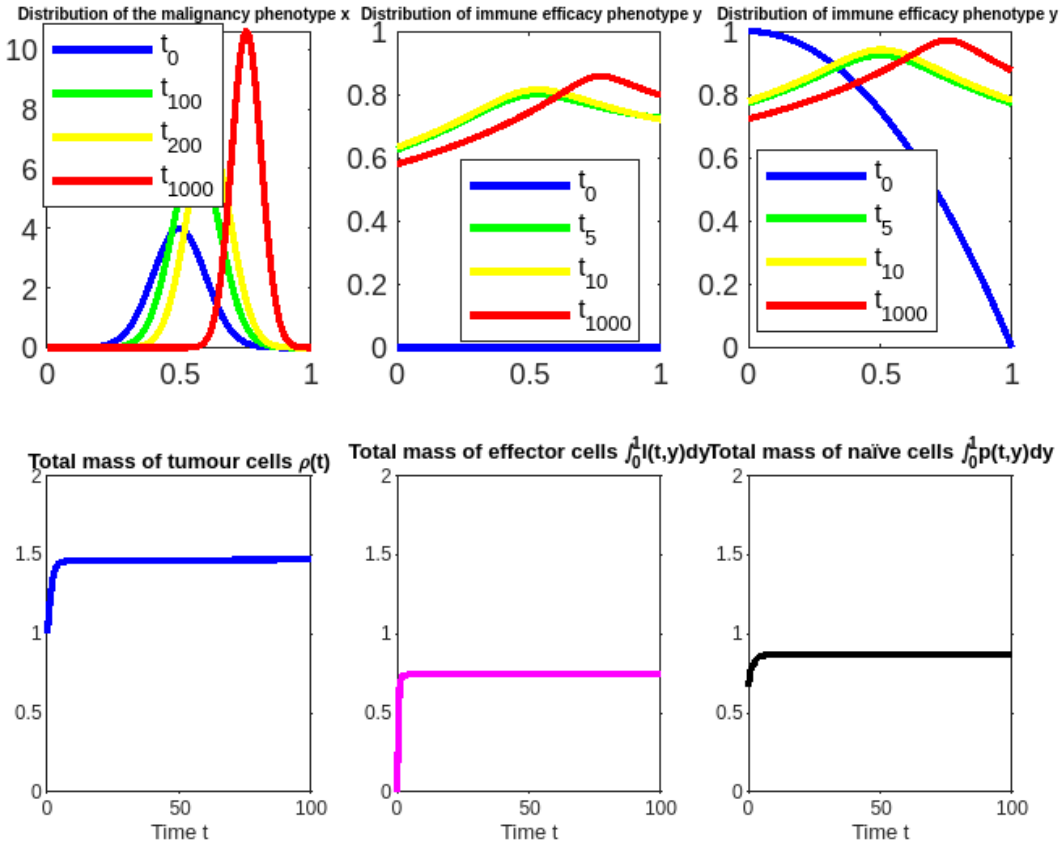

Figure 4.8: **Escape.** Strictly adaptive case ($\lambda = 1$). Numerical simulations of (4.11) with $(s, v) = (1, 2)$, plots of the population densities n, ℓ, p at different times up to $T = 1000$ in red (**upper row**) and initial evolution with time t from 0 to 100 of the total masses $\int_0^1 n(t, x)\, dx$, $\int_0^1 \ell(t, y)\, dy$, $\int_0^1 p(t, y)\, dy$ (**lower row**). Note that the total mass of tumour cells stabilises to a value close to the tumour carrying capacity $\rho^\star$ and the malignancy phenotype x concentrates onto a phenotype close to 1.

of immune cells and less effective immune response which may benefit tumour development. This is illustrated on the heatmap displayed on Figure 4.9, on which the value of the relative density $\frac{\rho^\infty}{\rho^\star}$ of total tumour cells at the end of numerical simulations are represented for different combinations of s and v, the values of the other parameters are as in Table 4.1, with $\lambda = 1$.

4.4.1.5 Combination of both innate and adaptive anti-tumour immune responses

In this subsection, we present numerical simulations that incorporate the innate and adaptive immune response by taking an intermediate value of the parameter $\lambda = 0.5$, and we compare

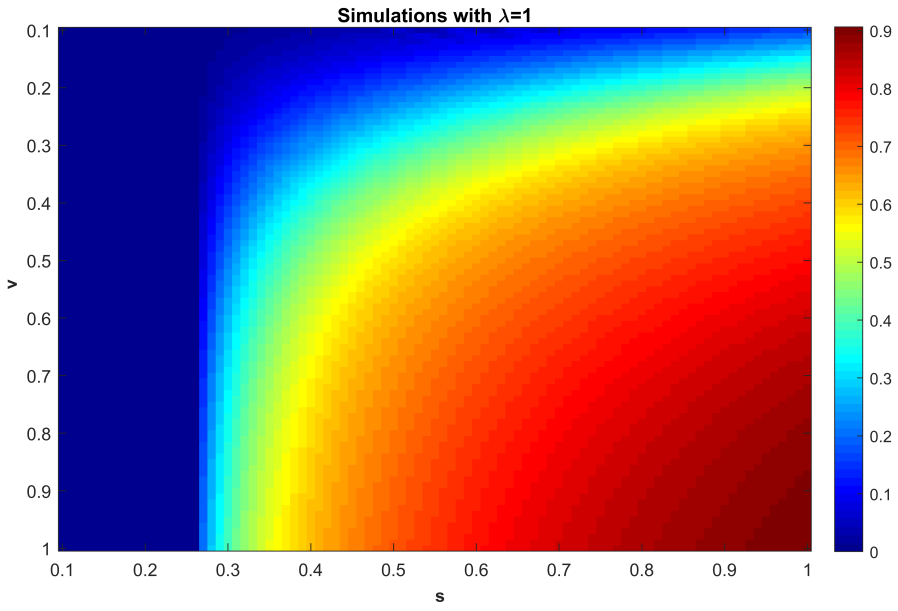

Figure 4.9: **Precision of detection parameter s vs. precision of targeting parameter v.** (Here, $\lambda = 1$). Heatmap representation of the contribution of the two localisation kernel parameters s and v to the relative density $\frac{\rho^\infty}{\rho^\star}$ of total tumour cells at the end of simulations, in the case without treatment. Recall that $\rho^\star$ is the maximum possible density (the carrying capacity) of tumour cells.

these results with those displayed in the previous paragraphs. We will numerically show how the outcomes of the tumour-immune response interactions change as we vary the specificity of the anti-tumour immune response v for a fixed value of $s = 1$. All the values of the other parameters and functions are as in Table 4.1. As shown on Figures 4.10-4.12, for intermediate values of the parameter λ in $[0, 1]$, dynamics similar to those of a strictly adaptive anti-tumour immune response are observed numerically in the case of a mixed anti-tumour immune response. More precisely, for low values of the parameter v, the specific anti-tumour immune response involving CD8+ T-lymphocytes is relatively high, leading to the total eradication of tumour cells; intermediate values of v lead to a co-existence state representing tumour-immune response equilibrium; and finally, sufficiently high values of v decrease the efficiency of the specific immune response and lead to the emergence of malignant tumour cells. This is illustrated on Figure **??**, on which one can in particular see (upper horizontal panel of the heatmap) that even with high values of s, low values of v (i.e., wide detection, narrow targeting), a mixed innate/adaptive immune response can still yield low values of the total density of tumour cells. Taken together, the numerical results that we

Dynamics of tumour cells, effector and naïve lymphocytes with $(s, v) = (1, 0.1)$

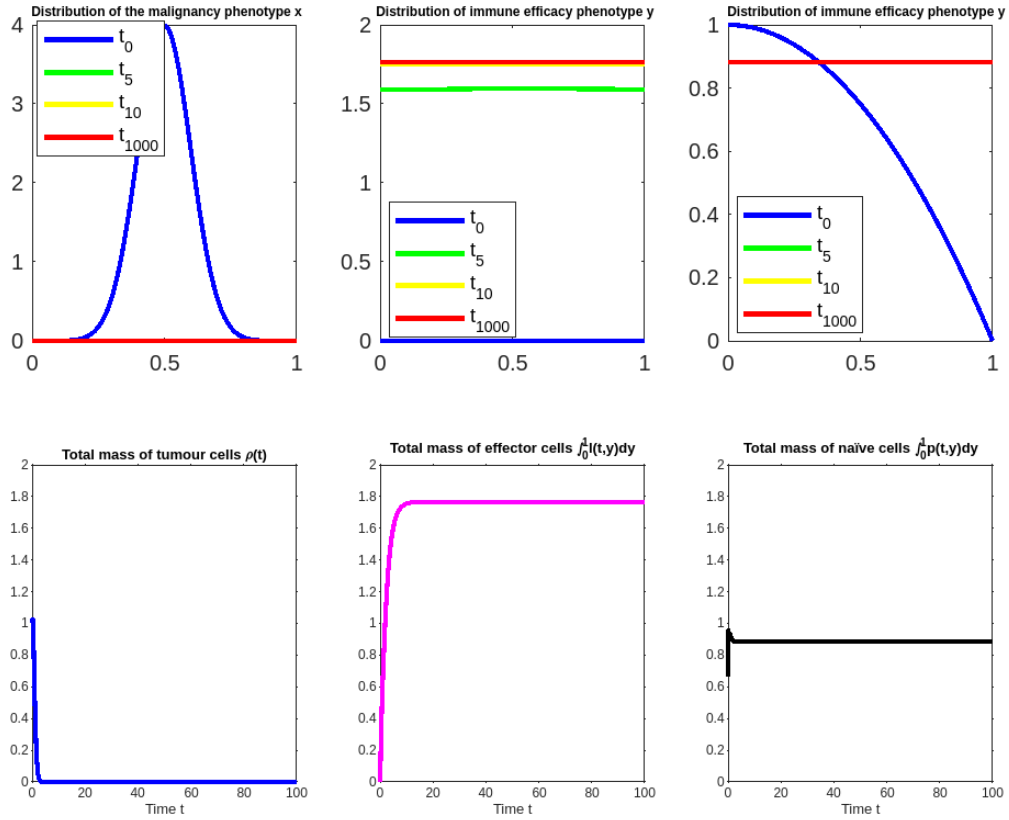

Figure 4.10: **Eradication.** Mixed innate/adaptive case ($\lambda = 0.5$). Numerical simulations of (4.11) with $(s, v) = (1, 0.1)$ at different times up to $T = 1000$ in red (**upper row**) and initial evolution with time t from 0 to 100 of the total masses of cells $\int_0^1 n(t, x)\, dx$, $\int_0^1 \ell(t, y)\, dy$, $\int_0^1 p(t, y)\, dy$. As one can see on the right panels, eradication comes quickly with this highly precise value of the targeting parameter v.

have presented in the previous subsections suggest that the model has validity for providing a consistent qualitative description of the anti-tumour immune response involving both NK cells and CD8+ T-lymphocytes.

Periodic solutions. We now numerically address the existence of periodic solutions. We first take all the parameters and functions to be equal to those chosen for the ODE model in the periodic case, those used to obtain Figure 3.3. Then, we perturb them by a small parameter $0 < \delta \ll 1$. In this case, an oscillatory behaviour also emerges, corresponding to a co-existence state representing a time-dependent periodic solution, see Figure 4.14. We have not been able to analytically address the existence of periodic solutions, except for the

Dynamics of tumour cells, effector and naïve lymphocytes with $(s, v) = (1, 0.5)$

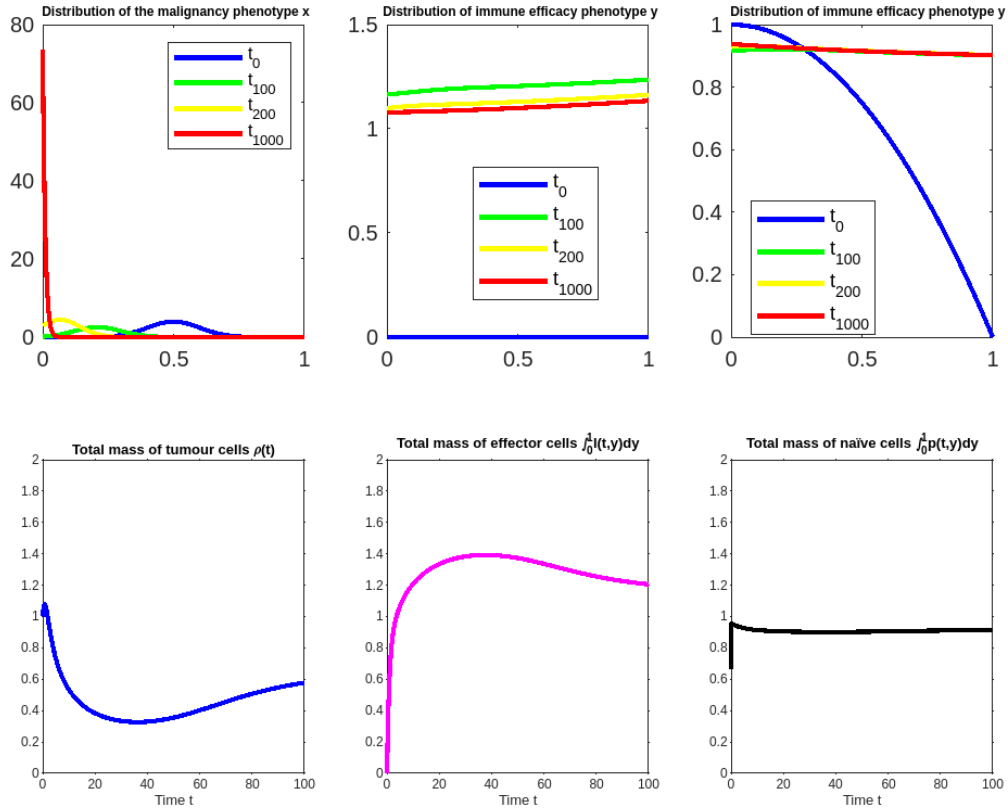

Figure 4.11: **Equilibrium.** Mixed innate/adaptive case ($\lambda = 0.5$). Numerical simulations of (4.11) with $(s, v) = (1, 0.5)$, plots of the population densities n, ℓ, p at different times up to $T = 1000$ in red (**upper row**) and initial evolution with time t from 0 to 100 of the total masses of cells $\int_0^1 n(t, x)\, dx$, $\int_0^1 \ell(t, y)\, dy$, $\int_0^1 p(t, y)\, dy$ (**lower row**). Note that the total mass of tumour cells stabilises at an intermediate value between extinction and the tumour carrying capacity, and that the malignancy phenotype x concentrates on the phenotype 0.

very specific case where all functions are constant, in which case we recover 3.3, for which we know periodic solutions do exist (cf. Theorem 3.4.1, Section 3.4 Chapter 3).

4.4.2 Numerical simulations with constant drug doses

4.4.2.1 Increasing *ICIs*: from escape to equilibrium

The results presented in the previous subsections summarise how the three Es of immunoediting can occur under different combinations of values for the parameters s and v. We now explore the possible outcomes of immunotherapy with immune checkpoint inhibitors where

Dynamics of tumour cells, effector and naïve lymphocytes with $(s, v) = (1, 1)$

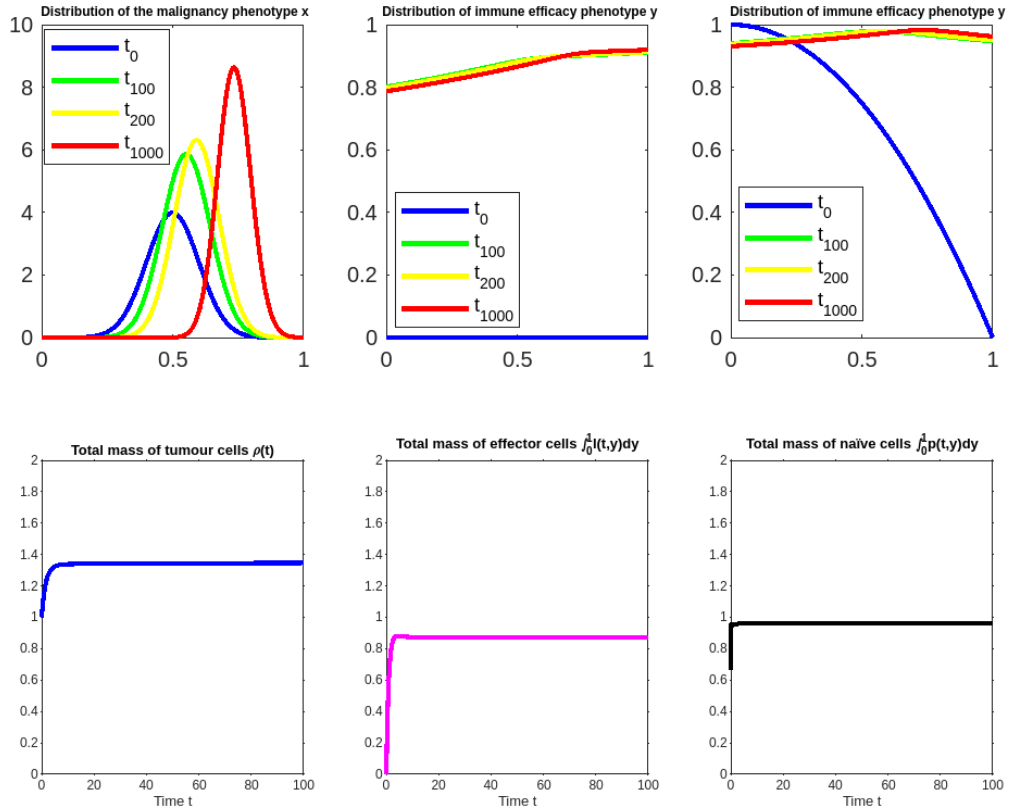

Figure 4.12: **Escape.** Mixed innate/adaptive case ($\lambda = 0.5$). Numerical simulations of (4.11) with $(s, v) = (1, 1)$, plots of the population densities n, ℓ, p at different times up to $T = 1000$ in red (**upper row**) and initial evolution with time t from 0 to 100 of the total masses $\int_0^1 n(t, x)\, dx$, $\int_0^1 \ell(t, y)\, dy$, $\int_0^1 p(t, y)\, dy$ (**lower row**). Note that the total mass of tumour cells stabilises to a value close to the tumour carrying capacity $\rho^\star$ and that the malignancy phenotype x concentrates around a phenotype close to 1.

only the adaptive anti-tumour immune response is active (i.e., $\lambda = 1$). This corresponds to a biological scenario in which anti-PD1 immunotherapy is used to boost the exhausted T-cells.

We will in what follows present numerical simulations with constant (in time) control ICI. In particular, we placed ourselves in the same configuration as on Figure 4.8, a choice of parameters that resulted, with $ICI = 0$, in tumour escape. We numerically solve the same mathematical problem considered in the previous subsections taking now ICI to be constant over time, from $ICI = 1$ to $ICI = 10$.

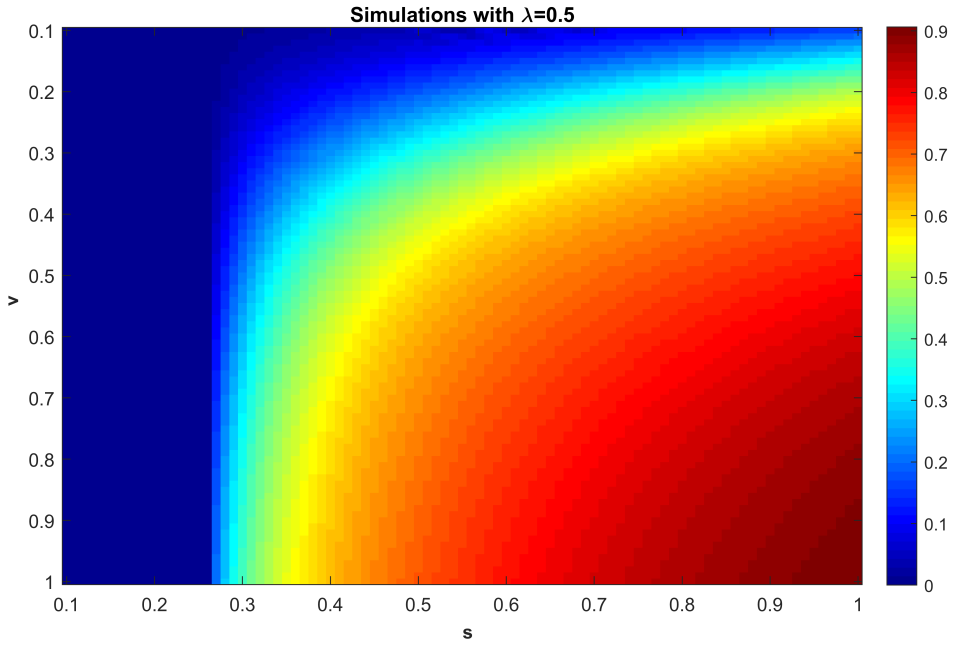

Figure 4.13: **Precision of detection parameter s vs. precision of targeting parameter v.** (Here again, $\lambda = 0.5$). Heatmap representation of the contribution of the two localisation kernel parameters s and v to the relative density $\frac{\rho^\infty}{\rho^\star}$ of total tumour cells at the end of simulations ($T = 500$), in the case without treatment. Recall that $\rho^\star$ is the maximum possible density (the carrying capacity) of tumour cells. Of note, as already mentioned above, one can see that, provided that the precision of detection is high enough (low values of the parameter s, between 0.1 and 0.25), whatever the precision of the targeting parameter v in a wide range between 0.1 and 1, the immune response yields extinction or quasi-extinction of the tumour mass (deep blue rectangular zone on the left). Conversely, for values of poor precision of s and v, here (s, v) in a neighbourhood of $(1, 1)$, one can see that anti-tumour efficacy of the immune response is poor.

Controlling tumour growth with $ICIs$. The numerical results shown on Figure illustrate the impact of a constant control $ICI = 10$, which allows to maintain the total mass of tumour cells $\rho(t)$ close to its initial value $\rho(0)$, whereas the population of tumour cells becomes concentrated as a Dirac mass centred at the point $x^\star 0.28$ corresponding to a less aggressive phenotype. Comparing these results with those displayed on Figure , we see that in general, for the same values of the parameters s and v, taking $ICI = 10$ slightly increases the number of competent immune cells and reduces tumour growth, taking the tumour below its carrying capacity, which represents an "equilibrium" among the three Es. However, one can note that the tumour is not eradicated (and this holds whatever the chosen level of ICIs).

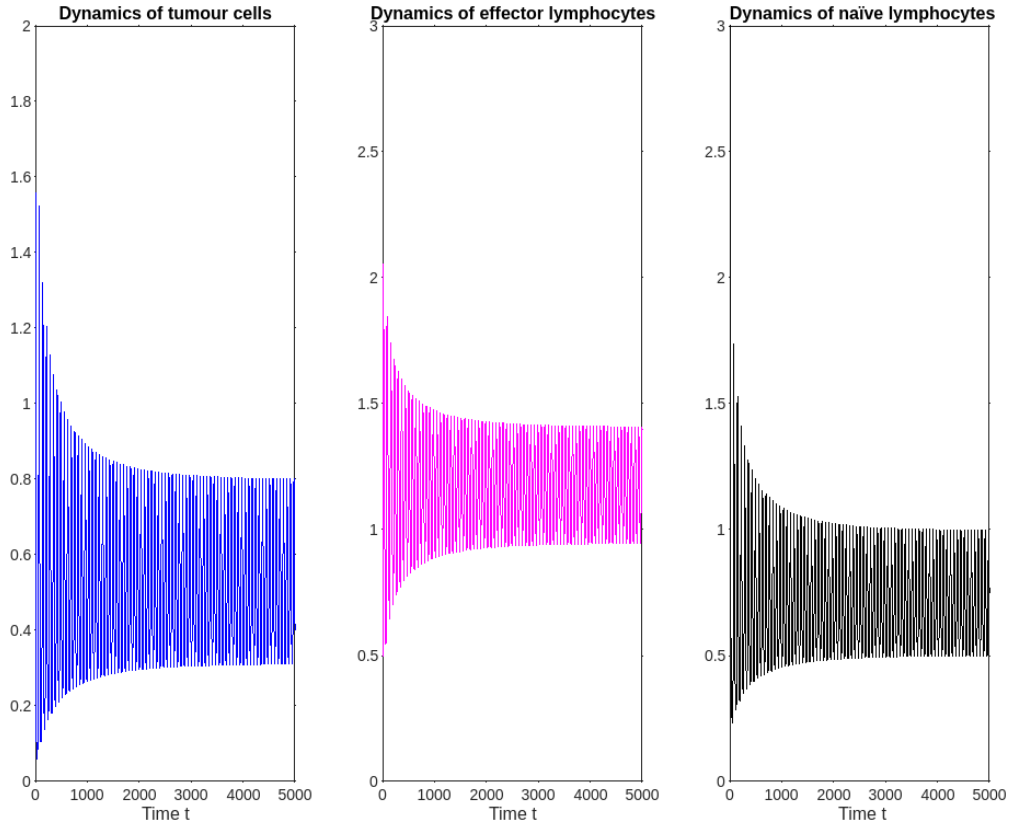

Figure 4.14: Evolution with time of the tumour total density $\rho(t)$ (in blue), competent T cells total density $\sigma(t) = \int_0^1 \ell(t,y)\,dy$ (in magenta), and the total density of naïve T cells $\int_0^1 p(t,y)\,dy$ (in black) for $T = 5000$.

4.4.2.2 Possible extinction with ICIs with a different function ν

This last unsatisfactory remark leads us to nevertheless illustrate how a slightly modified version of the same model can show a situation in which increasing the level of *ICIs* can bring the tumour from escape or equilibrium to extinction. We define a new version of the immunotolerance function ν by

$$\nu(y) = 1 - 0.1y, \tag{4.51}$$

and set the parameter for the natural death rate of competent T cells to $k_1 = 0.01$, keeping the other parameters as in Table 4.1.

Efficacy of the immune response. With this new function, the simulation shown on Figure 4.15, with $ICI = 10$ is completely modified, as can be seen on Figure 4.17, compared to Figures 4.15 and 4.16. Indeed, this time, the strategy consisting of taking a constant

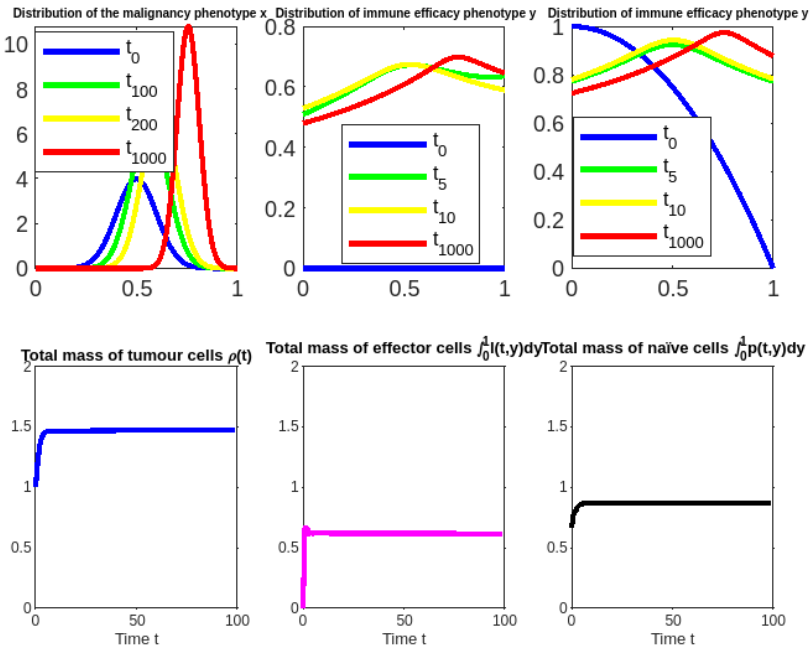

Figure 4.15: **Escape.** Numerical simulations of (4.1) with $\lambda = 1$ (T-cells only), $(s, v) = (1, 2)$, without treatment, and with the new function ν defined by 4.51, for the same simulation setup as of Figure 4.8 (strictly adaptive case, i.e., $\lambda = 1$). Here, $k_1 = 0.01$. Plots of the population density of tumour cells n at different times up to $T = 1000$ in red (**left panel**) and initial evolution with time t from 0 to 100 of the total mass $\int_0^1 n(t, x)\, dx$ (**right panel**). The black dashed line stands for the tumour carrying capacity $\rho^\star$. As shown on the left panel, the malignancy phenotype level is high.

control with *ICIs* restores the immune efficacy and allows for the total eradication of tumour cells. These results also suggest that acting by $ICIs$ to modify the immunotolerance function ν in a different way, not only by just dividing its amplitude by means of the term $1 + hICI$, and on k_1, may promote effective therapies with immune checkpoint inhibitors which affect the total density of tumour cells. Of course, one would then have to better define in some physiological way the immunotolerance function ν, which is so far arbitrary. Such better, more physiological, definition would nonetheless require access to experimental measurements, which is presently beyond our reach.

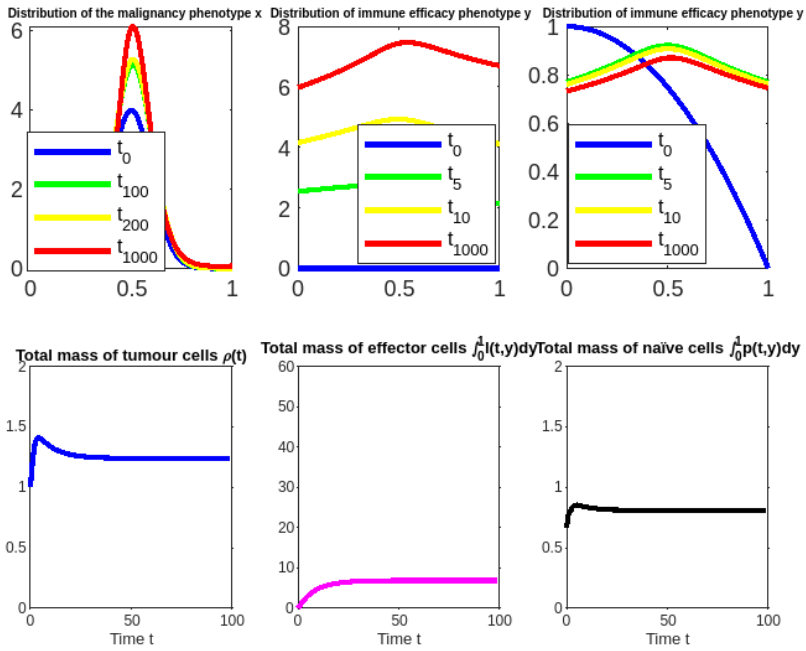

Figure 4.16: **Equilibrium.** Simulation with $ICI = 1$ and $h = 10$, with the new function ν defined by 4.51 (strictly adaptive case). Here, $k_1 = 0.01$, and all the other parameters and functions are as in Table 4.1. Increasing the level of $ICIs$ from 0 to 1 has led the tumour from escape to equilibrium. As shown on the left panel, the malignancy phenotype has notably decreased.

4.5 Discussion, conclusions and research perspectives

4.5.1 Summary of the mathematical results

In this chapter, we have proposed a new mathematical model of tumour-immune interactions in which cell populations are structured by continuous phenotype variables representing their aggressiveness. Despite its simplicity, our model features some relevant phenomena, and it captures the three *E*s of immunoediting - eradication, equilibrium and escape. In particular, it reproduces the formation of an equilibrium, which characterises the capacity of the immune system to contain tumour growth.

In Section 4.3, we showed through an asymptotic analysis of the model that under the *a priori* assumption that the population of tumour cells converges to a certain measure, such a measure can precisely be characterised when it is not the trivial measure.

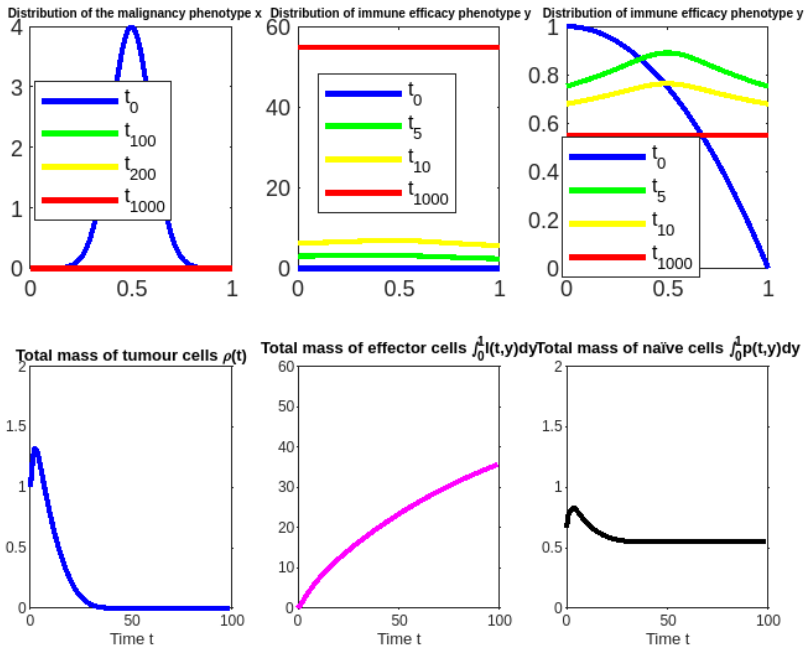

Figure 4.17: **Eradication**. Simulation with $ICI = 10$ and $h = 10$, with the new function ν defined by 4.51 (strictly adaptive case). Here, $k_1 = 0.01$, and all the other parameters and functions are as in Table 4.1. Increasing the level of $ICIs$ to 10 has led the tumour from escape/equilibrium to eradication.

Our model can incorporate three different types of anti-tumour immune responses: innate, adaptive, and a combination of both immune responses. By numerically comparing these three cases in Section 4.4, the outcomes are as follows:

Innate anti-tumour immune response. If the parameter s, which determines how localised the phenotype x is with respect to the phenotype y, is small enough, then the tumour is always eliminated. For intermediate values of s, we obtain convergence to a limit coherent with Theorem 4.3.1: a coexistence state occurs, yielding a persistent tumour cell population at a controlled level. Finally, high values of the parameter s reduce the efficiency of the anti-tumour immune response and lead to tumour escape. For particular choices of the model parameters, the numerical results also show periodic solutions, characterised by periodic alternating growth and decay of all the immune and tumour cell populations.

Adaptive anti-tumour immune response. The numerical results that we have presented demonstrate that within the adaptive anti-tumour response, both the specificity of

the response of competent immune cells (i.e., the parameter v) and the specificity of the message transmitted by APCs (i.e., the parameter s) play a key role in the tumour-immune interactions. In fact, when s and v are both small, our results indicate that tumour eradication can occur, while higher values of s or v may result in tumour escape.

Combination of the innate and the adaptive anti-tumour immune responses. Increasing the specificity of the adaptive immune response (low values of the parameter v) has a beneficial effect on the immune response to tumours, whereas higher values of the parameter v can be detrimental to the anti-tumour immune action.

Simulations of the effect of constant drug doses. The numerical simulations displayed in Section 4.4.2.1 show that a constant control allows to maintain the total density of tumour cells below its carrying capacity and prevents malignant tumour cells from taking over the whole population. We have also shown that slightly changing the immunotolerance rate along with the natural death rate of competent T cells improves the immune check-point inhibitor's immunotherapy efficacy and that they can bring tumours from escape to eradication.

4.5.2 Biological interpretations.

Taking for granted the existence of a continuous malignancy trait in tumour cells, that we relate to a 'degree of stemness' or de-differentiation potential, and similarly, of a continuous potential of tumour cell-kill in lymphocytes at the contact of tumour cells, we have qualitatively produced scenarios that reproduce the three Es of immunoediting. We have shown that the initial malignancy trait of tumour cells is affected by the immune response, with or without boosting by ICI therapy, and that it will always concentrate on a pointwise value, meaning that tumour cells as a population organise their stemness trait around a fixed dominant characteristic. Whether this sharp malignancy trait is increased or decreased by the immune response cannot *a priori* be decided, as its determinants depend in a complex way on the entangled functions d, r, μ and φ that govern the proliferation of the tumour cell population. If this model has some relevance with the reality of antitumoral immune response, it means that the effect of lymphocytes attacking a tumour may as well increase or decrease its stemness, which to the best of our knowledge is not inconsistent with biological

observations so far. From a therapeutic point of view, we have shown, as proofs of concept, numerical case studies in which a tumour can be brought from escape to extinction, or at least equilibrium, by continuous delivery of ICIs.

4.5.3 Possible generalisations.

i) Firstly, we plan to extend the model considered in this paper to carry out a mathematical study of tumour-response interactions, taking into account non-genetic instability, which may be considered as mediated by random epimutations in populations of tumour cells. In this respect, a modelling approach analogous to the one presented in [52], would consist in modifying system 4.1 as follows:

$$\begin{cases} \dfrac{\partial n}{\partial t}(t,x) = \left[r(x) - d(x)\rho(t) - \mu(x)\varphi(t,x)\right] n(t,x) \left[+\beta \dfrac{\partial^2 n}{\partial x^2}(t,x)\right], \\ \dfrac{\partial \ell}{\partial t}(t,y) = p(t,y) - \left(\nu(y)\rho(t) + k_1\right) \ell(t,y), \\ \dfrac{\partial p}{\partial t}(t,y) = \alpha\chi(t,y)p(t,y) - k_2 p^2(t,y). \end{cases} \tag{4.52}$$

The linear diffusion operator $\beta\frac{\partial^2 n}{\partial^2 x}(t,x)$, with $0 < \beta \ll 1$, represents here a malignancy phenotype lability (uncertainty) linked to the extreme plasticity of cancer cells [72], that are able to vary their phenotype in response to any (drug or other environmental) insult.
ii) Another natural way to extend our work would be to introduce a population of antigen-presenting cells (APCs), that recognises a tumour antigen as their cognate one to activate naive T-cells, instead of the time-independent shortcut function $\omega(x,y)$ (see Section 4.2.3). Delays might also naturally be introduced in this bidirectional communication process.
iii) Future research perspectives, from the point of view of confronting the model to data, are to identify its parameters, making use of preclinical and clinical data on the growth of in-vivo tumours in laboratory rodents and in melanoma patients exposed to ICI therapies. This, however, will necessarily rely on long-term collaborations with teams of laboratory experimentalists and clinicians, towards whom we have here only set this physiologically based model as a basis for interactive discussions to assess it qualitatively.
(iv) Finally, as exemplified in [65], it would be relevant to address numerical optimal control of model 4.1 in order to identify possibly optimal delivery schedules for the ICI therapies, which

will also be intended in the framework of an interactive collaboration with experimentalists and clinicians.

Conclusion and research perspectives

5.1 Discussions and conclusions

Several clinical and experimental studies have recently shown that the immune system plays a decisive role, providing tumour control, long-term clinical benefits, and prolonged survival. Nevertheless, the anti-tumour immune response is a complex process that depends on many factors. In this context, mathematical models are useful tools for describing and predicting the dynamics of interactions between tumour cells and immune cells in order to propose new therapeutic strategies.

In this thesis, two mathematical models have been proposed to describe the tumour-immune interactions, with the goal of investigating the biological settings that allow for tumour eradication, tumour-immune equilibrium, or tumour escape.

We began this thesis by discussing the key biological processes and mechanisms involved in tumour-immune interactions, with a focus on the role of two types of immune cells: NK cells and cytotoxic T lymphocytes, which are the main actors in the anti-tumour immune response. The rest of chapter 1 was then devoted to describe processes that allow for tumour-immune escape and some immunotherapy techniques developed to boost or restore an effective anti-tumour immune response.

Tumour-immune interactions are studied not only in labs, but mathematical modelling can help in gaining a better understanding of tumour development and its immune escape process.

In chapter 2, we provide a short review of certain mathematical models describing tumour-immune interactions and their applications, with a focus on ordinary differential equations models and phenotype-structured models.

After these background chapters, we provided the main body of this thesis. This work was organised into two complementary chapters. Each chapter focused on a modelling approach to describe the interactions between tumour cells and immune cells. In particular, these models have been developed to investigate:

(1) the outcomes of the tumour-immune response dynamics, depending on the values of the biological parameters;
(2) the adaptation of the malignancy phenotype of the tumour cell population to a natural immune response with or without immunotherapy;
(3) the effect of the immune checkpoint inhibitor immunotherapy on the adaptive anti-tumour immune response.

Pursuing these goals, we have proposed new mathematical models of tumour-immune interactions in which tumour-immune interactions are represented at the level of cancer and immune cell populations and include different aspects of tumour-immune interactions. In particular, the mathematical models proposed in this thesis were formulated as follows:

(a) an integro-differential equations model of Lotka-Volterra type (Chapter 4), in which heterogeneity of the cell populations is taken into account by structuring variables that are continuous internal traits (aka phenotypes), representing a potential of "aggressiveness" (tumour malignancy vs. anti-tumour efficacy). The development of this model allows for representing the action of drugs enhancing the immune response. It has also raised associated questions in adaptive dynamics about the selection of some traits, which are considered as dominant traits by the environment. We showed through an asymptotic analysis of the model that, under the a priori assumption, the population of tumour cells converges to a certain measure, which can be precisely characterized when it is not the trivial measure. By means of numerical simulations, we explored the outcomes of three different types of anti-tumour immune responses: innate, adaptive, and a combination of both immune responses. More precisely, we have shown that the tumour cell population concentrates on a single phenotype and that the initial

malignancy trait of tumour cells is always affected by the immune response, with or without enhancement by immune checkpoint inhibitor therapy.

(b) an ordinary differential model, which was not formulated on the basis of biological or biophysical aspects but has been formally derived from the integro-differential model. Through linear stability analysis, we identified possible conditions on the model parameters leading to different dynamics, aiming for a more in-depth theoretical understanding of the system under consideration. The ODE model also exhibits an oscillatory behaviour in some parameter regimes.

Both the IDE model and the ODE model reproduce the three Es of immunoediting: Elimination, Equilibrium, and Escape. An excellent quantitative agreement between the numerical simulations of the two models was obtained. However, regarding the theoretical aspect, no general convergence result is to be expected for the IDE model, since it does have an ODE system with known possible periodic behaviour as a particular case. In this regard, finding which parameters lead to convergence or to oscillatory behaviours is a completely open question.

The results obtained in this thesis have shed light on:

(a) the way in which different parameters impact the dynamics of tumour-immune response interactions and induce tumour escape.

(b) the way in which a simple mathematical model can qualitatively reproduce the three Es of immunoediting, and underline the importance of including the effect of different parameters when exploring the action of drugs boosting the immune response.

5.2 Research perspectives

Other extensions than those already introduced at the end of each chapter are summarized in the following paragraph:

As already mentioned in Chapter 1, recent research in oncology indicates that immunotherapy is a promising anti-cancer treatment. The response to this new targeted therapy depends on many factors, among them the infiltration of cytotoxic T lymphocytes into the tumour. Galon and collaborators ([31], [32]) suggest that the different types of infiltration of tumours

by T lymphocytes are indicators of the prognosis. Based on the level of Immunocore, the authors proposed a classification of tumours into four different categories. The “hot category”, refers to the inflamed and infiltrated tumours with a large number of cytotoxic T cells in the centre of it and high Immunoscore. In this particular category, infiltrated activated T cells are exhausted or dysfunctional and express a number of inhibitory receptors. The ”altered-immunosuppressed” category is characterised by tumours with a small amount of infiltrated T cells. Tumours that enter the ”altered-excluded” category are characterized by two different regions: their margin is infiltrated by activated T cells while the centre is deprived of lymphocytes. The last category is ”cold” tumours, which are characterised by a low Immunocore and are often correlated to a poor response to immunotherapy since activated T cells are absent within the tumour and at the tumour borders. Building upon the results of these recent works, and the modelling approaches developed in [49], it might be interesting to extend the models considered in this thesis to carry out a mathematical study of tumour-response interactions, taking into account the spatial distribution of CTLs within the tumour. With the aim to investigate the impact of cytotoxic T lymphocyte infiltration on tumour development. This should lead us to also structure the populations of cells according to an added space variable to describe the random motion of tumour cells and CTLs. For possible tumour-immune response interaction models taking space into account, we refer to ([5], [57], [58]).

The improvement of anti-tumour therapies and their combinations is an important goal in oncology. The improvement of anti-tumour therapies and their combinations is an important goal in oncology. In this context, it would be interesting to include in our models the effects of different types of therapies. By making use of optimization and optimal control methods, it would be possible to design the best delivery schedule for different therapeutic agents. For instance, the optimal control setting might consist of an objective function representing eradication or containment of the tumour cell population and of dynamic constraints such as the limitation (boundedness from below and from above) of the production of competent T lymphocytes.

A significant challenge of the modelling approach presented in this thesis is testing the validity of our models. In this framework, techniques of data processing and deep learning would be excellent tools for the identification of the model parameters. Moreover, collaborations between biologists, clinicians, and mathematicians would be helpful to construct

reasonable modelling assumptions, which in turn would increase the success of research on the development of new cancer therapies with the least possible side effects on healthy cells, and can spark new experimental or theoretical research in this field. In spite of their current limitation, we believe that the study presented in this thesis can be extremely beneficial in understanding tumour-immune interactions.

Appendix A

A.1 Proof of lemma 3.3.1

1. Let $r_0 < r < d+1$, then the inequality $k_5 < k_2$ is equivalent to

$$2\left(r-\frac{C}{\nu}\right)\left(d+\frac{A}{\nu}\right)\sqrt{4AC} < \left[(Ar+Cd)-2\left(r-\frac{C}{\nu}\right)A\right]\left(\frac{1}{\nu k_3}-(r-d)\right)$$
$$+(Ar+Cd)\sqrt{\left(\frac{1}{\nu k_3}-(r-d)\right)^2+4\left(d+\frac{A}{\nu}\right)\left(r-\frac{C}{\nu}\right)}.$$

Since

$$\begin{aligned}
\frac{1}{\nu k_3}-(r-d) &= -(\nu+d+1)(r-d-1)+(2\nu d+\nu+d)>0\\
(Ar+Cd) &= A\left(r-\frac{C}{\nu}\right)+\left(d+\frac{A}{\nu}\right)C>0\\
(Ar+Cd)-2A\left(r-\frac{C}{\nu}\right) &= \left(d+2\frac{A}{\nu}\right)C-Ar\\
&= -\left[A+\nu(d\nu+2A)\right](r-d-1)-A(d+1).
\end{aligned}$$

Therefore,

If $r_0 < r \leq r_1$, then $(Ar + Cd) - 2A\left(r - \frac{C}{\nu}\right) \geq 0$. Moreover,

$$2\left(r - \frac{C}{\nu}\right)\left(d + \frac{A}{\nu}\right)\sqrt{4AC} < (Ar + Cd)\sqrt{\left(\frac{1}{\nu k_3} - (r - d)\right)^2 + 4\left(d + \frac{A}{\nu}\right)\left(r - \frac{C}{\nu}\right)}. \tag{A.1}$$

In fact, the inequality (A.1) is equivalent to

$$4\left(d + \frac{A}{\nu}\right)\left(r - \frac{C}{\nu}\right)\left[4\left(r - \frac{C}{\nu}\right)\left(d + \frac{A}{\nu}\right)AC - (Ar + Cd)^2\right] < (Ar + Cd)\left(\frac{1}{\nu k_3} - (r - d)\right)^2.$$

That is,

$$-4\left(d + \frac{A}{\nu}\right)\left(r - \frac{C}{\nu}\right)\left[A\left(r - \frac{C}{\nu}\right) - \left(d + \frac{A}{\nu}\right)C\right]^2 < (Ar + Cd)\left(\frac{1}{\nu k_3} - (r - d)\right)^2.$$

Hence, $k_5 < k_2$.

If $r > r_1$, then $(Ar + Cd) - 2A\left(r - \frac{C}{\nu}\right) < 0$ and the inequality (A.1) is equivalent to

$$2\left(r - \frac{C}{\nu}\right)\left(d + \frac{A}{\nu}\right)\sqrt{4AC} - \left[\left(d + \frac{A}{\nu}\right)C - A\left(r - \frac{C}{\nu}\right)\right]\left(\frac{1}{\nu k_3} - (r - d)\right) <$$

$$\left[A\left(r - \frac{C}{\nu}\right) + \left(d + \frac{A}{\nu}\right)C\right]\sqrt{\left(\frac{1}{\nu k_3} - (r - d)\right)^2 + 4\left(d + \frac{A}{\nu}\right)\left(r - \frac{C}{\nu}\right)}.$$

That is

$$-4\left[\left(d + \frac{A}{\nu}\right)C - A\left(r - \frac{C}{\nu}\right)\right]\left(\frac{1}{\nu k_3} - (r - d)\right)\left(r - \frac{C}{\nu}\right)\left(d + \frac{A}{\nu}\right)\sqrt{4AC}$$

$$-4AC\left(r - \frac{C}{\nu}\right)\left(d + \frac{A}{\nu}\right)\left(\frac{1}{\nu k_3} - (r - d)\right)^2 < 4\left(d + \frac{A}{\nu}\right)\left(r - \frac{C}{\nu}\right)\left[A\left(r - \frac{C}{\nu}\right) - \left(d + \frac{A}{\nu}\right)C\right]$$

Therefore

$$\left[\sqrt{AC}\left(\frac{1}{\nu k_3} - (r - d)\right) - \left(A\left(r - \frac{C}{\nu}\right) - \left(d + \frac{A}{\nu}\right)C\right)\right]^2 > 0.$$

i.e. $F^2(r) > 0$ where F is given in (3.17). Hence,

- If $r = r_2$, then $k_2 = k_5$.
- If $r \neq r_2$ and $r > r_0$, then $k_5 < k_2$.

2. Let $0 < r < d+1$. Then the inequality $k_4 < k_2$ is equivalent to

$$\left(d+2\frac{A}{\nu}\right)\sqrt{4AC}+A\left(\frac{1}{\nu k_3}-(r-d)\right)<A\sqrt{\left(\frac{1}{\nu k_3}-(r-d)\right)^2+4r\left(d+2\frac{A}{\nu}\right)}.$$

That is,

$$\left(d+2\frac{A}{\nu}\right)C+\nu\left(\frac{1}{\nu k_3}-(r-d)\right)\sqrt{-A(r-d-1)}<Ar. \tag{A.2}$$

Therefore,

If $0 < r \leq r_1$, then $\left(d+2\frac{A}{\nu}\right)C - Ar \geq 0$. Hence, $k_2 < k_4$.

If $r_1 < r < d+1$, then (A.2) is equivalent to $F(r) < 0$. Since $F'(r) < 0$, $F(r_1) > 0$ and $F(d+1) < 0$, then there exists $r_1 < r_2 < d+1$ such that

- If $r < r_2$, then $k_2 < k_4$.
- If $r = r_2$, then $k_2 = k_4$.
- If $r_2 < r < d+1$, then $k_2 > k_4$.

3. From above, we can deduce that

- If $r_0 < r < r_2$, then $k_5 < k_2 < k_4$.
- If $r = r_2$, then $k_2 = k_4 = k_5$.

Moreover, we can show that (see Appendix, Subsection A.2)

- If $r_2 < r < d+1$, then $k_4 < k_5 < k_2$.
- If $r \geq d+1$, then $k_4 < k_5$.

A.2 Proof of theorems 3.3.5-3.3.7

To establish the local stability of the interior equilibrium $E^\star$, it remains to solve the inequality (3.21). Let

$$\begin{aligned}
f^\star(k) &:= \rho^\star = \frac{1}{2d}\left[r-d-\frac{1}{k\nu}+\sqrt{(r-d-\frac{1}{k\nu})^2+4rd}\right],\\
f_1(k) &:= \rho_1 = \frac{-B-\sqrt{\Delta}}{2A},\\
f_2(k) &:= \rho_2 = \frac{-B+\sqrt{\Delta}}{2A},\\
f_3(k) &:= \rho_3 = \frac{-B}{A}.
\end{aligned}$$

We have

$$\begin{aligned} f^{\star\prime}(k) &:= \frac{1}{k^2\nu}\left[\frac{\rho_*}{\sqrt{(r-d-\frac{1}{k\nu})^2+4rd}}\right] > 0, \\ f_1'(k) &:= \frac{\rho_1}{k^2\sqrt{\Delta}} > 0, \\ f_2'(k) &:= \frac{-\rho_2}{k^2\sqrt{\Delta}} < 0, \\ f_3'(k) &:= \frac{-1}{k^2 A} < 0. \end{aligned}$$

Since at point $r = d+1$, we have $f_2(k) = f_3(k)$, for all $k > 0$. Then our proof is divided into two cases.

1. Case 1: Let $r \geq d+1$. Since $f^\star$ is increasing and f_2 is decreasing, $\lim_{k\to 0} f^\star(k) = 0$, $\lim_{k\to 0} f_2(k) = +\infty$, $\lim_{k\to+\infty} f^\star(k) = \frac{r}{d}$, $\lim_{k\to+\infty} f_2(k) = \frac{\nu(r-1-d)}{(2d\nu+\nu+d+1)}$, and $\frac{\nu(r-1-d)}{(2d\nu+\nu+d+1)} < \frac{r}{d}$, then there exists a unique $k_c > 0$ such that
   - If $k < k_c$, then $f^\star(k) < f_2(k)$ $(i.e.\ \rho^\star < \rho_2)$.
   - If $k = k_c$, then $f^\star(k) = f_2(k)$ $(i.e.\ \rho^\star = \rho_2)$.
   - If $k > k_c$, then $f^\star(k) > f_2(k)$ $(i.e.\ \rho^\star > \rho_2)$.

   To find the value of k_c, it remains to solve the inequality $\rho_2 < \rho^\star$. In fact, $\rho_2 < \rho^\star$ is equivalent to

$$A\left[r-d-\frac{1}{k\nu}+\sqrt{\left(r-d-\frac{1}{k\nu}\right)^2+4rd}\right]+d\left(\frac{1}{k_3}-\frac{1}{k}\right) > d\sqrt{\left(\frac{1}{k_3}-\frac{1}{k}\right)^2-4AC}. \tag{A.3}$$

   To solve the inequality (A.3), the proof is divided into two steps.

   Step 1: We show that the inequality

$$A\left[r-d-\frac{1}{k\nu}+\sqrt{\left(r-d-\frac{1}{k\nu}\right)^2+4rd}\right]+d\left(\frac{1}{k_3}-\frac{1}{k}\right) > 0. \tag{A.4}$$

   is satisfied. In fact, (A.4) is equivalent to

$$A\sqrt{\left(r-d-\frac{1}{k\nu}\right)^2+4rd} > \left(d+\frac{A}{\nu}\right)\left(\frac{1}{k}-\frac{1}{k_6}\right),$$

where

$$\begin{aligned}\frac{1}{k_6}: &= \frac{1}{k_3}+\frac{A\left[(\nu+d+1)(r-d-1)-(2d\nu+\nu+d)\right]}{(d+\frac{A}{\nu})}\\ &= \frac{(d\nu+\nu+d+1)(\nu+d)(r-d-1)+d\nu(2d\nu+\nu+d+1)+A}{(d+\frac{A}{\nu})}>0.\end{aligned}$$

If $\frac{1}{k}\leq\frac{1}{k_6}$, then the inequality (A.4) is satisfied.
If $\frac{1}{k}>\frac{1}{k_6}$, then we have

$$d\left(d+2\frac{A}{\nu}\right)\left(\frac{1}{k}-\frac{1}{k_6}\right)^2-2\frac{A^2}{\nu^2}\left(\frac{1}{k_6}-\nu(r-d)\right)\left(\frac{1}{k}-\frac{1}{k_6}\right)-\frac{A^2}{\nu^2}\left[\left(\frac{1}{k_6}-\nu(r-d)\right)^2+4rd\nu^2\right]<0.$$

That is,

$$\frac{1}{k}<\frac{1}{k_6}+\frac{\frac{A^2}{\nu^2}\left(\frac{1}{k_6}-\nu(r-d)\right)+\frac{A}{\nu}\sqrt{\left[\left(d+\frac{A}{\nu}\right)^2\left(\frac{1}{k_6}-\nu(r-d)\right)^2+4rd^2\nu^2\left(d+2\frac{A}{\nu}\right)\right]}}{d\left(d+2\frac{A}{\nu}\right)}:=\frac{1}{k_4}.$$

Therefore, for all $\frac{1}{k}<\frac{1}{k_4}$, the inequality (A.4) is satisfied.
Step 2: Let $\frac{1}{k}<\frac{1}{k_4}$, then the inequality (A.3) is equivalent to

$$A^2\left[r-d-\frac{1}{k\nu}+\sqrt{\left(r-d-\frac{1}{k\nu}\right)^2+4rd}\right]^2$$

$$+2dA\left(\frac{1}{k_3}-\frac{1}{k}\right)\left[r-d-\frac{1}{k\nu}+\sqrt{\left(r-d-\frac{1}{k\nu}\right)^2+4rd}\right]>-4d^2AC.$$

That is,

$$-\frac{2A}{\nu}\left[\left(d+\frac{A}{\nu}\right)\left(\frac{1}{k}-\frac{1}{k_3}\right)+\frac{A}{\nu}\left(\frac{1}{k_3}-\nu(r-d)\right)\right]\sqrt{\left(\frac{1}{k}-\nu(r-d)\right)^2+4rd\nu^2}$$

$$>-\frac{A^2}{\nu^2}\left[2\left(\frac{1}{k}-(r-d)\nu\right)^2+4rd\nu^2\right]-\frac{2dA}{\nu}\left(\frac{1}{k}-\frac{1}{k_3}\right)\left(\frac{1}{k}-(r-d)\nu\right)-4d^2AC.$$

Therefore

$$\left(d+\frac{A}{\nu}\right)\left(r-\frac{C}{\nu}\right)\left(\frac{1}{k}-\frac{1}{k_3}\right)^2+\left[\frac{A}{\nu}r-\frac{C}{\nu}\left(2\frac{A}{\nu}+d\right)\right]\left(\frac{1}{k_3}-\nu(r-d)\right)\left(\frac{1}{k}-\frac{1}{k_3}\right) - \left[\frac{AC}{\nu^2}\left(\frac{1}{k_3}-(r-d)\nu\right)^2+(Ar+dC)^2\right]<0 \quad \text{(A.5)}$$

Since,

$$\frac{1}{k_3}-\frac{1}{k_6}=\frac{A}{\nu\left(d+\frac{A}{\nu}\right)}\left(\frac{1}{k_3}-\nu(r-d)\right),$$

the inequality (A.5) is equivalent to,

$$\left(d+\frac{A}{\nu}\right)\left(r-\frac{C}{\nu}\right)\left(\frac{1}{k}-\frac{1}{k_6}\right)^2-\left(\frac{A}{\nu}r+\frac{C}{\nu}d\right)\left(\frac{1}{k_3}-\nu(r-d)\right)\left(\frac{1}{k}-\frac{1}{k_6}\right)-(Ar+dC)^2<0.$$

We obtain,

$$\frac{1}{k}<\frac{1}{k_6}+\frac{[Ar+Cd]\left[\frac{1}{k_3}-\nu(r-d)\right]+[Ar+Cd]\sqrt{\left[\frac{1}{k_3}-\nu(r-d)\right]^2+4(d\nu+A)(r\nu-C)}}{2(d\nu+A)\left[r-\frac{C}{\nu}\right]}:=\frac{1}{k_5}.$$

Since the critical value k_c always exists, then we have $k_c=k_5>k_4$.

In conclusion, we have the following results.

- If $r\geq d+1$ and $k<k_5$, then $\rho^\star<\rho_2$.
- If $r\geq d+1$ and $k=k_5$, then $\rho^\star=\rho_2$.
- If $r\geq d+1$ and $k>k_5$, then $\rho^\star>\rho_2$.

2. Case 2: Let $r<d+1$. Since $f^\star$ and f_1 are increasing an f_2 is decreasing, $\lim\limits_{k\to 0}f_1(k)=\lim\limits_{k\to 0}f^\star(k)=0$, $\lim\limits_{k\to 0}f_2(k)=+\infty$, $\lim\limits_{k\to k_2}f^\star(k)=\dfrac{1}{2d}\left[r-d-\dfrac{1}{k_2\nu}+\sqrt{\left(r-d-\dfrac{1}{k_2\nu}\right)^2+4rd}\right]=h^\star(r)$, $\lim\limits_{k\to k_2}f_1(k)=\lim\limits_{k\to k_2}f_2(k)=\sqrt{\dfrac{C}{A}}=h_2(r)$. Then, when $h^\star(r)>h_2(r)$ (*i.e.* $F(r)<0$), then there exists a unique $0<k_c<k_2$ such that

- If $r_2<r<d+1$ and $k<k_c$, then $f_1(k)<f^\star(k)<f_2(k)$ (*i.e.* $\rho_1<\rho^\star<\rho_2$).
- If $r_2<r<d+1$ and $k=k_c$, then $f_1(k)<f^\star(k)=f_2(k)$ (*i.e.* $\rho_1<\rho^\star=\rho_2$).
- If $r_2<r<d+1$ and $k_c<k<k_2$, then $f_1(k)<f_2(k)<f^\star(k)$ (*i.e.* $\rho_1<\rho_2<\rho^\star$).
- If $r=r_2$ and $0<k<k_2$, then $f_1(k)<f^\star(k)<f_2(k)$ (*i.e.* $\rho_1<\rho^\star<\rho_2$).

Using the same argument as above, we can show that there exists $0 < k_c < k_2$ such that $k_4 < k_c = k_5 < k_2$.

Let now $0 < r < r_2$ and $k < k_2$, then the inequality $\rho_1 < \rho^\star$ is equivalent to

$$A\left[r-d-\frac{1}{k\nu}+\sqrt{\left(r-d-\frac{1}{k\nu}\right)^2+4rd}\right]+d\left(\frac{1}{k_3}-\frac{1}{k}\right) > -d\sqrt{\left(\frac{1}{k_3}-\frac{1}{k}\right)^2-4AC}. \tag{A.6}$$

From (A.4), if $r_2 < r < d+1$ and $k_4 \leq k < k_2$ then $\rho_1 < \rho^\star$.

If either $r_2 < r < d+1$ and $k < k_4$ or $r \leq r_2$ and $k < k_2$, then $\rho_1 < \rho^\star$ is equivalent to

$$\left(d+\frac{A}{\nu}\right)\left(r-\frac{C}{\nu}\right)\left(\frac{1}{k}-\frac{1}{k_3}\right)^2+\left[\frac{A}{\nu}\left(r-\frac{C}{\nu}\right)-\frac{C}{\nu}\left(\frac{A}{\nu}+d\right)\right]\left(\frac{1}{k_3}-\nu(r-d)\right)\left(\frac{1}{k}-\frac{1}{k_3}\right) - \left[\frac{AC}{\nu^2}\left(\frac{1}{k_3}-(r-d)\nu\right)^2+(Ar+dC)^2\right] > 0 \tag{A.7}$$

The inequality (A.7) is equivalent to

$$\left(d+\frac{A}{\nu}\right)\left(r-\frac{C}{\nu}\right)\left(\frac{1}{k}-\frac{1}{k_6}\right)^2-\frac{(Ar+Cd)}{\nu}\left(\frac{1}{k_3}-\nu(r-d)\right)\left(\frac{1}{k}-\frac{1}{k_6}\right)-(Ar+dC)^2 > 0.$$

Then, if $r > \frac{C}{\nu}$ (*i.e.* if either $r_2 < r < d+1$ and $k < k_4$ or $r_0 < r \leq r_2$ and $k < k_2$) we obtain

$$\frac{1}{k} > \frac{1}{k_6}+\frac{\frac{(Ar+Cd)}{\nu}\left(\frac{1}{k_3}-\nu(r-d)\right)+\frac{(Ar+Cd)}{\nu}\sqrt{\left(\frac{1}{k_3}-\nu(r-d)\right)^2+4\nu^2\left(d+\frac{A}{\nu}\right)\left(r-\frac{C}{\nu}\right)}}{2\left(d+\frac{A}{\nu}\right)\left(r-\frac{C}{\nu}\right)} := \frac{1}{k_5}$$

Since the critical value k_c is unique and exists always for $r_0 < r < d+1$, then we have $k_c = k_5 < k_2 < k_4$.

In conclusion, we have the following results.

- If $0 < r \leq r_0$ and $k < k_2$, then $\rho^\star < \rho_1 < \rho_2$.
- If $r_0 < r < r_2$ and $k_5 < k < k_2$, then $\rho^\star < \rho_1 < \rho_2$.
- If $r_0 < r < r_2$ and $k = k_5$, then $\rho_1 = \rho^\star < \rho_2$.
- If $r_0 < r < r_2$ and $k < k_5$, then $\rho_1 < \rho^\star < \rho_2$.

A.3 Proof of theorem 3.3.8

By means of a Lyapunov function, we show that the interior equilibrium $E^\star$ is globally asymptotically stable. We set

$$\begin{aligned} V(\rho,\sigma,\gamma) &= \left(\rho-\rho^\star-\rho^\star\ln\frac{\rho}{\rho^\star}\right)+\frac{1}{2}\left(\frac{2d-\sigma^\star}{\nu\sigma^{\star 2}}\right)(\sigma-\sigma^\star)^2 \\ &\quad+\left(\frac{2\nu dk\,(d-\sigma^\star)\,\sigma^\star+d\,(2d-\sigma^\star)}{\nu\,(2d-\sigma^\star)\,\sigma^\star}\right)\left(\gamma-\gamma^\star-\gamma^\star\ln\frac{\gamma}{\gamma^\star}\right) \end{aligned}$$

It is obviously that $V(\rho,\sigma,\gamma)>0$ when $d>\sigma^\star$ and $V(\rho,\sigma,\gamma)=0$ if and only if $\rho=\rho^\star$, $\sigma=\sigma^\star$ and $\gamma=\gamma^\star$. Further, calculating the time derivative of V along the positive solutions

of (3.3), we find

$$\begin{aligned}
\frac{dV}{dt} &= (\rho-\rho^\star)\left(r-d\rho-\sigma\right)+\left(\frac{2d-\sigma^\star}{\nu\sigma^{\star 2}}\right)(\sigma-\sigma^\star)\left(\gamma-\nu(1+\rho)\sigma\right)\\
&\quad+\left(\frac{2\nu dk\left(d-\sigma^\star\right)\sigma^\star+d\left(2d-\sigma^\star\right)}{\nu\left(2d-\sigma^\star\right)\sigma^\star}\right)(\gamma-\gamma^\star)\left(\rho-k\gamma\right)\\
&= (\rho-\rho^\star)\left(-d(\rho-\rho^\star)-\sigma+\sigma^\star\right)+\left(\frac{2d-\sigma^\star}{\nu\sigma^{\star 2}}\right)(\sigma-\sigma^\star)\left((\gamma-\gamma^\star)-\nu(\sigma-\sigma^\star)-\nu(\rho\sigma-\rho^\star\sigma^\star)\right)\\
&\quad+\left(\frac{2\nu dk\left(d-\sigma^\star\right)\sigma^\star+d\left(2d-\sigma^\star\right)}{\nu\left(2d-\sigma^\star\right)\sigma^\star}\right)(\gamma-\gamma^\star)\left(\rho-\rho^\star-k(\gamma-\gamma^\star)\right)\\
&= \left(-d(\rho-\rho^\star)^2-(\sigma-\sigma^\star)(\rho-\rho^\star)\right)\\
&\quad+\left(\frac{2d-\sigma^\star}{\nu\sigma^{\star 2}}\right)\left((\sigma-\sigma^\star)(\gamma-\gamma^\star)-\nu(\sigma-\sigma^\star)^2-\nu(\sigma-\sigma^\star)(\rho(\sigma-\sigma^\star)+(\rho-\rho^\star)\sigma^\star)\right)\\
&\quad+\left(\frac{2\nu dk\left(d-\sigma^\star\right)\sigma^\star+d\left(2d-\sigma^\star\right)}{\nu\left(2d-\sigma^\star\right)\sigma^\star}\right)\left((\rho-\rho^\star)(\gamma-\gamma^\star)-k(\gamma-\gamma^\star)^2\right)\\
&= -d(\rho-\rho^\star)^2-k\left(\frac{2\nu dk\left(d-\sigma^\star\right)\sigma^\star+d\left(2d-\sigma^\star\right)}{\nu\left(2d-\sigma^\star\right)\sigma^\star}\right)(\gamma-\gamma^\star)^2-\left(\frac{2d-\sigma^\star}{\nu\sigma^{\star 2}}\right)\nu(1+\rho)(\sigma-\sigma^\star)^2\\
&\quad+\left(\frac{2d-\sigma^\star}{\nu\sigma^{\star 2}}\right)(\sigma-\sigma^\star)(\gamma-\gamma^\star)-\left[\left(\frac{2d-\sigma^\star}{\nu\sigma^{\star 2}}\right)\sigma^\star\nu+1\right](\sigma-\sigma^\star)(\rho-\rho^\star)\\
&\quad+\left(\frac{2\nu dk\left(d-\sigma^\star\right)\sigma^\star+d\left(2d-\sigma^\star\right)}{\nu\left(2d-\sigma^\star\right)\sigma^\star}\right)(\rho-\rho^\star)(\gamma-\gamma^\star)\\
&= -d(\rho-\rho^\star)^2-\left(\frac{2d-\sigma^\star}{\sigma^{\star 2}}\right)(\sigma-\sigma^\star)^2-k\left(\frac{2\nu dk\left(d-\sigma^\star\right)\sigma^\star+d\left(2d-\sigma^\star\right)}{\nu\left(2d-\sigma^\star\right)\sigma^\star}\right)(\gamma-\gamma^\star)^2\\
&\quad-\left(\frac{2d}{\sigma^\star}\right)(\rho-\rho^\star)(\sigma-\sigma^\star)+\left(\frac{2\nu dk\left(d-\sigma^\star\right)\sigma^\star+d\left(2d-\sigma^\star\right)}{\nu\left(2d-\sigma^\star\right)\sigma^\star}\right)(\rho-\rho^\star)(\gamma-\gamma^\star)\\
&\quad+\left(\frac{2d-\sigma^\star}{\nu\sigma^{\star 2}}\right)(\sigma-\sigma^\star)(\gamma-\gamma^\star)-\left(\frac{2d-\sigma^\star}{\sigma^{\star 2}}\right)\rho(\sigma-\sigma^\star)^2\\
&= -WPW^T-\left(\frac{2d-\sigma^\star}{\sigma^{\star 2}}\right)\rho(\sigma-\sigma^\star)^2,
\end{aligned}$$

where

$$W=(\rho-\rho^\star,\sigma-\sigma^\star,\gamma-\gamma^\star),\qquad W^T=\begin{pmatrix}\rho-\rho^\star\\ \sigma-\sigma^\star\\ \gamma-\gamma^\star\end{pmatrix},$$

and

$$P=\begin{pmatrix} d & \frac{1}{2}\left(\frac{2d}{\sigma^\star}\right) & -\frac{d}{2}\left(\frac{2\nu k(d-\sigma^\star)\sigma^\star+(2d-\sigma^\star)}{\nu(2d-\sigma^\star)\sigma^\star}\right)\\ \frac{1}{2}\left(\frac{2d}{\sigma^\star}\right) & \left(\frac{2d-\sigma^\star}{\sigma^{\star 2}}\right) & -\frac{1}{2}\left(\frac{2d-\sigma^\star}{\nu\sigma^{\star 2}}\right)\\ -\frac{d}{2}\left(\frac{2\nu k(d-\sigma^\star)\sigma^\star+(2d-\sigma^\star)}{\nu(2d-\sigma^\star)\sigma^\star}\right) & -\frac{1}{2}\left(\frac{2d-\sigma^\star}{\nu\sigma^{\star 2}}\right) & kd\left(\frac{2\nu k(d-\sigma^\star)\sigma^\star+(2d-\sigma^\star)}{\nu(2d-\sigma^\star)\sigma^\star}\right)\end{pmatrix}.$$

According to Sylvester's criterion the matrix P is positive definite if $d - \sigma^\star > 0$ and

$$4kd\nu\sigma^\star \left[2d - \sigma^\star + k\nu\sigma^\star \left(d - \sigma^\star\right)\right] \left[2d(2k\nu\sigma^\star - 1) + \sigma^\star\right] \left(2d - \sigma^\star\right) > 0.$$

That is

$$\frac{1}{2k\nu} \leq \sigma^\star < d. \tag{A.8}$$

It follows from (A.8) that $\frac{dV}{dt} \leq 0$ for all $(\rho, \sigma, \gamma) \in \mathbb{R}^3_+$ and $\frac{dV}{t} = 0$, when $\rho = \rho^\star$, $\sigma = \sigma^\star$ and $\gamma = \gamma^\star$. The inequality (A.8) is saisfied if either

1. $d < r < 2d$ and $k \geq \frac{1}{2\nu(r-d)}$, or
2. $r \geq 2d$ and $k > \frac{(r-d)}{d\nu r}$.

Hence, LaSalle's theorem implies convergence of the solutions to the interior equilibrium $E^\star$, for all initial values not in the set $M = \{0\} \times \mathbb{R}^2_+ \bigcup \mathbb{R}^2_+ \times \{0\}$. This shows that the interior equilibrium $E^\star$ is globally asymptotically stable in $\mathbb{R}^3_+ / M$.

A.4 Proof of theorem 3.4.1

We have

$$
\begin{aligned}
Re(x_2 + y_2 - \frac{a_2}{3}) = 0 \quad &\Leftrightarrow \quad -\left(t_1^{\frac{1}{3}} + t_2^{\frac{1}{3}}\right) - 2\frac{a_2}{3} = 0 \\
&\Leftrightarrow \quad \left(t_1^{\frac{1}{3}} + t_2^{\frac{1}{3}}\right) = -2\frac{a_2}{3} \\
&\Leftrightarrow \quad t_1 + t_2 - 2t_1^{\frac{1}{3}} t_2^{\frac{1}{3}} a_2 = -8\frac{a_2^3}{27} \\
&\Leftrightarrow \quad -2t_1^{\frac{1}{3}} t_2^{\frac{1}{3}} a_2 = \left(a_0 - \frac{a_1 a_2}{3} - \frac{6a_2^3}{27}\right) \\
&\Leftrightarrow \quad \frac{8}{27}\left(a_1 - \frac{a_2^2}{3}\right)^3 a_2^3 = \left(a_0 - \frac{a_1 a_2}{3} - \frac{6a_2^3}{27}\right)^3 \\
&\Leftrightarrow \quad \frac{2}{3}\left(a_1 - \frac{a_2^2}{3}\right) a_2 = \left(a_0 - \frac{a_1 a_2}{3} - \frac{6a_2^3}{27}\right) \\
&\Leftrightarrow \quad a_0 = a_1 a_2 \\
&\Leftrightarrow \quad A\rho^{\star 2} + B\rho^{\star} + C = 0.
\end{aligned}
$$

Moreover, when $a_0 = a_1 a_2$, *i.e.* $k = k_c = k_5$, we obtain

$$
\frac{\partial Re(x_2 + y_2 - \frac{a_2}{3})}{\partial k} = \frac{\partial Re(x_2 + y_2 - \frac{a_2}{3})}{\partial \rho^{\star}} \frac{\partial \rho^{\star}}{\partial k},
$$

$$
\frac{\partial \rho^{\star}}{\partial k} = \frac{1}{\nu k^2}\left[\frac{\rho^{\star}}{\sqrt{(r - d - \frac{1}{k\nu})^2 + 4rd}}\right] > 0,
$$

and

$$\begin{aligned}
\frac{\partial Re(x_2+y_2-\frac{a_2}{3})}{\partial\rho^\star} &= -\frac{1}{2}\frac{\partial\left(t_1^{\frac{1}{3}}+t_2^{\frac{1}{3}}+\frac{2}{3}a_2\right)}{\partial\rho^\star}\\
&= -\frac{1}{2}\left[\frac{1}{3}t_1^{\frac{-2}{3}}\frac{\partial t_1}{\partial\rho^\star}+\frac{1}{3}t_2^{\frac{-2}{3}}\frac{\partial t_2}{\partial\rho^\star}+\frac{2}{3}\frac{\partial a_2}{\partial\rho^\star}\right]\\
&= \frac{1}{6}\left[\frac{t_2^{\frac{2}{3}}+t_1^{\frac{2}{3}}}{t_1^{\frac{2}{3}}t_2^{\frac{2}{3}}}\right]\frac{\partial}{\partial\rho^\star}\frac{\left(a_0-\frac{a_1a_2}{3}+\frac{2a_2^3}{27}\right)}{2}+\frac{1}{6}\left[\frac{t_2^{\frac{2}{3}}-t_1^{\frac{2}{3}}}{t_1^{\frac{2}{3}}t_2^{\frac{2}{3}}}\right]\frac{\partial}{\partial\rho^\star}\frac{\sqrt{D}}{2}-\frac{1}{3}\frac{\partial a_2}{\partial\rho^\star}\\
&= \frac{1}{6}\left[\frac{\left(t_2^{\frac{1}{3}}+t_1^{\frac{1}{3}}\right)^2-2t_2^{\frac{1}{3}}t_1^{\frac{1}{3}}}{t_1^{\frac{2}{3}}t_2^{\frac{2}{3}}}\right]\frac{\partial}{\partial\rho^\star}\frac{\left(a_0-\frac{a_1a_2}{3}+\frac{2a_2^3}{27}\right)}{2}\\
&\quad+\frac{1}{6}\left[\frac{\left(t_2^{\frac{1}{3}}-t_1^{\frac{1}{3}}\right)\left(t_2^{\frac{1}{3}}+t_1^{\frac{1}{3}}\right)}{t_1^{\frac{2}{3}}t_2^{\frac{2}{3}}}\right]\frac{\partial}{\partial\rho^\star}\frac{\sqrt{D}}{2}-\frac{1}{3}\frac{\partial a_2}{\partial\rho^\star}.
\end{aligned}$$

Since

$$\begin{aligned}
t_2^{\frac{1}{3}}+t_1^{\frac{1}{3}} &= -\frac{2}{3}a_2,\\
t_1^{\frac{1}{3}}t_2^{\frac{1}{3}} &= -\frac{1}{3}\left(a_1-\frac{a_2^2}{3}\right),\\
t_2^{\frac{1}{3}} &= -\frac{1}{3}a_2+\sqrt{\frac{1}{3}a_1},\\
t_1^{\frac{1}{3}} &= -\frac{1}{3}a_2-\sqrt{\frac{1}{3}a_1},\\
t_2^{\frac{1}{3}}-t_1^{\frac{1}{3}} &= 2\sqrt{\frac{1}{3}a_1},
\end{aligned}$$

we obtain

$$\begin{aligned}
\frac{\partial Re(x_2+y_2-\frac{a_2}{3})}{\partial \rho^\star} &= \frac{\left(a_1+\frac{a_2^2}{3}\right)}{2\left(a_1-\frac{a_2^2}{3}\right)^2}\frac{\partial}{\partial\rho^\star}\left(a_0-\frac{a_1a_2}{3}+\frac{2a_2^3}{27}\right)-\frac{a_2\sqrt{\frac{1}{3}a_1}}{\left(a_1-\frac{a_2^2}{3}\right)^2}\frac{\partial}{\partial\rho^\star}\sqrt{D}-\frac{1}{3}\frac{\partial a_2}{\partial\rho^\star}\\
&= \frac{1}{2\left(a_1+a_2^2\right)}\left[\frac{\partial}{\partial\rho^\star}\left(a_0-\frac{a_1a_2}{3}+\frac{2a_2^3}{27}\right)-\frac{2a_2}{3}\frac{\partial}{\partial\rho^\star}\left(a_1-\frac{a_2^2}{3}\right)-\frac{2}{3}\left(a_1+a_2^2\right)\frac{\partial a_2}{\partial\rho^\star}\right]\\
&= \frac{1}{2\left(a_1+a_2^2\right)}\left[\frac{\partial a_0}{\partial\rho^\star}-a_2\frac{\partial a_1}{\partial\rho^\star}-a_1\frac{\partial a_2}{\partial\rho^\star}\right]\\
&= \frac{1}{2\rho^\star\left(a_1+a_2^2\right)}\left[a_1\nu-a_2(\nu+d+2d\nu)\rho^{\star 2}\right]\\
&= \frac{1}{2\left(a_1+a_2^2\right)}\left[-(\nu+d+2d\nu)(\nu+d+1)\rho^{\star 2}+\nu^2(1+d-r)\right] \qquad \text{(A.9)}\\
&= \frac{1}{2\left(a_1+a_2^2\right)}\left[-(\nu+d+2d\nu)(\nu+d+1)\left(\frac{-B+\sqrt{B^2-4AC}}{2A}\right)^2+C\right]\\
&= \frac{1}{2\left(a_1+a_2^2\right)}\left[-(A+2d\nu)\left(\frac{2B^2-4AC-2B\sqrt{B^2-4AC}}{4A^2}\right)+C\right]\\
&= \frac{1}{\left(a_1+a_2^2\right)}\left[\frac{-(A+2d\nu)B^2+4AC(A+d\nu)+B(A+2d\nu)\sqrt{B^2-4AC}}{4A^2}\right]. \qquad \text{(A.10)}
\end{aligned}$$

1. From (3.25), if $r \geq d+1$, then $\frac{\partial Re(x_2+y_2-\frac{a_2}{3})}{\partial\rho^\star} < 0$.
2. From (3.25), if $r < d+1$ and $k < k_2$, then $\frac{\partial Re(x_2+y_2-\frac{a_2}{3})}{\partial\rho^\star} < 0$ since $B < 0$ and $(A+2d\nu)B^2 > 4AC(A+d\nu)$ $(B^2 > 4AC)$.

Hence, when $k = k_c$, we have

$$\frac{\partial Re(x_2+y_2-\frac{a_2}{3})}{\partial k} = \frac{\partial Re(x_2+y_2-\frac{a_2}{3})}{\partial\rho^\star}\frac{\partial\rho^\star}{\partial k} < 0,$$

for all $r > 0$.

Bibliography

[1] M. Abel, C. Yang, M.S. Thakar and S. Malarkannan, *Natural killer cells: development, maturation, and clinical utilization*, Frontiers in immunology, 9 (1869), 2018, pp. 1-23.

[2] L. Almeida, C. Audebert, E. Leschiera and T. Lorenzi, *Discrete and continuum models for the coevolutionary dynamics between CD8+ cytotoxic T lymphocytes and tumour cells*, Mathematical biology and medicine, 2023, pp. 1-34.

[3] L. Almeida, P. Bagnerini, G. Fabrini, B. D. Hughes and T. Lorenzi, *Evolution of cancer cell populations under cytotoxic therapy and treatment optimisation: insight from a phenotype-structured model*, ESAIM: Mathematical Modelling and Numerical Analysis, 53 (4), 2019, pp. 1157-1190.

[4] F.E. Alvarez, J.A. Carrillo and J. Clairambault, *Evolution of a structured cell population endowed with plasticity of traits under constraints on and between the traits*, Journal of Mathematical Biology, 85 (6-7), 2022, p.64.

[5] K.K. Atsou, Mathematical modeling of tumor-immune system interactions: equilibrium and escape phase, Doctoral dissertation, Universite Cote d'Azur, France, 2020.

[6] A. Balasubramanian, T. John and M. L. Asselin-Labat, *Regulation of the antigen presentation machinery in cancer and its implication for immune surveillance*, Biochemical Society Transactions, 50 (2), 2022, pp. 825-837.

[7] J. C. Becker, T. Brabletz, C. Czerny, C. Termeer and E.B. Bröcker, *Tumor escape mechanisms from immunosurveillance: induction of unresponsiveness in a specific MHC-restricted CD4+; human T cell clone by the autologous MHC class II+ melanoma*, International immunology, 5 (12), 1993, pp. 1501-1508.

[8] M. Bertolaso, Philosophy of Cancer, A dynamic and relational view, Springer Science + Business Media Dordrecht, 2016.

[9] M. Burnet, *Cancer—a biological approach: III. Viruses associated with neoplastic conditions. IV. Practical applications*, British medical journal, 1 (5023), 1957, pp. 7-841.

[10] M.V. Caisova, The study of cancer immunotherapy based on installation of phagocytosis stimulating ligands on the tumor cells surface and investigation of underlying mechanisms, Doctoral dissertation, Faculty of Science, University of South Bohemia, Czech Republic, 2017.

[11] C. Cattani, A. Ciancio, and A. d'Onofrio, *Metamodeling the learning–hiding competition between tumours and the immune system: a kinematic approach*, Math. Comput. Model. 52 (1), 2010, pp. 62–69.

[12] A. F. Chambers, A. C. Groom and I. C. MacDonald, *Dissemination and growth of cancer cells in metastatic sites*, Nature Reviews Cancer, 2 (8), 2002, pp. 563-572.

[13] N. Champagnat, R. Ferrière and S. Méléard, *From individual stochastic processes to macroscopic models in adaptive evolution*, Stochastic Models, 24 (sup1), 2008, pp. 2-44.

[14] D. D. Chaplin, *Overview of the immune response*, Journal of allergy and clinical immunology, 125 (2), 2010, pp. 53-523.

[15] N. Champagnat, R. Ferrière and S. Méléard, *From individual stochastic processes to macroscopic models in adaptive evolution*, Stochastic Models, 24 (sup1), 2008, pp. 2-44.

[16] D. S. Chen and I. Mellman, *Oncology meets immunology: the cancer-immunity cycle*, Immunity, 39 (1), 2013, pp. 1-10.

[17] J. Clairambault, *Stepping from modeling cancer plasticity to the philosophy of cancer*, Frontiers in Genetics, 11 (2020), p. 579738.

[18] J. Clairambault and Pouchol, *A survey of adaptive cell population dynamics models of emergence of drug resistance in cancer, and open questions about evolution and cancer*, BIOMATH, 8 (1), 2019, p. 23.

[19] E. X. DeJesus and C. Kaufman, *Routh-Hurwitz criterion in the examination of eigenvalues of a system of nonlinear ordinary differential equations*, Physical Review A, 35 (12), 1987, pp. 528-5290.

[20] M. Delitala and T. Lorenzi, *Recognition and learning in a mathematical model for immune response against cancer*, Discrete and Continuous Dynamical Systems-B, 18 (4), 2013, p. 891.

[21] L. Desvillettes, P. E. Jabin and S. Mischler, *On selection dynamics for continuous structured populations*, Communications in Mathematical Sciences, 6(3) 2008, pp. 729-747.

[22] J. Dine, R. Gordon, Y. Shames, M. K. Kasler and M. Barton-Burke, *Immune checkpoint inhibitors: an innovation in immunotherapy for the treatment and management of patients with cancer*, Asia-Pacific journal of oncology nursing, 4 (2), 2017, pp. 127-135.

[23] G. P. Dunn, A. T. Bruce, H. Ikeda, L. J. Old and R. D. Schreiber, *Cancer immunoediting: from immunosurveillance to tumor escape*, Nature immunology, 3 (11), 2002, pp. 991-998.

[24] G. P. Dunn, L. J. Old and R.D. Schreiber, *The three Es of cancer immunoediting.* Annu. Rev. Immunol, 22 (2004), pp. 329-360.

[25] A. D'Onofrio, *Tumor evasion from immune control: strategies of a MISS to become a MASS. Chaos*, Solitons and Fractals, 31 (2), 2007, pp. 261-268.

[26] H. Dritschel, S. L. Waters, A. Roller and H. M. Byrne, *A mathematical model of cytotoxic and helper T cell interactions in a tumor microenvironment*, Letters in Biomathematics, 5 (S1), 2018, p. 34.

[27] R. Eftimie, J. L. Bramson and D. J. Earn, *Interactions between the immune system and cancer: a brief review of non-spatial mathematical models*, Bulletin of mathematical biology, 73 (1), 2011, pp. 2-32.

[28] A. D. Fesnak, C. H. June and B. L. Levine, *Engineered T cells: the promise and challenges of cancer immunotherapy*, Nature reviews cancer, 16 (9), 2016, pp. 566-581.

[29] U. Forys, J. Waniewski and P. Zhivkov, *Anti-tumor immunity and tumor anti-immunity in a mathematical model of tumor immunotherapy*, Journal of Biological Systems, 14 (1), 2006, pp. 13-30.

[30] F. Frascoli, P. S. Kim, B. D. Hughes and K. A. Landman, *A dynamical model of tumour immunotherapy*, Mathematical biosciences, 253 (2014), pp. 50-62.

[31] J. Galon, and D. Bruni, *Approaches to treat immune hot, altered and cold tumours with combination immunotherapies*, Nature reviews Drug discovery, 18 (3), 2019, pp. 197-218.

[32] J. Galon, B. A. Fox, C. B. Bifulco, G. Masucci, T. Rau, G. Botti and M. Capone, *Immunoscore and Immunoprofiling in cancer: an update from the melanoma and immunotherapy bridge 2015*, 2016, pp. 1-6.

[33] G. Gross and Z. Eshhar, *Therapeutic potential of T cell chimeric antigen receptors (CARs) in cancer treatment: counteracting off-tumor toxicities for safe CAR T cell therapy*, Annual review of pharmacology and toxicology, 56 (2016), pp. 59-83.

[34] Y. Y. Han, D. D. Liu and L. H. Li, *PD-1/PD-L1 pathway: current researches in cancer*, American Journal of Cancer Research, 10 (3), 2020, pp. 727-742.

[35] D. Hanahan and R. A. Weinberg, *Hallmarks of cancer: the next generation*, Cell, 144 (5), 2011, pp. 646-674.

[36] D. Hanahan and R. A. Weinberg, *The hallmarks of cancer*, Cell, 100 (1), 2000, pp. 57-70.

[37] Y. Iwai, M. Ishida, Y. Tanaka, T. Okazaki, T. Honjo and N. Minato, *Involvement of PD-L1 on tumor cells in the escape from host immune system and tumor immunotherapy by PD-L1 blockade*, Proceedings of the National Academy of Sciences, 99 (19), 2002, pp. 12293-12297.

[38] P.E. Jabin and G. Raoul,*On selection dynamics for competitive interactions*, Journal of Mathematical Biology, 63(2011), pp. 493-551.

[39] R. W. Jenkins, D. A. Barbie and K. T. Flaherty, *Mechanisms of resistance to immune checkpoint inhibitors*, British journal of cancer, 118 (1), 2018, pp. 9-16.

[40] C.H. June, *Adoptive T cell therapy for cancer in the clinic*, The Journal of clinical investigation, 117 (6), 2007, pp. 1466-1476.

[41] Z. Kaid, A. Lakmeche, J. Clairambault and M. Helal, *Dynamics of tumor growth and of the immune response model*, Nonlinear Studies, 30(3), 2023, pp. 1-23.

[42] Z. Kaid, C. Pouchol, J. Clairambault. A phenotype-structured model for the tumour-immune response, Math Model Nat Phenomena, 18(22), 2023, pp. 1-27.

[43] H. K. Khalil, Nonlinear Systems, 3rd edition, Michigan State University, Prentice Hall, 1996.

[44] R. Kiessling, E. Klein and H. Wigzell, *Natural killer cells in the mouse. I. Cytotoxic cells with specificity for mouse Moloney leukemia cells*, Specificity and distribution according to genotype. European journal of immunology, 5 (2), 1975, pp. 112-117.

[45] D. Kirschner and J. C. Panetta, *Modeling immunotherapy of the tumor–immune interaction*, Journal of mathematical biology, 37 (3), 1998, pp. 235-252.

[46] V. A. Kuznetsov, I. A. Makalkin, M. A. Taylor and A. S. Perelson, *Nonlinear dynamics of immunogenic tumors: Parameter estimation and global bifurcation analysis*, Bulletin of Mathematical Biology, 56 (2), 1994, pp. 295-321.

[47] H. Ledford, H. Else and M. Warren, *Cancer immunologists scoop medicine Nobel prize*, Nature, 562 (7725), 2018, pp. 20-22.

[48] J. H. Lee, E. Shklovskaya, S. Y. Lim, M. S. Carlino, A. M. Menzies, A. Stewart, B. Pedersen, M. Irvine, S. Alavi, J. Y. H. Yang, D. Strbenac, R. P. M. Saw, J. F. Thompson, J. S. Wilmott, R. A. Scolyer, G. V. Long, R. F. Kefford and H. Rizos, *Transcriptional downregulation of MHC class I and melanoma de-differentiation in resistance to PD-1 inhibition*, Nature Communications, 11 (1), 2020, pp. 1-12.

[49] E. Leschiera, Mathematical models of tumour-immune interactions: discrete and continuum approaches, Doctoral dissertation, Sorbonne University, UPMC University of Paris 6, France, 2022.

[50] F. Le Louedec, F. Leenhardt, C. Marin, E. Chatelut, A. Evrard and J. Ciccolini, *Cancer Immunotherapy Dosing: A Pharmacokinetic/Pharmacodynamic Perspective*, Vaccines, 8 (4), 2020, p. 632.

[51] J. Li and B. Z. Stanger, *How tumor cell dedifferentiation drives immune evasion and resistance to immunotherapy*, Cancer research, 80 (19), 2020, pp. 4037-4041.

[52] T. Lorenzi, R.H. Chisholm and J. Clairambault, *Tracking the evolution of cancer cell populations through the mathematical lens of phenotype-structured equations*, Biology direct, 11 (1), 2016, pp. 1-17.

[53] A. Lorz, T. Lorenzi, M. E. Hochberg, J. Clairambault and B. Perthame, *Populational adaptive evolution, chemotherapeutic resistance and multiple anti-cancer therapies*, Mathematical Modelling and Numerical Analysis, 47 (2), 2013, pp. 377-399.

[54] T. Lorenzi and C. Pouchol, *Asymptotic analysis of selection-mutation models in the presence of multiple fitness peaks*, Nonlinearity, 33 (11), 2020, p. 5791.

[55] G. E. Mahlbacher, K. C. Reihmer and B. F. Hermann, *Mathematical modeling of tumor-immune cell interactions*, Journal of Theoretical Biology, 469 (2019), pp. 47-60.

[56] L. Martínez-Lostao, A. Anel and J. Pardo, *How do cytotoxic lymphocytes kill cancer cells?*, Clinical cancer research, 21 (22), 2015, pp. 5047-5056.

[57] A. Matzavinos and M. A. Chaplain, *Travelling-wave analysis of a model of the immune response to cancer*, Comptes rendus biologies, 327 (11), 2004, pp. 995-1008.

[58] A. Matzavinos, M. A. Chaplain and V. A. Kuznetsov, *Mathematical modelling of the spatio-temporal response of cytotoxic T-lymphocytes to a solid tumour*, Mathematical Medicine and Biology, 21 (1), 2004, pp. 1-34.

[59] L. G. Meza Guzman, L. Keating and S. E. Nicholson, *Natural Killer Cells: Tumor Surveillance and Signaling Cancers*, 12 (4), 2020, pp. 12-952.

[60] A. Oliveir and C. Pouchol, *Combination of direct methods and homotopy in numerical optimal control: application to the optimization of chemotherapy in cancer*, Journal of Optimization Theory and Applications, 181 (2019), pp. 479-503.

[61] K. Perica, J. C. Varela, M. Oelke and J. Schneck,*Adoptive T cell immunotherapy for cancer*, Rambam Maimonides medical journal, 6 (1), 2015, p. 1-9.

[62] S. Pesce, M. Greppi, F. Grossi, G. Del Zotto, L. Moretta, S. Sivori, C. Genova and E. Marcenaro, *PD/1-PD-Ls Checkpoint: Insight on the Potential Role of NK Cells*, Frontiers in Immunology, 10 (2019), pp. 1-8.

[63] B. Perthame. Transport equations in biology. Birkhäuser, Boston, 2007.

[64] S. Pesce, M. Greppi, G. Tabellini, F. Rampinelli, S. Parolini, D. Olive and E. Marcenaro, *Identification of a subset of human natural killer cells expressing high levels of programmed death 1: A phenotypic and functional characterization*, Journal of Allergy and Clinical Immunology, 139 (1), 2017, pp. 335-346.

[65] C. Pouchol, J. Clairambault, A. Lorz, and E. Trélat,*Asymptotic analysis and optimal control of an integro-differential system modelling healthy and cancer cells exposed to chemotherapy*, Journal de Mathématiques Pures et Appliquées, 116 (2018), pp. 268-308.

[66] C. Pouchol, Modelling interactions between tumour cells and supporting adipocytes in breast cancer, Internship report, 2015, https://hal. inria. fr/hal-01252122.

[67] T. Pradeu, Philosophy of immunology, Cambridge University Press, 2020.

[68] C. Robert, J. Schachter, G. V. Long, A. Arance,J. J. Grob, L. Mortier and J. Larkin, *Pembrolizumab versus ipilimumab in advanced melanoma*, New England Journal of Medicine, 372 (26), 2015, pp. 2521-2532.

[69] V. Shankaran, H. Ikeda, A. T. Bruce, J.M. White, P. E. Swanson, L. J. Old and R. D. Schreiber,*IFN_γ and lymphocytes prevent primary tumour development and shape tumour immunogenicity*, Nature, 410 (6832), 2001, pp. 1107-1111.

[70] J. Scholler, T. L. Brady, G. Binder-Scholl, W. T. Hwang, G. Plesa, K. M. Hege and C. H. June, *Decade-long safety and function of retroviral-modified chimeric antigen receptor T cells*, Science translational medicine, 4 (132), 2012, pp. 53-132.

[71] R. D. Schreiber, L. J. Old and M. J. Smyth,*Cancer Immunoediting: Integrating Immunity's Roles in Cancer Suppression and Promotion*, Science, 331 (6024), 2011, pp. 1565-1570.

[72] S. Shen and J. Clairambault, *Cell plasticity in cancer cell populations*, F1000Research, 9 (2020), pp. 635-650.

[73] L. M. Sompayrac, How the immune system works, John Wiley and Sons, 2022.

[74] O. Sotolongo-Costa, L. M. Molina, D. R. Perez, J. C. Antoranz and M. C. Reyes, *Behavior of tumors under nonstationary therapy*, Physica D : Nonlinear Phenomena, 178 (3-4), 2003, pp. 242–253.

[75] T. H. Stewart, *Immune mechanism and tumor dormancy*, Revista Medicina, 56 (1), 1996, p. 74.

[76] K. Takahashi and S. Yamanaka, *Induction of Pluripotent Stem Cells from Mouse Embryonic and Adult Fibroblast Cultures by Defined Factors*, Cell, 126 (4), 2006, pp. 76-663.

[77] L. Thomas and H. Lawrence, Cellular and humoral aspects of the hypersensitive states, New York: Hoeber-Harper, 1959, pp. 529-32.

[78] A. M. Van Der Leun, D. S. Thommen and T. N. Schumacher,*$CD8^+$ T cell states in human cancer: insights from single-cell analysis*, Nature Reviews Cancer, 20 (4), 2020, pp. 218-232.

[79] X. Wang and I. Rivière, *Clinical manufacturing of CAR T cells: foundation of a promising therapy*, Molecular Therapy-Oncolytics, 3 (2016), p. 16015.

[80] J. D. Wolchok, V. Chiarion-Sileni, R. Gonzalez, P. Rutkowski, J. J. Grob, C. L. Cowey and J. Larkin, *Overall survival with combined nivolumab and ipilimumab in advanced melanoma*, New England Journal of Medicine, 377 (14), 2017, pp. 1345-1356.

[81] A. Xia, Y. Zhang, J. Xu, T. Yin and X. J. Lu, *T cell dysfunction in cancer immunity and immunotherapy*, Frontiers in immunology, 10 (2019), pp.1-15.

[82] H. Zhang, Z. Y. Dai, W. T. Wu, Z. Y. Wang, N. Zhang, L. Y. Zhang, W. J. Zeng, Z. X. Liu and Q. Cheng, *Regulatory mechanisms of immune checkpoints PD-L1 and CTLA-4 in cancer*, Journal of Experimental and Clinical Cancer Research, 40 (1), 2021, pp. 1-22.

[83] Immune system, https://www.britannica.com/science/immune-system.

[84] Immunology of cancer, https://www.mayoclinic.org.

[85] Cancer biology, https://www.mayoclinic.org/cancer.

Abstract

In this thesis, we develop deterministic models to describe tumour-immune response interactions, with the goal to represent the recent immunotherapies using so-called immune checkpoint inhibitors aimed at enhancing the immune response. Through a combination of analytical studies and numerical simulations, our main findings were as follows: firstly, both models exemplify the three Es of immunoediting. Secondly, highlight the impact of different biological settings on the anti-tumour immune response.

Keywords: Tumour-Immune interactions, Phenotype-structured model, Ordinary differential equations, Asymptotic analysis, Immune checkpoint inhibitors.

Résumé

Dans cette thèse, nous développons des modèles déterministes pour décrire les interactions entre les tumeurs et la réponse immunitaire, dans le but de représenter les récentes immunothérapies utilisant des inhibiteurs de points de contrôle immunitaires visant à renforcer la réponse immunitaire. Grâce à une combinaison d'études analytiques et de simulations numériques, nos principaux résultats sont les suivants : premièrement, les deux modèles illustrent les trois Es de l'immunoéditation. Deuxièmement, ils mettent en évidence l'impact de différents paramètres biologiques sur la réponse immunitaire anti-tumorale.

Mots clefs : Interactions tumeur-système immunitaire, Modèle structuré en phénotype, Equations différentielles ordinaires, Analyse asymptotique, Inhibiteurs de points de contrôle immunitaires.

الملخص

في هذه الأطروحة، نطور نماذج حتمية لوصف تفاعلات الاستجابة المناعية للورم، بهدف تمثيل العلاجات المناعية الحديثة باستخدام ما يسمى بمثبطات نقاط التفتيش المناعية التي تهدف إلى تعزيز الاستجابة المناعية. من خلال مزيج من الدراسات التحليلية والمحاكاة العددية، كانت النتائج الرئيسية التي توصلنا إليها على النحو التالي: أولاً، يجسد كلا النموذجين النماذج الثلاثة لاستجابة المناعة. ثانيًا، تسليط الضوء على تأثير العوامل البيولوجية المختلفة على الاستجابة المناعية المضادة للورم.

الكلمات المفتاحية: تفاعلات الورم والجهاز المناعي، نموذج منظم حسب النمط الظاهري، المعادلات التفاضلية العادية، التحليل المقارب مثبطات نقاط التفتيش المناعية.